Ecophysiological, morphological and genetic differences between two Southern Ocean morphotypes of the coccolithophorid

Emiliania huxleyi (Lohm.) Hay and Mohler (Haptophyta).

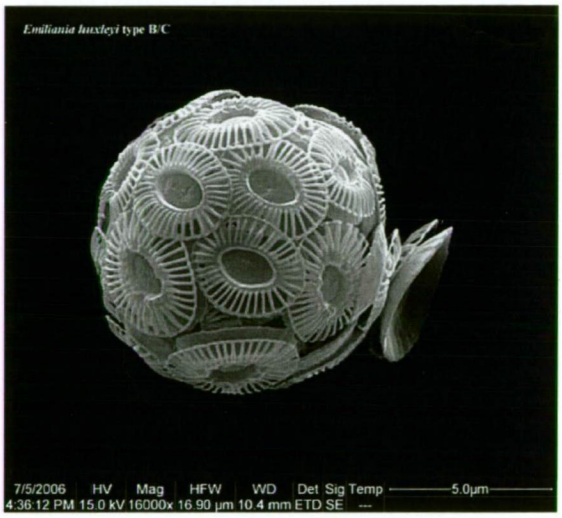

Suellen S. Cook BSc (Hons)

submitted in fulfillment of the requirements for the degree of Doctor of Philosophy

School of Plant Science, University of Tasmania
Hobart, Tasmania, Australia
April 2010

TABLE OF CONTENTS

Declaration

This thesis contains no material which has been accepted for a degree or diploma by the University or any other institution, except by way of background information and duly acknowledged in the thesis. To the best of my knowledge and belief, this thesis contains no material previously published or written by another person except where due acknowledgment is made in the text of the thesis, nor does the thesis contain any material that infringes copyright.

This thesis may be made available for loan and limited copying in accordance with the Copyright Act 1968.

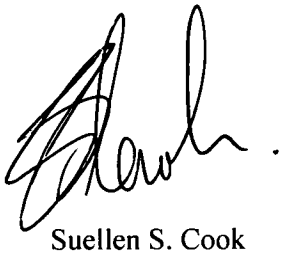

Suellen S. Cook
April 2010

Acknowledgements

Undertaking this doctorate has been wonderfully challenging and has made me a much stronger, resilient person. I have stretched myself beyond what I ever thought possible. The journey has only been possible with the enduring support of my family, my partner Glenn, your devotion and love have been invaluable, my daughter Lucy, who has made significant compromises above and beyond what is normally expected of a young teenager but who is ultimately very proud of her mum, my mother Margaret who has valued the benefits of higher education and my recently deceased father, Denis, I know he was and would be very proud of what I have achieved.

I wish to sincerely thank my supervisors for their invaluable support, guidance and their individual talents and expertise that have contributed much to this research. They are Prof Gustaaf Hallegraeff, A/Prof Mark Hovenden and A/Prof René Vaillancourt

Importantly this body of research would not have been possible without assistance from the following, to whom I give special thanks:-
Helen Bond, a deep well of algal culturing tricks, without whom, remaining sane and solving seemingly insurmountable problems would have been impossible. Dr Rebecca Jones from the School of Plant Science so generously provided a level of support, instruction and knowledge about genetic analysis and microsatellite processes second to none. Dr Will Howard, ACE CRC made possible my participation in the 2007 SAZ SENSE Marine Science Voyage on Aurora Australis enabling the collection of Southern Ocean algal samples. A/Prof Peter Ralph for valuable ongoing support and highly skilled assistance with the dark art of PAM data interpretation. Also my fellow Plant Science PhD candidates, Kate, Joana and Ben, technical assistance from Adam Smolenski, Dr Simon Wright and Rick van den Enden (AAD) Kate Evans, Dr Karsten Gorman (SEM), Dr Miguel de Salas and Ian Cummings. There are a number of people I would like to acknowledge here that although they may not consider their contribution large they have been pivotal in my candidature; Prof Jim Reid, Assoc Prof Anthony Koutoulis, Dr Gay McKinnon and Prof Andrew McMinn.

I have been gratefully supported by an Australian Post-graduate scholarship throughout my candidature along with additional financial assistance generously provided by a Bookend Trust-Lynchpin Fund Scholarship with the support of Dr Niall Doran and Susan Anderson, thank you.

A heartfelt thank you to everyone who have helped me reach my goal and increase our collective knowledge of the exciting "Pandora's Box" that is microalgae and in particular the exquisite *Emiliania huxleyi*.

Emiliania huxleyi var. *aurorae*

Abstract

The coccolithophorid *Emiliania huxleyi* has long been considered a cosmopolitan species occurring from the tropics to polar waters. This keystone marine phytoplankton through its shedding of delicate and intricately beautiful calcium carbonate coccoliths is a major contributor to the global geochemical cycling of carbon and is attracting widespread interest as to whether it will increase photosynthesis or reduce calcification in response to current climate change. To gain an understanding of the ecology of little studied Southern Hemisphere populations of *E. huxleyi* 423 single cell isolates were established from 10 sampling locations encompassing 5 ocean currents/systems around southern Australia, Tasmania and the Southern Ocean, including below the Antarctic Polar Front. Two distinct coccolith morphotypes were recognised which remained stable during long-term culturing: type A and type B/C.

DNA was extracted from these strains and each was amplified with 8 microsatellite markers developed for the species. The amplification success of the microsatellites was low (65%) but comparable between this and a previous study using the same markers with *E. huxleyi* (61%). Low to moderate genetic differentiation (from pairwise comparisons between populations F_{ST} range = 0.01 - 0.09) was apparent among type A populations despite considerable admixture suggesting that gene flow is not sufficient to completely prevent differentiation. Moderate to high levels of genetic differentiation (F_{ST} range 0.14 - 0.16) were observed between the Southern Ocean morphotype B/C and all type A populations. The genetic differences may arise from an ecological or environmental constraint to this unique Southern Ocean B/C morphotype.

Pigment analyses of the two morphotypes revealed significant differences in fucoxanthin pool composition and size. The 19′-hexanoyloxyfucoxanthin:chlorophyll *a* ratio (Hex:chl *a*) in type A strains was always <1, but > 1 in type B/C strains indicating an important role for Hex in managing light harvesting in type B/C strains. Based on non-Chl *a* normalized pigment data type B/C strains had a larger fucoxanthin pool due to 11 x greater

Hex:fucoxanthin ratio and a higher ratio of carotenoids to chlorophylls. Type A strains had an 8x higher concentration of fucoxanthin. Type A possessed the carotenoid 4-keto-19′-hexanoyloxyfucoxanthin (4-keto-hex) but this pigment was never detected in over 30 type B/C strains.

Related physiological differences between the two morphotypes were evident in the response to light, both in short and long term exposure experiments. Non-photochemical quenching (NPQ) of chlorophyll fluorescence and xanthophyll de-epoxidation were induced twice as rapidly in type A than in type B/C. Recovery of photosynthetic yield from short-term high light exposure was 12.5 x faster in type A than in type B/C. The Ek value of neither morphotype reflected either low or high steady state growth irradiance level (i.e. having an E_k value near the ambient irradiance) nevertheless in high growth irradiance the light saturation index (E_k) for type A was higher than type B/C. Upon exposure to simulated midday sea surface irradiance, the high light grown type B/C more than doubled its E_k value to surpass type A. Low light acclimated strains of both morphotypes suffered long term photodamage when exposed to sea surface irradiance levels.

The two *E. huxleyi* morphotypes, A and B/C, use and are affected by light differently according to the light level to which they have previously been acclimated.
With its higher fucoxanthin content, rapid xanthophyll de-epoxidation activity and recovery/repair mechanisms, type A is adapted to a narrower light intensity range but is more efficient under sustained high light conditions than type B/C. Accelerated xanthophyll cycling that increases the short-term photoprotective capacity of cells may be an important factor contributing to the ecological success of *E. huxleyi* type A during surface blooms at high light intensities. In contrast, type B/C, although possessing the capacity to acclimate to high light, has slower light response rates and takes longer to recovery and therefore may be compromised in its ability to adapt and optimise photosynthesis to reach the rapid growth rates required to form blooms. Furthermore, if as predicted under climate change models, ocean stratification and shallow mixing increase, then these conditions will have serious implications for the survival of the type B/C as it will potentially be exposed to longer

periods of high light conditions which may prove permanently damaging over a sustained period of time.

The degree of genetic differentiation along with the difference in pigment composition and photophysiological properties between the two morphotypes reflects an adaptive evolutionary divergence due to isolation of type B/C by the Antarctic Circumpolar Current. It is proposed that morphotype B/C be recognized as variety *aurorae* var. nov distinct from the more widespread type A (var. *huxleyi*). Recognition of strain variation of this previously considered cosmopolitan taxon is critical in order to predict the future success of this key ocean plankton.

1 Introduction

1.1 Background

The coccolithophorid *Emiliania huxleyi,* a ubiquitous member of the marine phytoplankton, first appeared in the geological record approximately 270,000 years ago and is numerically the most important coccolithophorid in the present-day world oceans (Brand 1994). *Emiliania huxleyi* forms large blooms contributing significantly to the global carbon pump by producing organic carbon from photosynthesis and inorganic carbon in the form of elegantly sculptured calcium carbonate coccoliths covering each cell (Balch *et al.* 1992; Holligan 1992; Westbroek *et al.* 1994). *Emiliania huxleyi* is widely considered to be a cosmopolitan marine microalga since it occurs from tropical to polar waters. Despite intensive research over many years, most of what is known about *E. huxleyi* has been derived from experimental studies on a limited number of North Atlantic and North-Eastern Pacific derived strains (Paasche 2001). We lack information about its global population structure in view of the increasing recognition that there exists a significant degree of morphological and physiological variation within this species complex (Stolte *et al.* 2000; Young *et al.* 2003; Hagino *et al.* 2005; Leonardos and Harris 2006).

1.2 Thesis Aims

The aim of this thesis is to explore the genetic, morphological and photophysiological variability between Southern Hemisphere populations and in particular the differentiation between the principal Southern Ocean morphotypes type A and B/C (*sensu* Young *et al.* 2003). Each chapter examines aspects of difference between the two morphotypes and culminates in an interpretation of findings in light of the evolutionary pressures and environmental influences that together have shaped their Southern Ocean distribution.

1.3 Genetic variability

In 1982 Brand reported evidence for genetic differences in growth rates between *E. huxleyi* culture strains originating from water of differing temperature. This was seen as a reflection of phenotypic plasticity within a cosmopolitan species (Medlin *et al.* 1994a). *Emiliania*

huxleyi populations may comprise significant genetic structure that has not been detectable with traditional highly conserved markers (Medlin *et al.* 2000) thus prompting the development and use of microsatellite molecular markers to investigate population structure (Iglesias-Rodriguez *et al.* 2002; Iglesias-Rodriguez *et al.* 2006b). These studies found populations from the different water masses were not clonal and individuals sampled from the same bloom were genetically distinct suggesting that sexual reproduction plays an important role in adaptation to changing environmental conditions (Iglesias-Rodriguez *et al.* 2006b). Chapter 2 of this thesis examines the genetic variability in Southern Hemisphere populations of *E. huxleyi* using the published microsatellite markers with a focus on the genetic differentiation among populations of type A strains from nine locations sampled from five ocean currents around SE Australia and also between type A and Southern Ocean type B/C sampled from two locations, the Antarctic Circumpolar Current and below the Antarctic Polar Front.

1.4 Morphology and pigment profiling

Distinguishing morphotypes of the polymorphic coccolithophorid *E. huxleyi* has been a topic of investigation for decades. Much of the early work on *E. huxleyi* concerned the biology of cells, describing sessile, motile, and naked cells either with or without flagella (Paasche 2001) and a number of coccolith bearing morphotypes which Medlin *et al.* (1996) suggested should be recognised as separate varieties but which have not been widely accepted. Currently there are five recognised *Emiliania* morphotypes (Young *et al.* 2003) all of which are illustrated in Fig. 1.1 including the morphotype B/C from this study.

Type A is globally widespread and the most prevalent bloom-forming morphotype (Paasche *et al.* 1996), while type B is primarily found in the North Sea (van Bleijswijk *et al.* 1991) and the type B/C (referred to as type K by Hiramatsu & De Deckker 1996 and type C by Findlay and Giraudeau 2000) has thus far only been found in the Southern Ocean (Findlay and Giraudeau 2000; Cubillos *et al.* 2007), the Kuroshio Current, east of Japan (Findlay and Giraudeau 2000; Hagino *et al.* 2005) and off the coast of Namibia (J. Henderiks, pers.comm.).

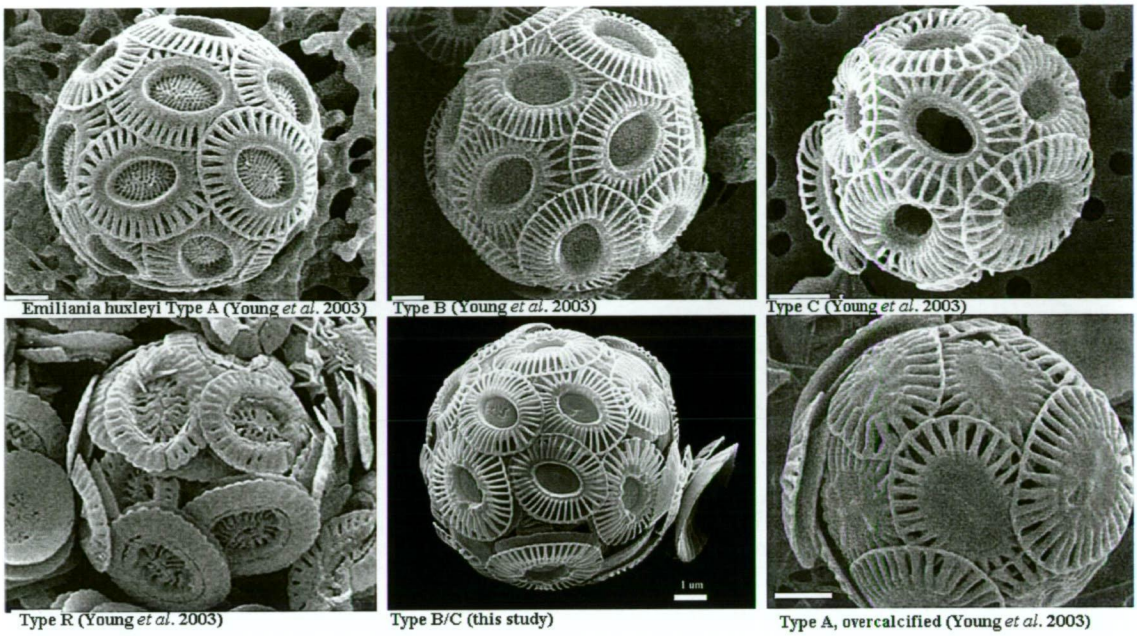

Fig. 1.1. Recognised morphotypes of *Emiliania huxleyi.* From top left, clockwise, type A, type B, type C, Type R (all Young *et al.* 2003), type B/C (this study) and overcalcified type A (Young *et al.* 2003). All scale bars = 1 μm.

Pigment composition has been used extensively to characterise haptophyte algae as a means of identifying the taxonomic composition of mixed phytoplankton field samples from marker pigment signatures (Jeffrey and Allen 1964; Arpin *et al.* 1976; Garrido and Zapata 1998; Jeffrey and Vesk 2005) including *E. huxleyi*. Zapata *et al.* 2004 identified eight groups of haptophyte pigment signatures stating the presence of monovinyl-chlorophyll c_3, 4-keto-19'-hexanoyloxyfucoxanthin and 19'-butanoyloxyfucoxanthin and the absence of chlorophyll c_1 as diagnostic for *E. huxleyi*.

Despite advances in technology, pigment analysis alone has so far not been explored to discriminate between *E. huxleyi* morphotypes. When significant variability exists in a species it is important to differentiate morphotypes or ecotypes to prevent generalisation and extrapolation from the study of a limited number of strains or populations. Therefore in

Chapter 3 the morphology and pigment profile of type B/C is characterised and compared to that of the widely studied type A.

1.5 Photophysiology

1.5.1 Short term photoprotective responses

If, as argued by Medlin (2007) genetic differences are based on local adaptation then this may be reflected in functional ecophysiological differences. Chapters 4 and 5 test the hypothesis that the Southern Ocean *E. huxleyi* type B/C population has become physiologically and ecologically distinct due to adaptation and isolation made possible by the Antarctic Circumpolar Current.

Efficient photosynthesis requires optimal utilisation of absorbed photons when light is limiting, however transport of plankton cells from depth to the surface exposes them to irradiance levels that can be much higher than needed to reach maximum photosynthetic capacity (Falkowski, 1994, Litchman & Klausmeier, 2001, Muller *et al.*, 2001). Plant cells must take photoprotective measures but these impose a cost in terms of carbon fixation (Long *et al.* 1994). Therefore, the ability to rapidly optimise photochemistry to prevailing light conditions is critically important for survival, growth and competitive advantage in changeable light environments (Huismann *et al.* 1999a, b, Litchman & Klausmeier, 2001, MacIntyre *et al.* 2002). To manage high light intensities over short time scales (seconds to hours), photosynthesis in many algae species, is down-regulated by dissipating excess energy in part by enzymatic xanthophyll pigment conversion. The xanthophyll cycle is thus critical to prevent permanent cell damage (Olaizola *et al.* 1994; Falkowski and Raven 1997; Gorbunov *et al.* 2001). Xanthophyll pigments fulfil a dual function, with the epoxidised forms assisting in light harvesting, whereas de-epoxidised forms dissipate excessive energy in high light (Olaizola *et al.* 1994; Owens 1994).

Chapter 4 describes the similarities and differences in the photophysiological response to light between triplicate strains of the two dominant Southern Ocean morphotypes of *E. huxleyi,* A and B/C using pulse amplitude modulation fluorometry (PAM) and HPLC

pigment analysis. The kinetics of xanthophyll pigment de-epoxidation and epoxidation are compared to the induction and relaxation of photochemical and non-photochemical quenching.

1.5.2 Long term acclimation and response

Emiliania huxleyi appears to be tolerant of the effects of extreme irradiance levels, particularly in bloom conditions (Tyrrell and Taylor 1996; Nielsen 1997; Iglesias-Rodriguez *et al.* 2002; Merico *et al.* 2004; Harris *et al.* 2005; Harris *et al.* 2009). Irradiance appears to be a key factor determining the occurrence of *E. huxleyi* blooms (Nanninga and Tyrrell 1996; Iglesias-Rodriguez *et al.* 2002; Siegel *et al.* 2007; Zondervan 2007). Where in diatom assemblages at light levels of 1700 µmol photons $m^{-2} s^{-1}$ a reduction of 80% in the photosynthetic rate is likely (Kirk 1994), no evidence of photoinhibition in *E. huxleyi* has been reported. The objective of Chapter 5 is to characterise the response of morphotypes A and B/C of *E. huxleyi* to long-term low and high growth irradiance and to assess the susceptibility to irradiance based photoinhibition and recovery using PAM fluorometry.

1.6 Concluding Remarks

Chapter 6 brings together the key findings, namely genetic differentiation (chapter 2), morphological characterisation and pigment signature of type B/C (Chapter 3), xanthophyll activity (Chapter 4) and long term acclimation to variable light intensity (Chapter 5). The evolutionary pressures of circumpolar entrainment forming a barrier to gene flow and allowing adaptation to the environmental gradients created at the Antarctic Polar Front are presented as causative factors in the distribution of the two morphotypes and the fragmentation of the Southern Ocean type B/C. Furthermore the implications for the survival of the B/C morphotype and its capacity to form blooms under current climate change predictions are explored.

2 Genetic variability in Australian and Southern Ocean populations of *Emiliania huxleyi.*

2.1 Abstract

To gain an understanding of the genetic variability within Southern Hemisphere populations of *Emiliania huxleyi,* a collection was established which consisted of 423 single cell isolates collected from five ocean currents in southern Australia, west and east coast of Tasmania and from the Southern Ocean, including below the Antarctic Polar Front. Two of the five currently recognised morphotypes were represented, A and B/C, both of which remained stable during long-term culturing. DNA was extracted from these strains and each was amplified for eight microsatellite markers developed for this species. The amplification success of the microsatellites was low (65%), but comparable between this and a previous study using the same markers with *E. huxleyi* (61%). Levels of diversity (H_e, H_o and F_{IS}) across markers were also comparable. Patterns of allele frequency indicated differentiation between western, eastern and southern populations through factors such as genetic drift. Low to moderate genetic differentiation (F_{ST} range = 0.01 - 0.09) was apparent among type A populations despite considerable admixture suggesting that gene flow is not sufficient to completely prevent differentiation. Moderate to high levels of genetic differentiation (F_{ST} range 0.14 - 0.16) were observed between the Southern Ocean type B/C and type A populations. Structuring of populations and differentiation among type A populations appeared to be associated with ocean currents. The level of differentiation found between morphotypes supports the existence of some form of barrier, be it reproductive, environmental or biogeographical and provides evidence of considerable divergence and differentiation of *E. huxleyi* type B/C and that despite significant admixture among type A populations, genetic differentiation persists.

2.2 Introduction

Emiliania huxleyi, a ubiquitous member of the marine phytoplankton, first appeared in the geological record 270,000 years ago and is numerically the most important coccolithophorid in the present-day world oceans Despite recognition that there exists a significant degree of morphological and physiological variation within the microalga *E. huxleyi* little is known regarding the genetic differences and the ecology of each of the five currently recognised morphotypes (Young 1994; Hiramatsu and DeDeckker 1996; Findlay and Giraudeau 2000; Young *et al.* 2003; Findlay *et al.* 2005; Schroeder *et al.* 2005) (Fig. 1.1). Most attempts to differentiate between the morphotypes have focused almost exclusively on morphological characterisation.

Genetic variation between and within populations and/or blooms of *E. huxleyi* has been investigated in a number of studies over the last 30 years using a variety of methods, proxies and molecular markers. In 1982, Brand examined the genetic variability between and within populations of *E. huxleyi* by determining the growth rate of cultured strains from different parts of the North Atlantic. Brand's results indicated genetic differences between populations originating from water of differing temperature but was unable to find any correlation to morphotypes (Brand 1982). Because of this lack of genetic differences, morphological variation was believed to reflect the phenotypic plasticity of a cosmopolitan species (Medlin *et al.* 1994a).

In 2005 a genetic marker was identified within the 3' untranslated region of a coccolith associated protein mRNA separating the A and B morphotypes, and also showed that type A was composed of a number of distinct genotypes (Schroeder *et al.* 2005). The study was conducted on seven known type A isolates and two known type B isolates all originating from Northern Hemisphere waters. Medlin *et al.* (1996) included three Southern Hemisphere cultures in a genetic analysis of variation in the nuclear-encoded small sub-unit ribosomal RNA gene and spacer region but no genetic differences were identified between individuals. It should be noted however that this latter study did not include the morphotype

B/C from the Southern Ocean and that ribosomal genes are renowned for their slow rate of evolution (Avise 1994).

Measuring levels of genetic diversity and population fragmentation has now become possible using microsatellite markers. Microsatellite molecular markers have recently been developed for a number of marine phytoplankton species including the diatoms *Ditylum brightwellii* (Rynearson and Armbrust 2000), *Pseudo-nitzschia multiseries* (Evans *et al.* 2004), the dinoflagellates *Alexandrium tamarense, A. catenella* and (Nagai *et al.* 2006a), rhapidophytes *Heterosigma akashiwo, Chattonella antique, C. marina* and *C. ovata* (Nagai *et al.* 2006b; Demura *et al.* 2007) and haptophytes *Phaeocystis antarctica, P. globosa* , *P. pouchetii* (Gaebler *et al.* 2007) and the coccolithophorid *E. huxleyi* (Iglesias-Rodriguez *et al.* 2002) but only in a few cases have genetic studies been published.

Microsatellite markers consist of segments of DNA that contain tandem repeats of simple motif sequences usually between 1 and 5 base pairs which are flanked by less repetitive sequences which serve as primers sites (Halliburton 2004). Due to their high mutation rate in the number of repeats, microsatellite markers are highly polymorphic with many alleles per marker. Hence, microsatellite markers have proven highly informative for DNA fingerprinting applications, analysis of paternity, patterns of gene flow, genetic variability, population structure and differentiation (Halliburton 2004). It is apparent from previous research that *E. huxleyi* may hold significant population structure that has not been detectable with traditional highly conserved markers thus prompting the use of microsatellite markers to investigate population structure.

By 2006, ten polymorphic microsatellite markers had been isolated from one strain (B92-11, Norway) of *E. huxleyi* (Iglesias-Rodriguez *et al.* 2002; Iglesias-Rodriguez *et al.* 2006b). These microsatellite markers were used to genotype 85 strains of *E. huxleyi* from different geographical origins (including 4 strains from the Southern Hemisphere). They suggested that populations were not clonal either within or among the different water masses from which samples were taken and further that even individuals sampled from the same bloom were genetically distinct, questioning the notion that blooms arise primarily from binary cell

division. The authors suggested that sexual reproduction plays an important role during bloom events with the resulting assortment of genotypes enabling adaptation to changing environmental conditions (Iglesias-Rodriguez *et al.* 2006b). It is also likely that genetically diverse seed populations contribute to the genetic diversity of blooms, even with binary fission (Brand 1982).

AFLPs have also been used to analyse genetic variability of *E. huxleyi* populations from seven North Atlantic strains and two Southern Hemisphere strains, one from South Africa and one from New Zealand (Iglesias-Rodríguez et al. 2002). Results indicated that no two strains shared an identical genotype and this posed the question of how a single species can bloom in both Northern and Southern Hemispheres with widely differing environmental conditions? They suggested that the genetic diversity and differentiation found could be interpreted as arising from mutation/selection pressures that ensures survival in changing oceanic conditions and that ocean currents create the barriers to dispersal isolating Northern and Southern Hemisphere populations (Iglesias-Rodríguez *et al.* 2002). Medlin (2007) in a review of cosmopolitan phytoplankton species concluded that planktonic populations can be genetically distinct through fragmentation and that we are merely looking at a snapshot in species evolution.

There is sufficient evidence to suggest that there maybe considerable genetic variability within and between populations of *E. huxleyi* worldwide and that there is some genetic basis for at least two morphotypes A and B. Nevertheless most studies exclude completely or include very few Southern Hemisphere strains in their analyses making extrapolation problematic and no studies have examined genetic differentiation between Southern Ocean morphotypes.

2.2.1 Aims

The aim of this study was to use existing microsatellite markers to characterise the patterns of genetic variability among oceanographically separate populations of *E. huxleyi* from the Southern Hemisphere. To gain an understanding of the genetic variability within the little

studied Southern Hemisphere populations of *E. huxleyi* a collection of 423 single cell isolates was established from 5 ocean currents in southern Australia, Tasmania and the Southern Ocean, including below the Antarctic Polar Front. Two morphotypes were recognised which remained stable during long-term culturing: type A, and type B/C. Specifically, this study aims to look for genetic differentiation among sampled populations of type A strains and for differentiation between the two principal morphotypes found in the Southern Ocean.

2.3 Materials and Methods

2.3.1 Culture material

Emiliania huxleyi cells were collected at 10 locations around SE Australia, Tasmania and the Southern Ocean (Fig. 2.1). Samples originated from 5 ocean current systems; the Leeuwin current moving east from Western Australia, the Zeehan Current, an extension of the Leeuwin Current, that travels south along the west coast of Tasmania, the East Australian Current (EAC) that travels south along the east coast of Australia and Tasmania, also from an eddy of the EAC that formed off the south east coast of Tasmania and from the Antarctic Circumpolar Current (Fig. 2.2). Populations in this study are defined as the set of strains isolated from 1 water sample at specific geographic location except for type A strains isolated from the two locations within the Southern Ocean which were combined to form one population as were all type B/C strains (Table 2.1).

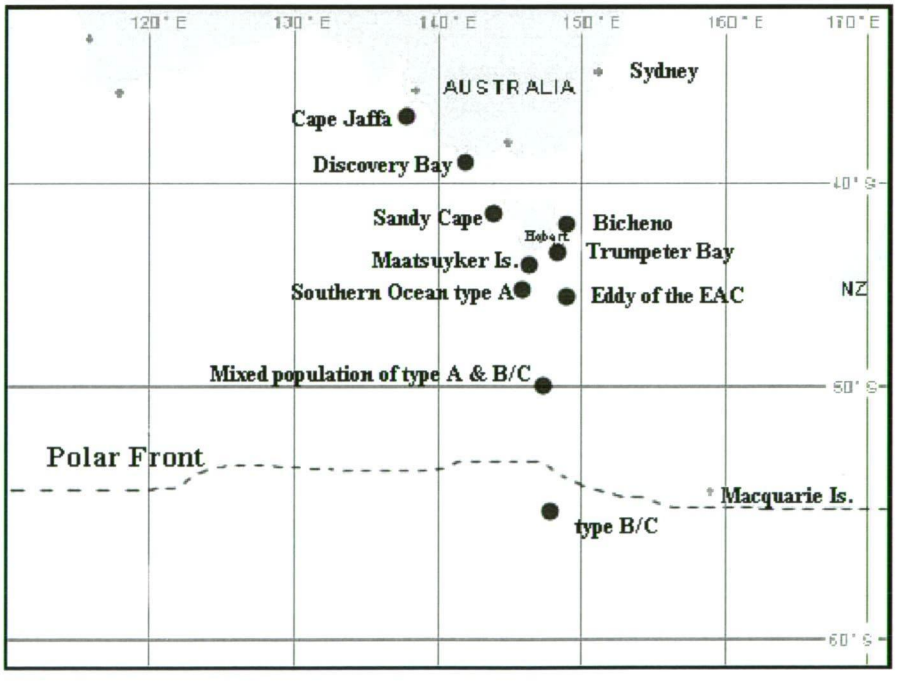

Fig. 2.1 Location map showing the sampling location (populations) of strains used in this study.

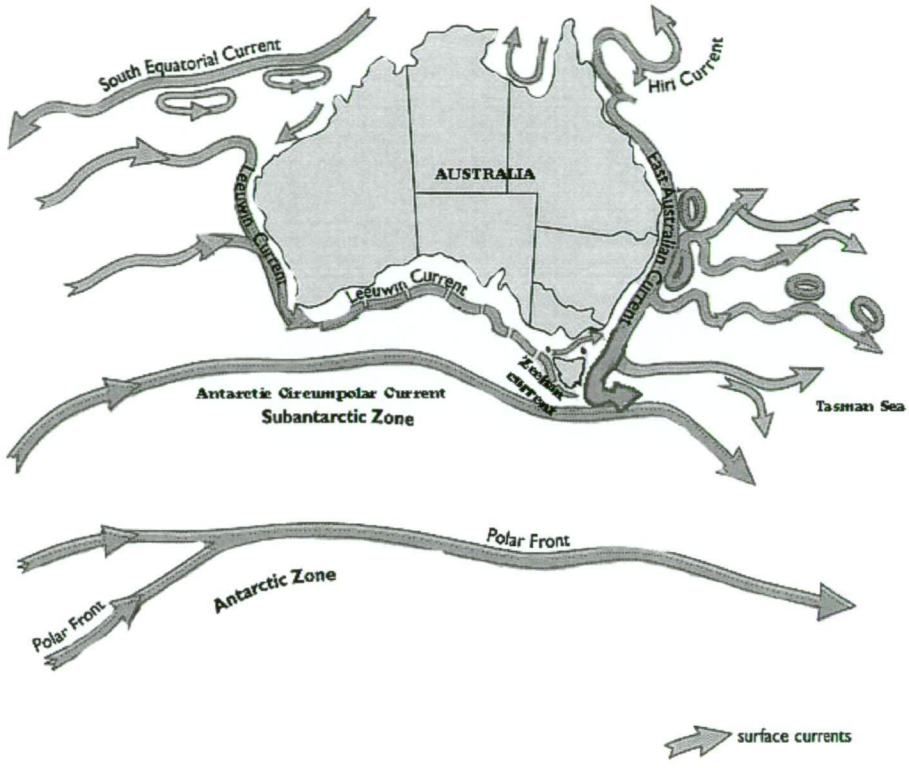

Fig. 2.2 Major surface ocean currents surrounding Australia. Modified from www.srfme.org.au

Seawater samples (two litre) were collected at each location and immediately filtered through a 25 µm plankton net to remove large zooplankton and phytoplankton, concentrated and aliquotted into 96 well microplates with added K media (Keller *et al.* 1987). After a period of approximately 1 week incubation a single cell was isolated from each well of the microplate using a micropipette under a Zeiss Axiovert 25 inverted light microscope. Under a Zeiss Stemi 2000C stereo microscope the single cell was washed in sterile media twice and established as an individual strain. Strains were cultured initially in 24 well microplates then, once established, stock cultures were maintained in sterile 70 ml specimen containers with K_2 media (Keller *et al.* 1987). Morphotypes were identified using scanning electron microscopy. Morphology remained stable during three years of long-term culturing.

Table 2.1. *Emiliania huxleyi* strains used for microsatellite analysis and amplification success

Population .	Location	ocean current	Isolation Date	n = (1-8 markers)	n (> 6 markers)
Bicheno	148.3759E 41.947234S	Coastal waters/EAC	June 2006	37	35
Trumpeter Bay	147.45300E 43.153102S	Coastal waters/EAC	May 2006	52	41
EAC Eddy	148.3505E 43.3950S	EAC	Jan 2007	39	26
Cape Jaffa	139.30664E 37.02009S	Leeuwin	Nov 2006	49	28
Discovery Bay	141.2518E 38.8907S	Leeuwin	Nov 2006	40	32
Sandy Cape	143.7136E 41.5507S	Zeehan	Nov 2006	66	46
Maatsuyker Is	146.36860E 43.6300S	Mixed	Nov 2006	70	44
Southern Ocean Type A	7m depth at 149.2500E 49.5900S	Mixed	Feb 2007	9	9
	Transect b/w 146.0489E 48.3447S and 146.5919E 45.0760S	Mixed	March 2006	5	3
Southern Ocean Type B/C	7m depth at 149.2500E 49.5900S	Mixed	Feb 2007	3	0
	7m depth at 145.5519E 53.5973S	Circumpolar Current	Feb 2007	6	0
	65m depth at 146.1813E 54.0850S	Circumpolar Current	Feb 2007	25	5
	80m depth at 145.5519E 53.5973S	Mixed	Feb 2007	12	3
	Transect b/w 142.4706E 59.4853S and 145.3450E 50.3251S	Mixed	Feb 2006	10	1
TOTAL				423	273

2.3.2 DNA extraction and PCR

Total genomic DNA was extracted using a phenol:chloroform:isoamyl alcohol extraction method following a modified protocol of Scholin and Anderson (1994). Approximately 50 ml of mid-log phase culture was harvested by gentle centrifugation. The cell pellet was resuspended in approximately 400 ul of autoclaved Milli-Q water (Millipore Corp.) at room temperature with the addition of 50 µl of 10% SDS sodium dodecyl sulphate, 50 µl of 10x STE (100 mM Tris, 100 mM EDTA and 100 nM NaCl, pH 8.0) and 5 µl RNase (100 mg/mL). The mixture was incubated with gentle mixing at 65° C for 10 min.

After incubation, the nucleic acids in this solution were purified by extracting once with 500 µl of phenol:chloroform:isoamyl alcohol (24:24:1) followed by two 500 µl chloroform:isoamyl extractions. Total nucleic acids were precipitated with the addition of 10% volume of 3 M Na-acetate (pH 5.2) and two volumes of cold 100% ethanol and held on ice for 20 min followed by centrifugation for 20 min in a 4° C centrifuge. The resulting pellet was washed with 70% ethanol and resuspended in 100 µl of TE (10 mM Tris-HCL, pH 7.5, 1 mM EDTA, pH 8.0). Where necessary DNA was cleaned by re-precipitation in the presence of high salt concentration (2.0 M NaCL).

Genomic DNA concentration was estimated by comparison with a known concentration of a standard molecular-weight marker (Lambda HindIII) by electrophoretic separation in 1% (w/v) agarose gels and also using a Picofluor Handheld Fluorometer (Turner Biosystems). Picogreen® dyes were used for DNA quantification and compared with a λDNA standard according to the manufacturer's instructions.

The PCR conditions for all microsatellite markers were as in Iglesias-Rodriguez *et al.* (2002) but with some modifications (Table 2.3). Forward primers were synthesized with a WellRED fluorescent label (Proligo) attached to the 5' end to allow detection of PCR product on a CEQ fragment analysis system (Beckmann Coulter). Microsatellite amplification products were initially visualized by electrophoretic separation on agarose gels in TAE buffer with ethidium bromide staining (0.5 µg/mL) before running on the CEQ.

PCR were performed separately for each marker and products co-loaded for fragment analysis in three sets (Set 1: P02E09, P02B12; Set 2: P02E10, P01E05, EHMS37; Set 3: P02F11, P01F08, P02E11) and sized in comparison with the CEQ™ DNA size standard-400 by using the associated Fragment Analysis software (Beckman Coulter) for allele binning and manual checking. Microsatellite scoring products assessed to be artefacts based on size and intensity, i.e. stutter bands, resulting from the imperfect amplification of repeats were associated with some markers. However, these additional products artifacts were usually distinguishable by their smaller size and low intensity and did not generally compromise the identification of alleles for the genotype analysis. Where accurate scoring was questionable the process was further optimized and amplification repeated.

Table 2.2. Ten microsatellite markers developed for *Emiliania huxleyi* strain B11 by Iglesias-Rodriguez *et al.* (2002, 2006b)

Marker	Expected repeat[1]	Primer sequences	T_a (°C)	Published size range of alleles (bp)
P02F11	$(GT)_{11}$	F: CTCGTGTGGCTATGCCTATG R: TCCAAGAGCAAAGTGCAAAA	58	100-149
P02E11	$(GA)_7TA\ (GA)_7$	F: CGGTGCTACGAGGTGTGTAA R: CACGCGCTTCACAATGTAAT	58	206-251
P01F08	$(GT)_{14}$	F: CGGAGCAGTCCAGTACACAA R: CGCATCTCAGTCGTTCTTCA	60	144-198
P02E09	$(GT)_9$	F: ACTCGGACTGGACGCACA R: GGCTGCTCTTCCCCTCTCCTA	59	82-104
P02B12	$(GT)_{10}$	F: GGTTAATCGCAGCAAAGAGC R: CAGTCTTGATCGGGACGA	58	204-220
P01E05	$(GA)_{14}GG\ (GA)_{21}$	F: GTGTGCCCTTTTGTGCTTTT R: GTGATGGTGTGCCTGTGTTC	57	120-190
P02E10	$(GT)_{11}GCAA(GT)_{11}$	F: CTCGTGTAGTCGGGGAGTGT R: CACGCGGTCCAATATTACCT	58	164-180
EHMS37	$(GT)_{23}$	F: TGTGAGAGTGAGCACGCA R: TTGAGGAGGATTACGAGGTC	60	203-240
EHMS15	$(GT)_{27}GC$	F: TCGAGGCGCGTCACACAC R: GCGAGCGGTGGGCAATGT	54	72-149
P02A08	$(GA)_6GG\ (GA)_{23}$	F: CCCCGTGTTTGAGAGAGAGA R: TCGGAGATCAGGGAGTTGTC	58	281-331

[1] Expected repeat is the repetitive pattern observed in the original clone *Emiliania huxleyi* B11 .

2.3.3 Molecular data analysis

GenAlEx6.2 (Peakall and Smouse 2006) was used to calculate the following parameters of genetic diversity, averaged for each marker: number of alleles (A), number of effective alleles (A_e) allele frequencies, observed (H_o) and expected heterozygosity (H_e) and Wright's (1978) fixation index (F). Comparison of pairwise F_{ST} values based on Nei's (1978) genetic

distance and their statistical significance were calculated using GenAlEx (Peakall and Smouse 2006).

Null allele frequencies were estimated using the Inbreeding Population Method (PIM) in INEst (Chybicki and Burczyk 2009). INEst allows the estimation of the frequency of null alleles taking into account the possibility of inbreeding within a population. The reported F_{IS} index represents the degree of inbreeding within a population after the effect of null alleles has been subtracted (Chybicki and Burczyk 2009). Allelic richness was calculated at the population level for type A populations using Fstat (Goudet 2002).

To assess allelic fixation the proportion of markers with an allele greater than 0.5 frequency was calculated. Inbreeding coefficients F_{IS}, F_{IT}, F_{ST} (F statistics) (Weir and Cockerham 1984) were calculated for each marker using Fstat (Goudet 2002). Jost's (2008) estimated D (D_{est}) was calculated using SMOGD v. 1.2.5. (Crawford 2009). D_{est} is a recently developed measure of differentiation that reportedly avoids the mathematical problems that surround statistics such as F_{ST} and G_{ST} which, according to Jost (2008) can give a misleading hierarchy of differentiation among populations. D_{est} accounts for differences in allele diversity among populations and types of markers (Jost 2008) and is suggested to provide a more realistic comparison between studies or among samples within a study.

2.3.4 Bayesian structure analysis

The population structure was assessed using two different approaches (1) with no *a priori* grouping by population or morphotype and 2) using population grouping to assess spatial differentiation (Fig. 2.1, Table 2.1)

2.3.4.1 Undefined populations

STRUCTURE 2.2.3 (Pritchard *et al.* 2000) was used to search for population structure without prior information on sample locations. The number of clusters of genetically similar individuals (K) and the affinities of individuals to these clusters (Q) were determined using the ΔK method described in Evanno *et al.* (2005). Assuming no prior population structure

and using the admixture model the estimated K was determined by comparing the estimated log probability of data at different values of K (from $K = 1$ to $K = 10$) using 100 000 MCMC repetitions following a burn-in of 100 000 repetitions (at which point stationarity had been reached). Five independent runs for each value of K were performed and the results were interpreted using the three runs with the highest likelihood.

Independent runs of STRUCTURE at a given K can result in different solutions simply due to label-switching across different runs or due to true multimodality (distinct solutions across different runs). Jakobsson and Rosenberg (2007) developed three algorithms which combine independent runs into a single solution; these are implemented in the software programme CLUMP. The *Fullsearch* algorithm in CLUMP was used to derive a single output from the three independent runs at each K from 2 to 9. DISTRUCT (Rosenberg 2004) was used to display the probability of membership (Q) of each individual into each of the inferred clusters. The average proportion of membership of each of the nine populations into the K clusters from the analysis of all sampled strains of *E. huxleyi* was also plotted on a separate map for each level of K.

2.3.4.2 Pre-defined populations

Strains were assigned to a population using individual assignment tests calculated in GeneClass 2.0 (Piry *et al.* 2004). This used the Bayesian computation criteria of Rannala and Mountain (1997) and an α level of 0.01 to calculate the likelihood that a given isolate originated from a given population. The process used genotype likelihoods to draw inferences about the population to which individuals belong. A self-assignment process (leave one out) calculated the likelihood of identifying genotypes in each population and assigned each genotype to the population for which it had the highest likelihood of belonging and secondly determined the likelihood of belonging to either morphotype group.

A principal coordinate analysis (PCA) was used to identify clusters based on similarity among locations. Nei's genetic distance was calculated in GenAlEx6 (Peakall and Smouse 2006) and then subjected to PCA also in GenAlEx.

2.4 Results

2.4.1 Success of microsatellite amplification

PCR amplification conditions were optimized by varying DNA template purity and concentration, primer concentration, number of PCR cycles and annealing temperature (Table 2.3). Adjustment of DNA template purity and concentration required considerable testing and optimizing to produce scorable PCR product. Initially ten nuclear microsatellite markers were tested; however due to inconsistencies with amplification and scoring EHMS15 and P02A08 were excluded. Formal testing of the consistency of PCR amplification over repeated runs was not tested for each marker due to lack of good quality template stock. However, repeats were conducted on co-loaded samples for optimization purposes, allele scoring of successful amplifications matched with previous allele sizes.

Table 2.3. Annealing temperatures and allele size range for each marker used in this study

Marker	Annealing temperature	Size range of alleles (bp)
P02F11	60	63-175
P02E11	58	125-267
P01F08	60	92-298
P02E09	62	73-127
P02B12	58	197-229
P01E05	58	102-222
P02E10	62	151-207
EHMS37	60	186-336

Successful amplification of alleles at each marker was achieved for between 66% and 79% of the original 423 *E. huxleyi* strains (Table 2.1). In particular Southern Ocean type B/C returned a very low amplification rate in 5 of the eight markers in comparison with type A populations (Fig. 2.3). Eastern Tasmanian populations had the highest PCR amplification success of any group.

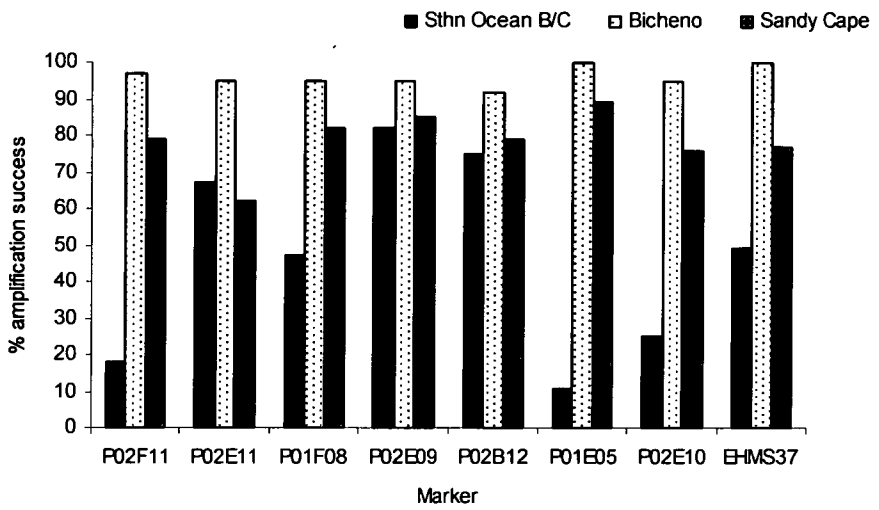

Fig. 2.3. Amplification success for *Emiliania huxleyi* strains from Southern Ocean type B/C, Bicheno and Sandy Cape populations.

Successful amplification in at least six of the eight microsatellite markers used was achieved in 86% - 97% of strains per population. Of these strains, 152 (56%) gave amplification products for all eight markers ranging from 13% in the Southern Ocean B/C population (one of nine strains) to 100% in the Bicheno population. The Southern Ocean type B/C population was problematic in that initially 37 out of 55 strains produced amplification products in at least one marker, however only nine remained after culling all strains that failed to amplify at a minimum of six markers. Of those nine, seven amplified at six markers, one at seven and one at all eight. P01E05 and P02F11 proved particularly problematic for the type B/C strains in that PCR product was absent in eight of the nine strains at P01E05 and absent in four of the nine in P02F11. Overall only strains with results for six or more markers were retained, resulting in a final data set of 273 individual strains representing nine populations and two morphotypes (A and B/C).

The frequency of null alleles was highest for markers P01F08 and EHMS37 and lowest for P02E09 (Table 2.4). There was evidence of a null allele at four or more markers in the

populations from Trumpeter Bay, EAC eddy, Cape Jaffa, Discovery Bay and Sandy Cape (Fig. 2.4).

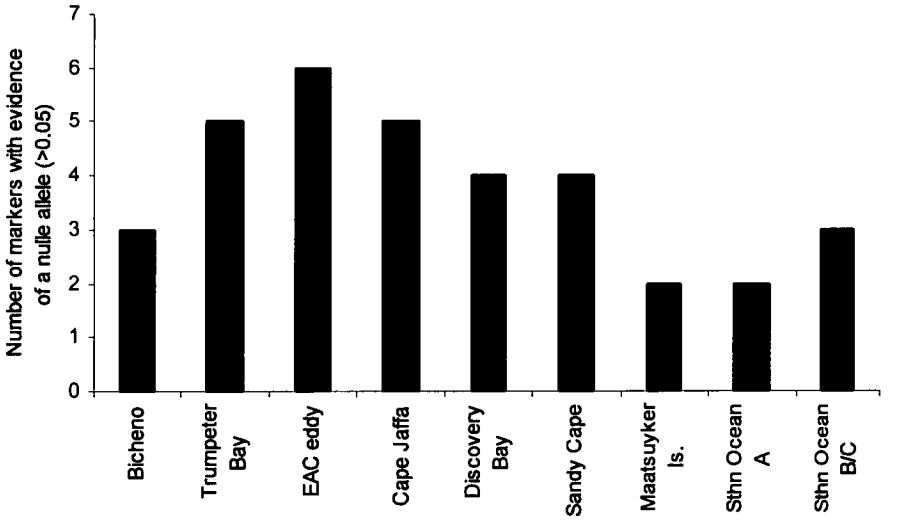

Fig. 2.4. The number of markers with evidence of a null allele (frequency likelihood > 0.05) after accounting for inbreeding (Chybicki and Burczyk 2009).

2.4.2 Microsatellite marker diversity

All eight markers were highly polymorphic, with between 14 and 59 observed alleles per marker (mean A across all markers, $A = 31$) (Table 2.4). All markers, however, had many rare alleles that contributed little to differentiating populations therefore the mean effective alleles (A_e) per marker of 6.4 was low (Table 2.4). The high level of polymorphism was also reflected in the moderately high levels of expected heterozygosity (mean H_e across markers, $H_T = 0.78$) (Table 2.4). EHMS37 produced the highest number of alleles. Expected heterozygosity was also highest at this marker but a reasonably high level of homozygote excess was evident. The observed heterozygosity was lower than the expected heterozygosity at all markers, but the least difference was at P02E09 and P02B12 and both also had a low likelihood of null alleles. Two markers (P01F08 and EHMS37) had high F_{IS} and F_{IT} values (Table 2.5). Both markers showed a high frequency of null alleles averaged

over all populations (Table 2.4). F_{ST} was highest for P02E11 then P02F11and lowest for markers P02B12 and P02E10, whereas D_{est} ranked EHMS37 highest. F_{ST} and D_{est} measures were not significantly different ($r^2 = 0.42$).

Table 2.4. Overall genetic diversity parameters for all microsatellite markers. N = Number of individual strains, A= observed number of alleles per marker, Ae = effective number of alleles per marker, Ho = observed heterozygosity, He = expected heterozygosity, Null = frequency of null alleles, averaged over populations and after inbreeding has been accounted for (Chybicki and Burczyk 2009).

Marker	*N*	*A*	A_e	H_o	H_e	Null
P02F11	263	32	6.32	0.75	0.82	0.08
P02E11	236	38	8.12	0.67	0.84	0.08
P01F08	238	37	6.09	0.46	0.83	0.18
P02E09	255	19	4.01	0.66	0.71	0.03
P02B12	248	15	2.61	0.55	0.60	0.05
P01E05	258	36	8.91	0.70	0.85	0.08
P02E10	248	14	3.14	0.55	0.66	0.04
EHMS 37	265	59	11.90	0.64	0.90	0.10
Mean		31.3	6.39	0.62	0.78	0.08
SE		5.3	0.47	0.02	0.02	0.02

Table 2.5. Inbreeding coefficients (F_{IS}, F_{IT}, F_{ST}) (Fstat) and Jost's (2008) estimated D (D_{est}) calculated for each marker. F_{IS}, inbreeding in individuals relative to their population; F_{IT}, inbreeding in individuals relative to the total species; F_{ST}, inbreeding in populations relative to the total species. D_{est}, measure of diversity among populations.

Marker	F_{IS}	F_{IT}	F_{ST}	D_{est}
P02F11	0.01	0.07	0.07	0.35
P02E11	0.24	0.30	0.08	0.60
P01F08	0.46	0.48	0.05	0.44
P02E09	0.09	0.13	0.04	0.21
P02B12	0.15	0.17	0.02	0.06
P01E05	0.26	0.28	0.03	0.35
P02E10	0.13	0.15	0.02	0.08
EHMS 37	0.31	0.33	0.04	0.67
Mean	0.22	0.25	0.05	0.34
SE	0.05	0.05	0.01	0.08

2.4.3 Population diversity

Genetic diversity, measured as expected heterozygosity, was highest in the EAC eddy population (H_e = 0.85, A = 14.8), Sandy Cape (H_e = 0.82, A = 15.8) and Maatsuyker Island (H_e = 0.80, A = 15.0) and lowest in the Southern Ocean B/C population (H_e = 0.68, A = 5.9) (Table 2.6). Population samples from Cape Jaffa, Discovery Bay and Sandy Cape, west of Tasmania, all showed high allelic richness (R_t) with low expected heterozygosity (Table 2.6) while those populations east of Tasmania, Trumpeter Bay and Bicheno had the lowest R_t.

Table 2.6 Genetic diversity parameters for all populations of *Emiliania huxleyi*, calculated from eight microsatellite markers. N = the number of individuals in each population, n = average number of individuals analysed per marker per population, A = observed number of alleles per marker per population, H_e = expected heterzygosity, H_o = observed heterozygosity, F = Wright's fixation index, Null = frequency of null alleles, averaged over populations and after inbreeding has been accounted for (Chybicki and Burczyk 2009). F_{IS} (INEst) = inbreeding co-efficient after null alleles have been accounted for; R_t = allelic richness.

Population	N	n	A	H_o	H_e	F	Null	F_{IS}	R_t
Bicheno	35	34.5	10.6	0.72	0.75	0.05	0.04	0	0.68
Trumpeter Bay	41	38.4	12.5	0.69	0.79	0.14	0.07	0	0.74
EAC eddy	26	24.0	14.8	0.62	0.85	0.27	0.12	0	0.81
Cape Jaffa	28	24.3	11.1	0.56	0.74	0.25	0.05	0.13	1.00
Discovery Bay	32	30.0	12.8	0.56	0.78	0.29	0.12	0.04	0.84
Sandy Cape	46	42.9	15.8	0.67	0.82	0.18	0.09	0.01	0.88
Maatsuyker Is	44	39.1	15.0	0.59	0.80	0.24	0.02	0.30	0.80
Sthn Ocean A	12	11.1	8.4	0.68	0.77	0.11	0.06	0	0.75
Sthn Ocean B/C	9	7.1	5.9	0.53	0.68	0.18	0.14	0	-
MEAN		27.9	11.9	0.62	0.78	0.19	0.08		

Southern Ocean B/C population was excluded from the allelic richness analysis due to low sample size. High F values were evident in Discovery Bay, EAC eddy, Cape Jaffa and Maatsuyker Is due to the presence of null alleles in the former two populations and inbreeding in the latter two populations (Table 2.6). Southern Ocean B/C population had a moderately high F value due to the presence of null alleles.

The most northern populations, Cape Jaffa and Discovery Bay and the two Southern Ocean populations, all with an H_e lower than the mean, showed a higher level of allelic fixation than

eastern and western Tasmanian populations as measured by the proportion of markers with an allele frequency greater than 0.5 (Fig. 2.5).

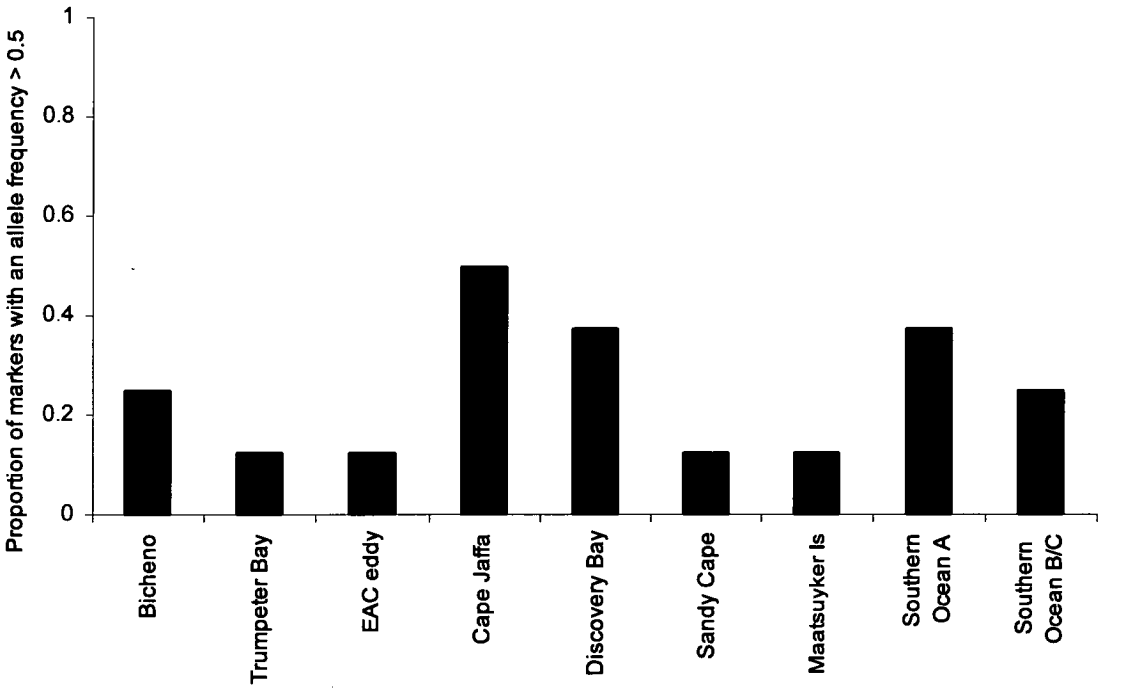

Fig. 2.5. Proportion of markers with an allele at a frequency greater than 0.5 ($L_{0.5}$) in each population

In eastern Tasmanian populations H_e and R_t increased with latitude until reaching the Southern Ocean where H_e decreased, whilst allelic fixation followed the opposite pattern, being higher in more northern populations, decreasing with latitude and increasing again in Southern Ocean populations (Table 2.6; Fig. 2.5). In western populations H_e increased whilst R_t and allelic fixation decreased until reaching the Southern Ocean populations. A pattern of increasing allelic fixation and decreasing H_e was evident in Southern Ocean populations. The Southern Ocean B/C population was unable to be analysed for allelic richness due to the small sample size.

2.4.4 *Population and morphotype differentiation*

Allele frequency varied considerable among populations (Table 2.7) with the Type B/C showing a marked difference from other populations. For example, allele 177 at P02E10 with an overall frequency of 0.20 had a higher frequency at Bicheno (0.32) Cape Jaffa (0.23) and Sandy Cape (0.24) but was completely absent from the Southern Ocean type B/C. Similar occurrences of alleles being absent in the B/C population occurred in markers P02E11, P01E05 and EHMS37. In contrast the frequency of allele 99 at P02E09 in Southern Ocean B/C (0.72) was much greater than the overall frequency of 0.210, whilst type A populations hovered around the mean (0.13-0.23). A similar situation occurred with allele 205 at P02B12 and 156 at P01F08 (Table 2.7). The complete list of allele frequencies is in the Appendix.

Table 2.7. Examples of the variation in allele frequencies among populations

Marker	P02F11	P02E11	P01F08	P02E09	P02B12	P01E05	P02E10	EHMS37
Allele	99	201	156	99	205	150	177	272
Bicheno	0.29	0.47	0.24	0.21	0.26	0.11	0.32	0.06
Trumpeter Bay	0.28	0.36	0.14	0.13	0.22	0.09	0.20	0.13
EAC eddy	0.10	0.13	0.06	0.21	0.08	0.06	0.14	0.08
Cape Jaffa	0.59	0.07	0.09	0.22	0.22	0.04	0.23	0.02
Discovery Bay	0.06	0.16	0.00	0.19	0.11	0.02	0.11	0.00
Sandy Cape	0.06	0.10	0.00	0.18	0.07	0.00	0.24	0.05
Maatsuyker Is	0.30	0.26	0.01	0.21	0.14	0.04	0.20	0.07
Southern Ocean Type A	0.25	0.20	0.00	0.23	0.05	0.05	0.17	0.04
Southern Ocean Type B/C	0.20	0.00	0.39	0.72	0.33	0.00	0.00	0.00

Mean F_{ST} across all markers was = 0.05 and D_{est} = 0.34 (Table 2.5). Pairwise F_{ST} values revealed that the Southern Ocean type A population was the least differentiated with two non-significant comparisons. Maatsuyker Is. population was also low when compared to other western populations (Table 2.8). Comparison between Southern Ocean type A population and Sandy Cape had the lowest non-significant pairwise F_{ST} (F_{ST} = 0.014) of the

western populations whereas Trumpeter Bay and Bicheno had the lowest pairwise F_{ST} of the eastern populations and the lowest genetic distance (0.83). Greatest differentiation was found in the Southern Ocean B/C population in both F_{ST} and genetic distance. The ranking of F_{ST} values for Southern Ocean B/C followed the increase in latitude of the populations, i.e. being most differentiated from Cape Jaffa, and least differentiated from the EAC eddy. D_{est} pairwise comparisons were in close agreement with F_{ST} comparisons (not shown).

Table 2.8. Pairwise F_{ST} values between populations (below diagonal) and Nei's (1978) genetic distance (above diagonal)among populations of *Emiliania huxleyi*. Significant differences of F_{ST} from zero were tested using Bonferroni correction and using P, 0.001. F_{ST} values in italics were not significant. Permutations = 1000.

	Bicheno	Trump. Bay	EAC eddy	Cape Jaffa	Discovery Bay	Sandy Cape	Maatsuy. Is.	Sth Ocean Type A	Sth Ocean Type B/C
Bicheno		0.083	0.341	0.387	0.457	0.413	0.244	0.427	0.716
Trumpeter Bay	*0.013*		0.254	0.304	0.383	0.291	0.130	0.334	0.724
EAC eddy	0.060	0.037		0.458	0.299	0.199	0.167	0.289	0.632
Cape Jaffa	0.088	0.061	0.057		0.537	0.439	0.192	0.455	0.721
Discovery Bay	0.082	0.057	0.042	0.089		0.151	0.230	0.231	0.788
Sandy Cape	0.074	0.043	0.021	0.067	0.023		0.135	0.186	0.771
Maatsuyker Is	0.053	0.026	0.020	0.034	0.038	0.014		0.233	0.690
Sth Ocean Type A	0.071	0.042	0.030	0.070	*0.026*	*0.014*	0.026		0.733
Sth Ocean Type B/C	0.163	0.143	0.124	0.164	0.157	0.136	0.140	0.135	

2.4.5 Genetic affinities among populations

All morphotype A populations clustered separately from the Southern Ocean type B/C population in the PCA analysis of axis one and two (Fig. 2.6A). Axis one and two showed the two most north- eastern populations (Bicheno and Trumpeter Bay) forming a unique cluster with Cape Jaffa, however, axis one and three clearly separate Cape Jaffa from the eastern populations. The east-west-south geographical clusters are clearer in Fig. 2.6B. Cape Jaffa on the South Australian coast stood alone as did Southern Ocean B/C.

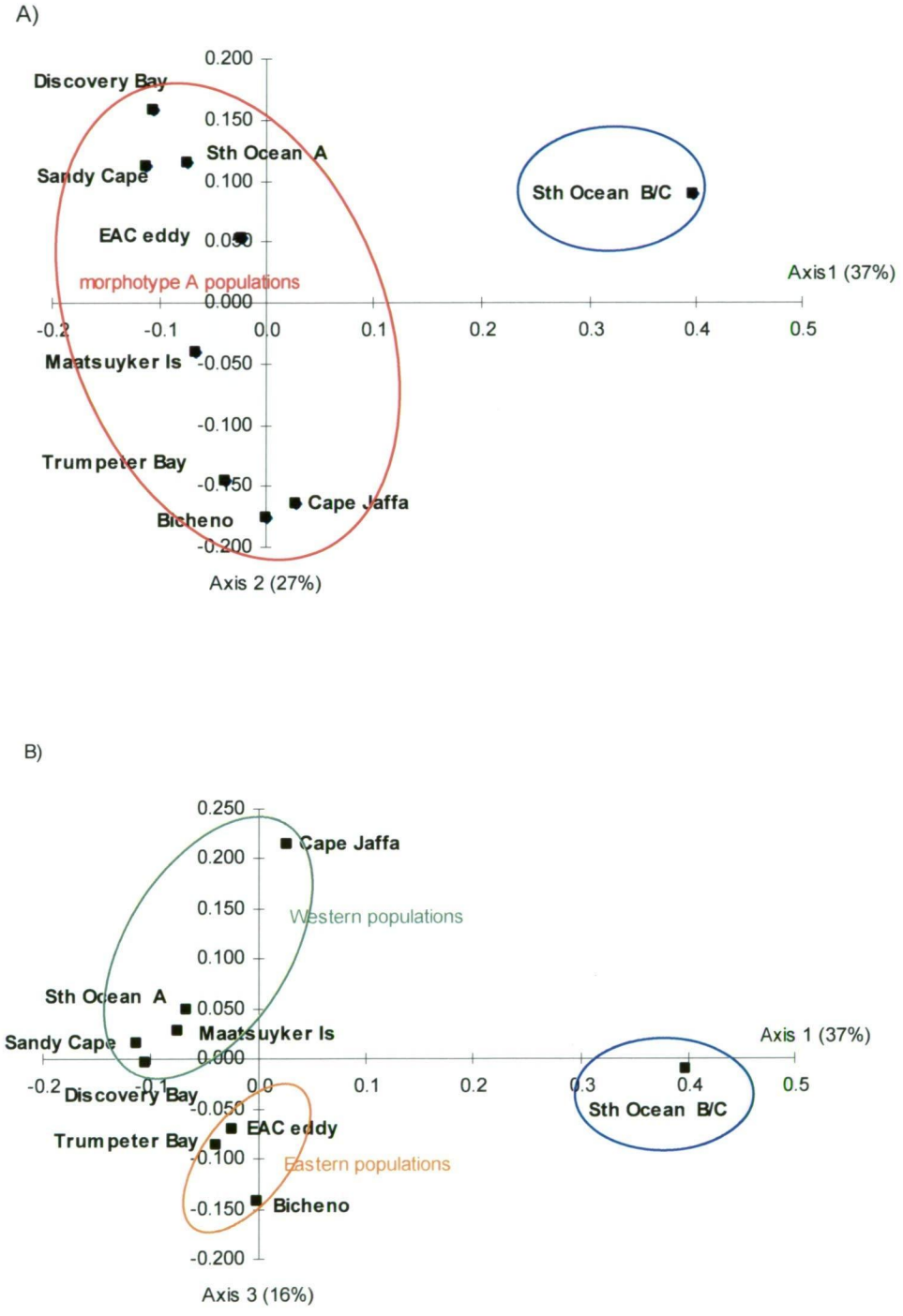

Fig. 2.6. Two dimensional PCAs of Nei's genetic distances between populations, A) axis 1 and 2, and B) axis 1 and 3.

2.4.5.1 Population structure analysis

In examining population structure with no priori subdivisions within the strain collection the Δ K method of Evanno *et al.* (2005) indicated either 3 or 6 genetic population groups (Fig. 2.7). Results of the STRUCTURE analysis of the data set with the number of groupings (K) varying from two to six are presented in Fig 2.8.

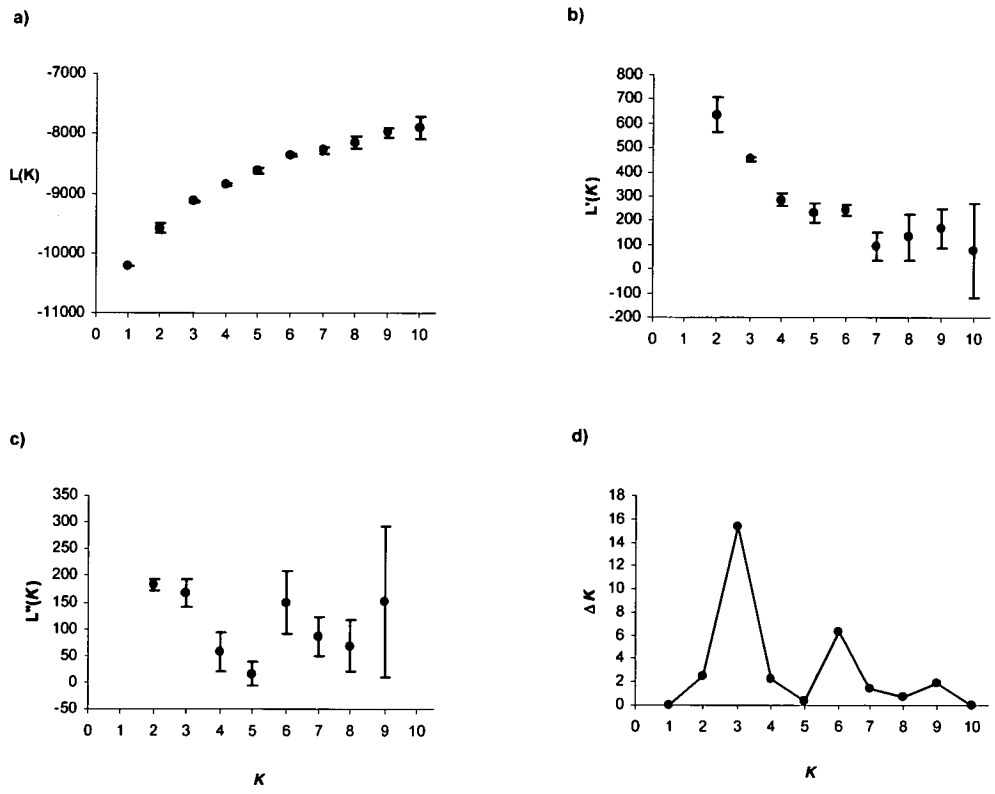

Fig. 2.7. The four steps used for the calculation of Δ *K* for 273 strains of *Emiliania huxleyi* from 9 populations following the calculations of Evanno *et al.* (2005). A) Mean *L(K)* (± SD) over the three highest likelihood runs. B) Mean rate of change of the likelihood distribution *L'(K)* (± SD). C) Mean absolute values of the second order rate of change of the likelihood distribution *L"(K)* (± SD). D) Δ *K* calculated as the mean in c) divided by the SD in a). The modal value indicates the "true" *K*, or number of clusters; in this case *K* = 3.

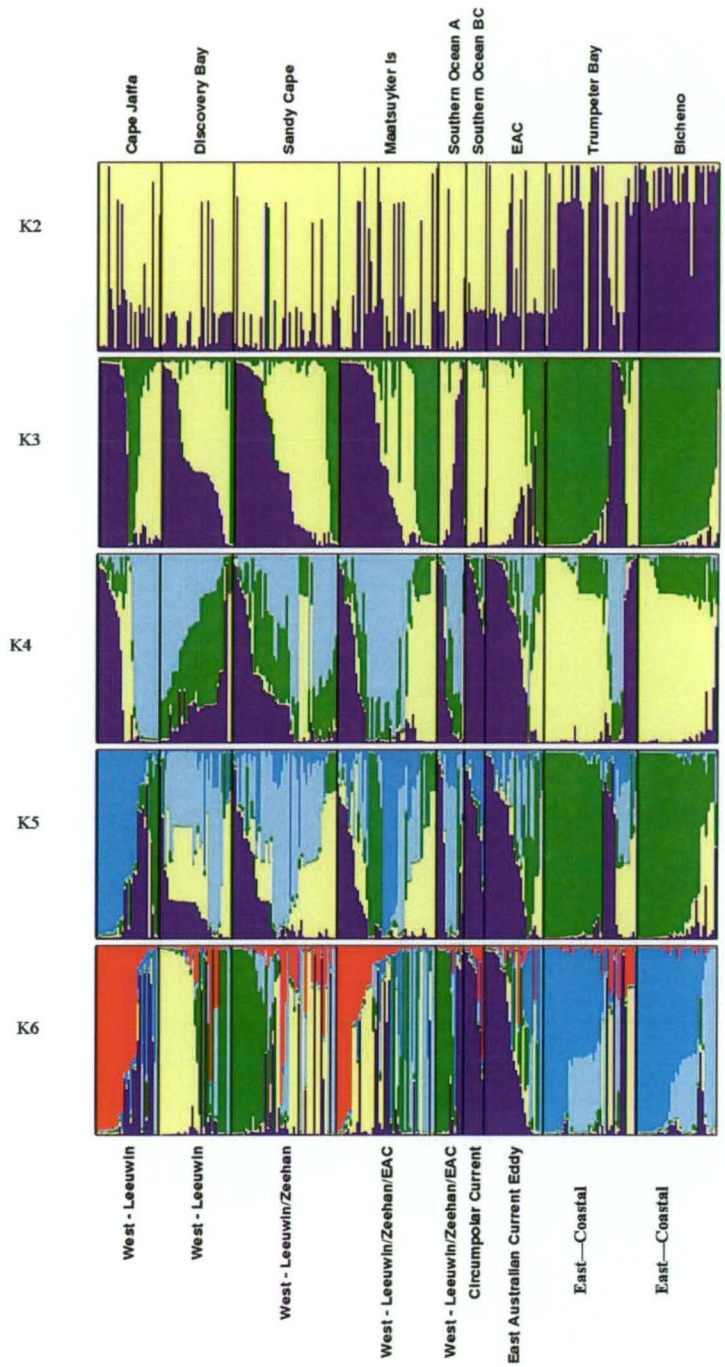

Fig. 2.8. Proportion of membership of all strains of *Emiliania huxleyi*. Each strain is represented by a thin vertical line partitioned into K coloured segments representing the strain's estimated membership into the K genetic clusters. Individuals are grouped by population (indicated above the figure) and the ocean system of origin shown below.

Considerable admixture is apparent at all values of K. When K = 2 the east-west division is apparent, although not strong. When K=3 the division appears stronger. Table 2.9 shows the proportional affinity (Q values) of each population to each of the K = 3 clusters. Cluster 1 comprised western populations and a high proportion of the Southern Ocean type A population. Cluster 2 comprised the eastern populations and cluster 3 the Southern Ocean populations. Although Discovery Bay and Sandy Cape contributed a major proportion to cluster 3 they had almost identical contributions in cluster 1. The EAC eddy falls into cluster 3. The Southern Ocean B/C population is almost exclusively cluster 3.

Table 2.9. Average Q value for each population of *Emiliania huxleyi* in each of the K = 3 clusters inferred by STRUCTURE.

	Cluster		
	1	2	3
Bicheno	0.022	0.909	0.068
Trumpeter Bay	0.174	0.650	0.176
EAC eddy	0.144	0.237	0.619
Cape Jaffa	0.452	0.201	0.347
Discovery Bay	0.454	0.090	0.457
Sandy Cape	0.424	0.136	0.440
Maatsuker Is	0.454	0.290	0.256
Southern Ocean type A	0.380	0.101	0.519
Southern Ocean type B/C	0.063	0.045	0.892

When K = 6 the evidence for the east-west-southern groupings became clearer but with populations still consisting of admixed individuals throughout. It is important to note that the small population sizes of the Southern Ocean groups may have been swamped by the much larger type A populations. To illustrate the extent to which individuals were assigned to the appropriate cluster the Q value (admixture proportions) at K = 6 are given in Table 2.10. It can be seen from the proportions that cluster 3 had only weak membership in comparison to other clusters, the strongest being cluster 5 with the Southern Ocean B/C as its

major member. The Maatsuyker Is. population showed the highest degree of admixture with small contributions to each of the STRUCTURE defined clusters.

The western populations are spread between 3 clusters (1, Sandy Cape and Southern Ocean type A; 4, Discovery Bay & 6, Cape Jaffa and Maatsuyker Is). In addition to its high Q value in cluster 4, Discovery Bay showed an affinity for cluster 1 situating itself alongside Sandy Cape and Southern Ocean type A as the highest contributors. As was the case when K= 3, Bicheno and Trumpeter Bay form a fairly unique cluster by themselves and again, the majority of Southern ocean B/C genotypes fall strongly into one cluster.

Table 2.10. Average Q value for each population of *Emiliania huxleyi* in each of the K = 6 clusters inferred by STRUCTURE.

Population	Cluster 1	2	3	4	5	6
Bicheno	0.015	0.647	0.266	0.018	0.042	0.012
Trumpeter Bay	0.019	0.468	0.193	0.105	0.164	0.052
Cape Jaffa	0.015	0.114	0.073	0.021	0.222	0.557
Maatsuker Is	0.116	0.116	0.196	0.211	0.135	0.227
Discovery Bay	0.246	0.016	0.118	0.475	0.077	0.069
Sandy Cape	0.314	0.016	0.177	0.247	0.140	0.105
Southern Ocean type A	0.561	0.094	0.038	0.023	0.261	0.024
EAC eddy	0.109	0.157	0.089	0.101	0.496	0.047
Southern Ocean type B/C	0.013	0.056	0.019	0.013	0.773	0.126

2.4.5.2 Assignment analysis

Using an assignment routine in GeneClass2, each strain was assigned to the population in which its expected genotype frequency had the highest likelihood of belonging (greatest probability of occurrence) (Fig. 2.9).

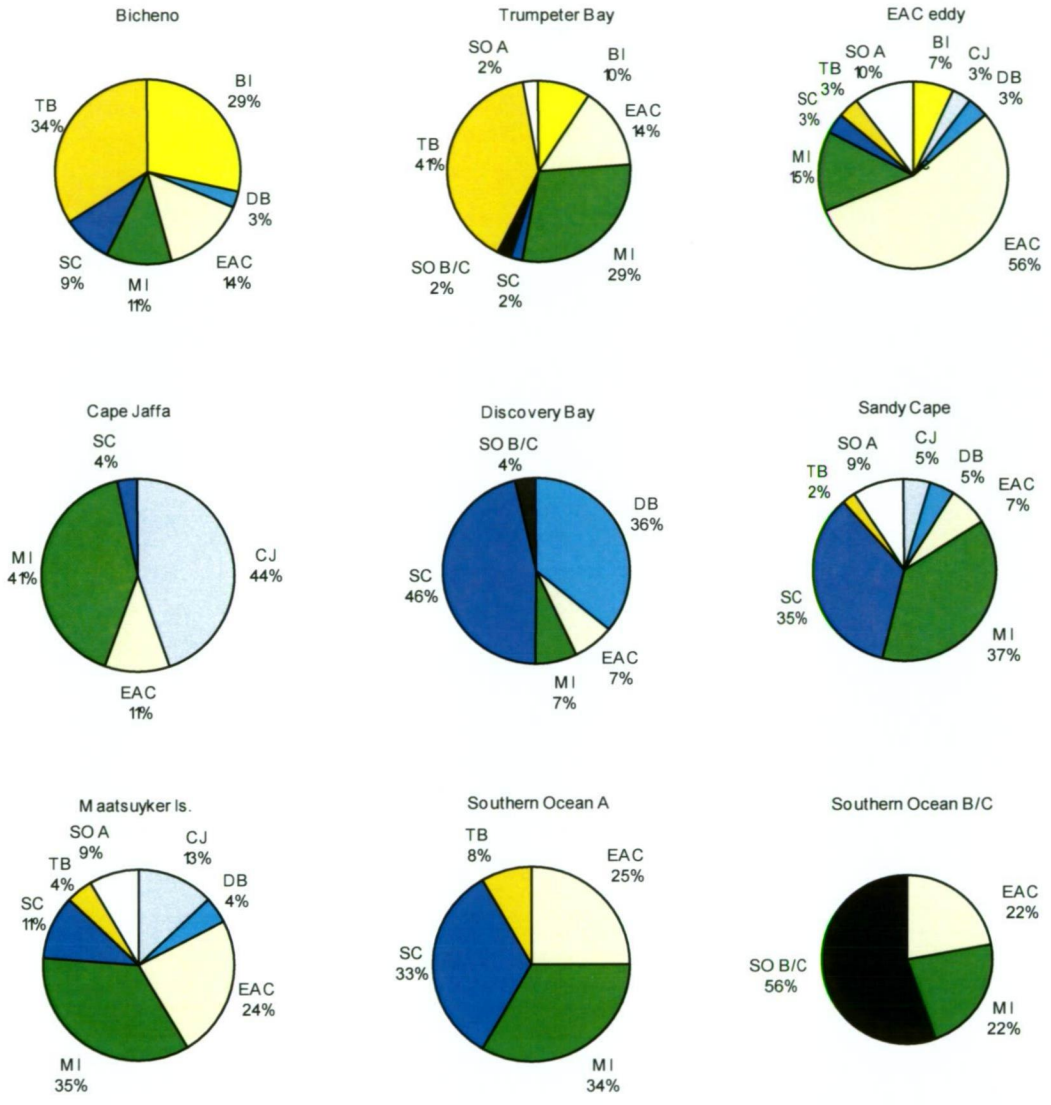

Fig. 2.9. Assignment of strains to the population in which its expected genotype frequency was the highest using the criterion of Rannala & Mountain (1997) and simulation algorithm of Paetkau *et al.* (2004) using 10 000 simulations.

Admixture was evident in the assignment analysis as it was in the STRUCTURE 2.2.3 analysis. However again there was separation between east and west groupings and the Southern Ocean B/C being distinct from other populations.

A further analysis of the likelihood of populations grouped into east, west and southern regions consisting of either morphotype A or B/C corresponded well with their morphological identification (Fig. 2.10). East, west and southern type A groups overlap but still the majority fall into the portion of the graph that indicates a greater likelihood of belonging to the morphotype A group. Some strains fall into the type B/C sector however this does not necessarily mean they have a type B/C genotype; it may be influenced by the presence of null alleles or missing data. All the type B/C strains showed a greater likelihood of being in their own population group rather than to the type A groups.

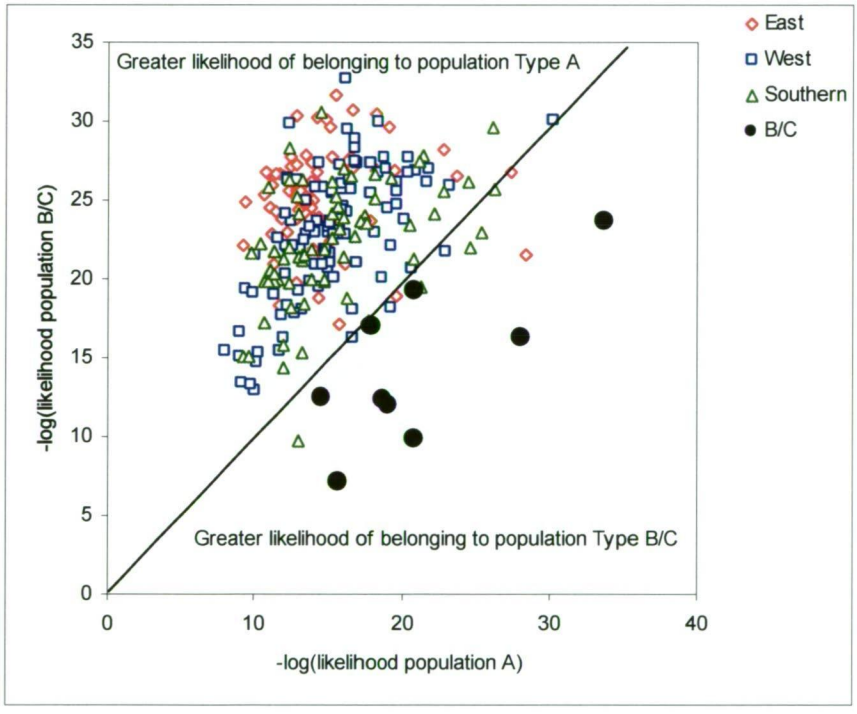

Fig. 2.10. Genetic likelihood of belonging to either morphotype A or morphotype B/C based on allele frequencies. The line terminating at the origin indicates the location where the genetic likelihoods of belonging to either morphotype A or B/C are equal. The area above the line indicates a greater likelihood of belonging to morphotype A and the area below the line indicates a greater likelihood of belonging to morphotype B/C.

2.5 Discussion

2.5.1 Molecular variation and diversity

Two of the original 10 markers produced a high degree of PCR failure with the original complete sample set of 423 strains. Further in the case of the Southern Ocean type B/C population, a high level of PCR failure was evident in 5 of the 10 markers resulting in a major reduction in sample size from 55 to nine strains. This failure rate is most likely due to mutations in flanking sequences that prevented amplification (Halliburton 2004). Four of the same *E. huxleyi* markers were used in a cross-amplification study with the closely related haptophyte *Gephyrocapsa oceanica* and distantly related *Coccolithus pelagicus,* (Iglesias-Rodriguez *et al.* 2006a). Amplification success in morphotype B/C strains in the present study was between 25 and 57% lower in 3 of the 4 markers reported for these two related species. Nevertheless the results presented here provide an extensive analysis of microsatellite markers for the 9 populations of *E. huxleyi* and indicate that, overall, genetic differentiation exists among sampled populations of morphotype A, despite the presence of null alleles and admixture. Furthermore the results unambiguously show that morphotype B/C is genetically differentiated from type A.

A total of 250 alleles were recorded from 273 *E. huxleyi* strains across the eight microsatellite markers, an average of 31.3 per locus. From the same markers, Iglesias-Rodriguez *et al.* (2006b) found an average of 14.5 alleles per marker from 87 strains of *E. huxleyi* only 4 of which originated in the Southern Hemisphere. The difference in allele detection is likely due to sample size as the range size of alleles increased between 1.5 and 5 times, depending on the marker. The degree of success in PCR amplification was similar between the present study and that of Iglesias-Rodriguez *et al.* (2006b), 61% of their strains amplified at 6 or more markers compared to 65% of the original 423 strains here. In the present study, despite due care in peak scoring, stuttering was a common problem, therefore samples were repeated where appropriate to confirm allele sizes. Iglesias-Rodriguez *et al.* (2006b) developed the primers used in the present study for a Nowegian Fjord strain of *E. huxleyi* B92 - 11, which itself failed to generate detectable alleles for markers P02A08 (a marker excluded from the present study) and P01E05. In that study marker P01E05 also

failed to amplify in any of their Southern Hemisphere strains however in the present study the amplification success of P01E05 was one of the highest in all Southern Hemisphere type A strains. Nevertheless both the present study and that of Iglesias-Rodriguez *et al.* (2006b) experienced high probability of null alleles. This was particularly prevalent in type B/C strains where only 9 of the original 55 strains produced PCR product for at least 6 markers. Considering the origin of the primers it is not surprising that the microsatellite markers proved more successful in type A strains than in the type B/C strains.

Levels of diversity (H_e, H_o and F_{IS}) estimated here across markers were comparable to previously reported measures in *E. huxleyi* for the same markers (Iglesias-Rodriguez *et al.* 2002; Iglesias-Rodriguez *et al.* 2006b). Despite the present study tripling the number of strains used, the overall similar levels of heterozygote deficiency apparent in both studies suggests this is a consistent representation for *E. huxleyi* populations. Other plankton species also show heterozygote deficiency, for example in the diatom *Ditylum brightwellii*, (Rynearson and Armbrust 2005) and *Pseudo-nitzschia pungens* (Evans *et al.* 2004) and the dinoflagellate *Alexandrium catenella* (Masseret *et al.* 2009).

Heterozygote deficiency can be attributed to a number of factors (Pemberton *et al.* 1995; Lowe *et al.* 2004; van Oosterhout *et al.* 2006), a Wahlund effect, where undetected population sub-structure leads to a deficiency of heterozygotes (Halliburton 2004), non-random mating caused by factors such as binary cell division, which is common among algal species, the presence of null alleles or inbreeding. Inbreeding (selfing or mating between relatives) may be a likely contributing factor although there is considerable evidence to suggest that sexual reproduction does occur, even in blooms (Rynearson and Armbrust 2005; Iglesias-Rodriguez *et al.* 2006b). Heterozygote deficiency is often seen in the presence of null alleles, arising either from non-amplification due to mutations in the priming sites or undetected PCR failure (Callen *et al.* 1993; Halliburton 2004; Chapuis and Estoup 2007; Carlsson 2008). .

None of the populations or strains were identical. In the present study, because Wright's Fixation index (F) was positive in all populations indicating the presence of inbreeding or

null alleles, a new software programme "INEst" was used to partition the traditional results into null alleles and inbreeding (Chybicki and Burczyk 2009). The results obtained enabled the determination of which populations are more affected by inbreeding after removing the effect of null alleles that lead to an underestimation of observed heterozygosity (Chybicki and Burczyk 2009). Null alleles were frequent in two markers in particular but present in all populations. However, after accounting for null alleles the four western populations (Cape Jaffa, Discovery Bay, Sandy Cape and Maatsuyker Is.) still produced positive F_{IS} (inbreeding coefficient) values. This is most likely due to the Wahlund effect (undetected population subdivision) as the Bayesian analysis found that the populations with the highest F_{IS} were also most likely to be admixed populations.

2.5.2 Population differentiation

Allelic frequencies differed markedly between populations of the two morphotypes. Where a particular allele was of high frequency in the type B/C population, it was more often of low frequency in type A populations. Furthermore, when an allele frequency was high in eastern populations it was frequently low in western populations and/or absent in the B/C population. These patterns of allele frequency indicate differentiation between western, eastern and southern populations through factors such as genetic drift where populations become subdivided into fragments, decrease in heterozygosity and thus of genetic diversity (Lowe *et al.* 2004), particularly evident in the type B/C population.

According to Wright (1978) F_{ST} values range between 0 (lack of genetic differentiation between populations) and 1 (complete isolation) with values of 0 - 0.05 implying little genetic differentiation, 0.05-0.15 moderate genetic differentiation, 0.15 - 0.25 great genetic differentiation and > 0.25 very great genetic differentiation. The global F_{ST} value for the 9 populations was low (F_{ST} = 0.05) and was considerably lower than the global F_{ST} = 0.10 reported by Iglesias-Rodriguez *et al.* (2006b) although that study covered populations from a much greater geographic range than the present study. It should be noted however that Iglesias-Rodriguez *et al.* (2006b) indicated null alleles were responsible for the poor amplification results and therefore as indicated F_{ST} values may have been overestimated.

Pairwise tests of genetic differentiation between populations were mostly low but still highly significant. The Southern Ocean type B/C F_{ST} values in comparison to all other populations were in the moderate to high category of genetic differentiation (0.12-0.16) in conjunction with almost twice the genetic distance between it and all other populations. The F_{ST} value reported for populations of the diatom *Pseudo-nitzschia pungens* sampled from two locations 100 km apart along the German coast in the North Sea, was much lower at 0.0016 (Evans *et al.* 2005) and the same was also found between populations of the same diatom along the Belgian coast F_{ST} = 0.0038 (Casteleyn *et al.* 2009). In contrast, F_{ST} for the diatom *Ditylum brightwellii*, in Puget Sound, was 0.245 (Rynearson and Armbrust 2004). F_{ST} between Japanese and French populations of the dinoflagellate *Alexandrium catenella* ranged between 0.15 and 0.29 (Masseret *et al.* 2009). Microsatellite DNA markers have identified significant but low levels of genetic structuring between New Zealand and Australian populations of cephalopods with F_{ST} values between 0.03-0.04 (Doubleday *et al.* 2009) and between populations of the sea urchin *Centrostephanus rodgersii* separated by 1000's of kilometers in Australian waters with F_{ST} values between 0.02-0.11 (Banks *et al.* 2007).

The genetic variability and population differentiation is markedly different between microalgal species despite often being considered cosmopolitan species (Medlin *et al.* 2000; Iglesias-Rodríguez *et al.* 2002). In the present study the type A populations pairwise F_{ST} values were lower between neighbouring populations such as between Bicheno and Trumpeter Bay (East) Sandy Cape and Maatsuyker Is or Discovery Bay (west) indicating a greater degree of gene flow between neighbouring populations than between those originating from different ocean currents or separated by the Tasmanian land mass. The most highly and significantly differentiated populations were the Southern Ocean type B/C and the most northerly, the Cape Jaffa population. Both populations are most likely influenced by significantly different origins of the ocean currents from which they were sampled; Cape Jaffa by the Leeuwin Current originating off the west coast of northern Australian and the type B/C population by the Antarctic Circumpolar Current. Ocean currents have previously been associated with the distribution of *E. huxleyi* types A, B, C and B/C-2 off the coast of Japan (Hagino *et al.* 2005).

Using F_{ST} and its relatives (G_{ST}) as a measure of differentiation has been challenged by Jost (2008) considers them to be defective measures of differentiation as they are affected by levels of genetic diversity within populations as well as the presence of null alleles. Jost (2008) claimed that traditional measures of differentiation do not rank populations correctly. Such discrepancies between F_{ST} type statistics and the true levels of differentiation could create confusion and provide false comparisons between studies as they are commonly used to draw conclusions about levels of gene flow and examine relationships between populations. Hence Jost (2008) proposed a new measure of differentiation (D) to allow mathematically more accurate comparisons. Whilst F_{ST} (or G_{ST}) is still useful in some circumstance such as estimating migration rates (Ryman and Leimar 2009) others have shown that these statistics have led to under estimations of differentiation (Heller and Siegismund 2009). Heller & Siegismund (2009) consider that discrepancies are highest in situations where high levels of within-population diversity exist as is the case in the present study of *E. huxleyi* and recommend using D. Despite some small differences the overall result is similar regardless of which statistic was used. As the use of D is only recent there are as yet no studies of microalgae that report this statistic.

The PCA grouped eastern populations together and western populations in a separate cluster and delineates the two morphotypes quite clearly closely associated with the ocean currents from which the cells originated. Interestingly the EAC eddy population showed closer genetic affinities with the two southern populations at Maatsuyker Is and Southern Ocean Type A. This was probably not surprising as this eddy, at the time of sampling, was located off the SE corner of Tasmania within close proximity to those aforementioned populations providing a distinct possibility of a mixture of type A cell genotypes. The assignment analysis showed that the Southern Ocean A population is primarily an artificial population with all its members drawn from other populations.

High levels of admixture were also evident from the STRUCTURE analysis. Considering that *E. huxleyi* is at the vagaries of ocean mixing and prevailing currents and has no known capacity to determine its geographic location it is not altogether surprising that populations

would consist of highly admixed genotypes. Admixture between populations maybe a reason for the relatively low F_{ST} found in this study.

2.5.3 Genetic differentiation between morphotypes

Significant but generally low levels of genetic differentiation among type A populations together with moderately high levels of genetic diversity within populations suggest that there are no major barriers other than land masses and entrainment in ocean currents, to gene flow between type A populations. Structuring of populations and differentiation among populations of type A appears to be associated with ocean currents. However, there appears to be a stronger restriction of gene flow between type A populations and the type B/C population. It is not known if there is any form of reproductive barrier to the forming of crosses between type A and type B/C cells. The genetic diversity reported for *E. huxleyi* indicates that sexual reproduction must be dominant in the lifecycle of this algal species (Paasche 2001). Furthermore both morphotypes are known to inhabit the same region of water forming a mixed population of morphotypes (Findlay and Giraudeau 2000; Cubillos *et al.* 2007). From SEM and mixed culture observations there appears to be no "mixed" morphotype that might represent a cross between A and B/C (unpublished obs.).

E. huxleyi diverged from its closest relative *Gephyrocapsa* sp. merely 268,000 ya and only became prominent in the geological record about 73,000-85,000 ya (Thierstein *et al.* 1977) therefore type B/C population with its lower diversity but higher degree of differentiation from type A populations suggests that this population may be in the process of diverging from the type A populations.

However, the data presented here should be interpreted with some caution. Amplification rate in the Southern Ocean B/C population was merely 15%, resulting in a usable population of only 9 strains that still failed to amplify at all 8 markers (except 1 strain). Therefore developing markers specific for Southern Ocean B/C strains and Southern Hemisphere type A strains could prove advantageous to investigate differentiation of the B/C morphotype in more depth.

2.6 Conclusions

The results of this study show that *E. huxleyi* exhibits low genetic diversity but strong differentiation between the two most geographically separated populations, Cape Jaffa and the Southern Ocean B/C, potentially due to the environmental gradient that exists between the two populations and the origin of ocean currents. Furthermore there is evidence of differentiation among all sampled populations of *E. huxleyi* morphotype A despite considerable admixture. This argues that gene flow between populations is not sufficient to prevent differentiation. There are a number of factors that may contribute to differentiation such as adaptation to environmental conditions and genetic drift. However the origin and isolating capacity of ocean currents, oceanographic fronts, and separation by land masses restricting the larger scale mixing of local populations are the common features of the populations studied and therefore likely to be major factors in genetic differentiation. Similar conclusions have been drawn to explain the genetic differentiation found in invertebrates with planktonic larvae (Lind *et al.* 2007; Thornhill *et al.* 2008), krill (Patarnello *et al.* 1996) and the diatom *Ditylum brightwelli* (Rynearson and Armbrust 2004). The apparent genetic separation between populations west and east of Tasmania although far from absolute, further supports a biogeographical barrier to gene flow, promoting the development of differentiation.

Importantly, the low PCR amplification success with many of the microsatellite markers in type B/C and the existence of a moderately high degree of genetic differentiation between the B/C population and all others, suggests that the Antarctic Polar Front and Antarctic Circumpolar Current act as open-ocean barriers to gene flow (Clarke *et al.* 2005) allowing divergence from the type A and perhaps, even a reproductive barrier. The opportunity for divergence in marine species has been reviewed in some detail (Palumbi 1994; Knowlton 2000; Medlin *et al.* 2000; Doney *et al.* 2004; Weisse 2008) and a number of studies have investigated the role of Antarctic ocean currents and Polar Fronts as barriers or otherwise to gene flow (Medlin *et al.* 1994b; Patarnello *et al.* 1996; Page and Linse 2002; Thornhill *et al.* 2008). The timing of a large phylogenetic divergence between Antarctic krill and sub-Antarctic species was attributed to the formation of Antarctic Polar Front by Patarnello *et al.*

(1996), whereas Clarke *et al.* (2005) and Norris (2000) suggest that many species are limited by their ability to maintain viable populations rather than by any inability to disperse past hydrographic barriers to gene flow.

More investigation is required into life cycle and reproductive habits and processes in both morphotypes of *E. huxleyi* as to date very little is known (Paasche 2001). The level of differentiation presented here support the existence of some form of barrier, be it reproductive, environmental or biogeographical. It is unlikely, however, that it is purely geographical as both morphotypes are known to be found in a mixed population just north of the Polar Front (this study and Cubillos *et al.* 2007). Clarke *et al.* 2005 suggest that the Southern Ocean may receive many more potential colonists from warmer northern regions than actually become established due to the difficulty in managing the rapid drop in temperature across the Polar Front. It appears that the sudden temperature drop has potentially limited the distribution of type A cells further poleward than the Antarctic Polar Front (Cubillos *et al.* 2007).

It is clear from the results presented here, evidence of considerable divergence and differentiation of *E. huxleyi* type B/C has occurred and that despite significant admixture among type A populations, genetic differentiation persists. Developing a set of microsatellite primers specific to the Southern Ocean type B/C would enable in-depth study of genetic differentiation and structure within this population.

3 Photosynthetic Pigment Profiles and Morphotaxonomy of *Emiliania huxleyi* morphotypes from the Southern Ocean

Submitted to Journal of Phycology as:

Ecophysiological differences between two Southern Ocean morphotypes of *Emiliania huxleyi* (Haptophyta): 1. Photosynthetic Pigment Profiles and Morphotaxonomy

Suellen S. Cook, Mark J. Hovenden,
School of Plant Science, University of Tasmania, Private Bag 55, Hobart, Tasmania 7001, Australia

Simon W Wright,
Australian Antarctic Division and Antarctic Climate and Ecosystems CRC, Kingston, Tasmania 7050, Australia

and Gustaaf M. Hallegraeff
Institute of Marine and Antarctic Studies, University of Tasmania, Private Bag 55, Hobart, Tasmania

Author for correspondence: email sscook@utas.edu.au

3.1 Abstract

The widespread coccolithophorid *Emiliania huxleyi* (Lohm.) Hay & Mohler, plays a pivotal role in the global carbon pump, and has long been known to exhibit significant morphological, genetic and physiological diversity. In this study we compared photosynthetic pigments and morphology of triplicate strains of morphotypes A and B/C from the Southern Ocean, grown in nutrient replete, semi-continuous batch culture. The two morphotypes differed in the width of coccolith distal shield elements (0.11 – 0.24 μm type A; 0.06 – 0.12 μm type B/C), morphology of the distal shield central area (grill of curved rods in type A ; thin plain plate in type B/C) and also showed significant differences in carotenoid composition despite possessing the same complement and relative proportions of chlorophylls. The mean Hex:Chl *a* ratio in type B/C was >1, whereas in type A the ratio was <1. The Hex:fucoxanthin ratio for type B/C was 11 x greater than in type A, and the proportion of fucoxanthin in type A was 8 x higher than in type B/C. The fucoxanthin derivative 4-keto-19′-hexanoyloxyfucoxanthin (4-keto-hex) was present in type A but undetected in 33 type B/C strains. We propose that the morphologically and physiologically distinct Southern Ocean morphotype B/C *sensu* Young *et al.* (2003) be recognized as *Emiliania huxleyi* var. *aurorae* var. nov. Cook et Hallegraeff.

3.2 Introduction

The traditional taxonomic interpretation of marine phytoplankton such as *Emiliania huxleyi* being cosmopolitan with a common gene pool has come into question in recent years (Iglesias-Rodriguez *et al.* 2006b; Medlin 2007). Medlin (2007) suggests that gene pools become fragmented and isolated as local populations adapt to their environment, where eventually morphological and physiological differentiation occurs. Identifying genetic diversity and gene flow between populations has now become possible using techniques such as microsatellite markers that help to determine population fragmentation and establish whether a common gene pool is shared at the local level (Rynearson and Armbrust 2004; Evans *et al.* 2005; Iglesias-Rodriguez *et al.* 2006b; Medlin 2007). When significant variability exists in a species it is important to differentiate morphotypes or ecotypes to prevent generalisation and extrapolation from the study of a limited number of strains or populations.

Identifying genetic diversity and physiological plasticity in phytoplankton species is particularly important when considering impacts of global climate change (Iglesias-Rodriguez *et al.* 2008; Beardall *et al.* 2009). The coccolithophorid *Emiliania huxleyi* forms large blooms in the world's oceans, contributing significantly to the global carbon pump to the sediments by producing and releasing calcium carbonate coccoliths (Balch *et al.* 1992; Beaufort *et al.* 2007). However there have been contradictory claims on how *E. huxleyi* will respond to ocean acidification (Riebesell *et al.* 2000; Iglesias-Rodriguez *et al.* 2008). It is probable that some of this variation arises from substantial differences in the physiology and ecology of the limited number of strains studied (Langer *et al.* 2009). Evaluation of ecophysiological responses to climate change must therefore take into consideration not only the environmental pressures but the genetic, morphological and physiological variability that exists within geographically widespread species.

Distinguishing morphotypes of the polymorphic coccolithophorid *E. huxleyi* has been a topic of investigation for decades. Much of the early work on *E. huxleyi* concerned the biology of cells, describing sessile, motile, and naked cells either with or without flagella (Paasche

2001) and a number of coccolith bearing morphotypes which Medlin *et al*.(1996) ultimately suggested should be recognised as separate varieties. This work was based on molecular DNA-based RAPD techniques which showed limited genetic separation between the type A and type B strains (Medlin *et al.* 1996). Further work has identified another 2 or 3 morphotypes (Okada and Honjo 1973; Findlay and Giraudeau 2000; Hagino *et al.* 2005). All five currently recognised *E. huxleyi* morphotypes are illustrated and described by Young *et al* (2003) (Table 3.1).

Table 3.1. Morphotaxonomy of four *Emiliania huxleyi* morphotypes.

Morphotype	Coccolith length (µm)	Distal shield elements	Element width (µm)	Central area	Geographic distribution
var. *huxleyi;* type A *sensu* Young & Westbroek 1991; Van Bleijswijk *et al.* 1991	(2.0) 2.5-3.5 (4.0) (Medlin *et al.* 1996); 2.89-(3.68)-4.39 present work (n=153)	Moderately elevated	0.5-0.12 (Medlin *et al.* 1996); 0.11-(0.17)-0.24 present work	Grill of 20-23 curved rods	Ubiquitous; Dominant in Southern Australian coastal waters
var. *pujosae* (Verbeek) Young et Westbroek ex Medlin et Green 1996, p.29;type B *sensu* Young & Westbroek 1991; Van Bleijswijk *et al.* 1991	Large (3.4) 3.8-4.8 (5.0) µm	Elevated	Narrow, 0.05-0.08 µm	Lath like elements	North Sea; Van Bleijswijk *et al.* 1991, figs 2,4
var. kleijniae Young et Westbroek ex Medlin et Green 1996, p.29 ; type C *sensu* Young *et al.* 2003	Small, 2.5-3.5	?	Narrow, 0.07-0.09	Lath-like, often forming a complete plate	Indian Ocean (Young & Westbroek 1991); Atlantic Ocean (McIntyre and Be 1967, plate 6B)
var. *aurorae* Cook et Hallegraeff var. nov.; type B/C *sensu* Young *et al.*2003, Hagino *et al.* 2005; Cubillos *et al.*2007; type C *sensu* Findlay & Giraudeau 2000; type K Hiramatsu & De Deckker 1996.	Large 2.65-(3.65)-4.80 (n=144)	Moderately elevated	Narrow, 0.06-(0.09)-0.12	Thin plain plate, rarely with superimposed lath element: often absent in corroded specimens	Dominant in the Australian and Indian sectors of the Southern Ocean, south of 50° (Cubillos *et al.* 2007; Mohan *et al.* 2008; Winter *et al.* 1999); Kuroshio current off Japan (Hagino *et al.*2005); Namibia (J.Hendriks, pers.comm)

More recently the geographic distribution of these morphotypes has been investigated in an attempt to unravel the morphological and genetic variability within semi-discrete populations of the species (van Bleijswijk *et al.* 1991; Hagino *et al.* 2005). The type A morphotype is

globally widespread and the most prevalent bloom-forming morphotype (Paasche *et al.* 1996), while the type B is primarily found in the North Sea (van Bleijswijk *et al.* 1991) and the type B/C (referred to as type K by Hiramatsu & De Deckker 1996 and type C by Findlay and Giraudeau 2000) has thus far only been found in the Southern Ocean (Findlay and Giraudeau 2000; Cubillos *et al.* 2007), the Kuroshio Current, east of Japan (Findlay and Giraudeau 2000; Hagino *et al.* 2005) and off the coast of Namibia (J. Henderiks, pers.comm.).

Populations of *E. huxleyi* are widely distributed and exhibit a high degree of ecological, physiological and morphological plasticity (Paasche 2001). In-depth studies into the variability within this species are few and these have investigated only a limited number of strains, most commonly of type A (Brand 1982; Young and Westbroek 1991; Medlin *et al.* 1996). In the largest study undertaken so far, Iglesias-Rodriguez *et al.* (2006b) found considerable genetic variability (up to 89% unique genotypes) among 82, principally North Atlantic Ocean strains of *E. huxleyi* type A, one type B strain from the English Channel and four Southern Hemisphere type A strains; two from tropical Australia and one each from New Zealand and South Africa. Southern Hemisphere strains were recognised as being genetically distinct from the Northern Hemisphere strains. Schroeder *et al.* (2005) located a genetic marker that correlated significantly with the separation of seven strains of *E. huxleyi* type A from two strains of type B. However, most attempts to differentiate between the morphotypes have focused exclusively on morphological characterisation.

If, as argued by Medlin (2007) genetic differences are based on local adaptation then this should be reflected in functional ecophysiological differences. One such characteristic is the photosynthetic pigment profile. Pigment composition has been used extensively not only for photophysiological research, but also to identify chemotaxonomic groupings. Over the past 50 years or so considerable progress has been made to characterise the pigment content of the haptophyte algae as a means of identifying the taxonomic composition of mixed phytoplankton field samples from marker pigment signatures (Jeffrey and Allen 1964; Arpin *et al.* 1976; Garrido and Zapata 1998; Jeffrey and Vesk 2005). Following recent developments in HPLC methods, Zapata *et al* (2004) resolved a pigment signature from 11

strains of *E. huxleyi,* 7 type A strains from the Northern Hemisphere and 4 type A from the Southern Hemisphere.

Despite advances in the identification, characterisation and detection of pigments, pigment analysis alone has so far not been used to discriminate between *E. huxleyi* morphotypes. In this study, we test the hypothesis that Southern Ocean *E. huxleyi* populations have become physiologically fragmented into semi-discrete populations arising from some form of environmental barrier and reflected as morphotypes. This has been approached using pigment and morphometric analysis to determine if reliable differences exist between two morphotypes (A and B/C) isolated from the Southern Ocean. Such an examination should provide useful insights into whether the two morphotypes are physiologically and ecologically distinct.

3.3 Methods

3.3.1 Algal strains and culture conditions for pigment analysis.

For an analysis of chloroplast pigments, 3 strains of each morphotype were selected as a representative sample from a collection of over 400 strains of *E. huxleyi* established from samples taken in the Southern Ocean and the South Eastern Australia region, based on co-occurance of morphotypes at similar latitudes and being collected during the same season. Fig. 3.1 shows the geographic location and morphotype of each of the 6 strains used in this study. These strains have remained morphologically stable in culture at tempertures ranging between 4 and 20° C for over three years.

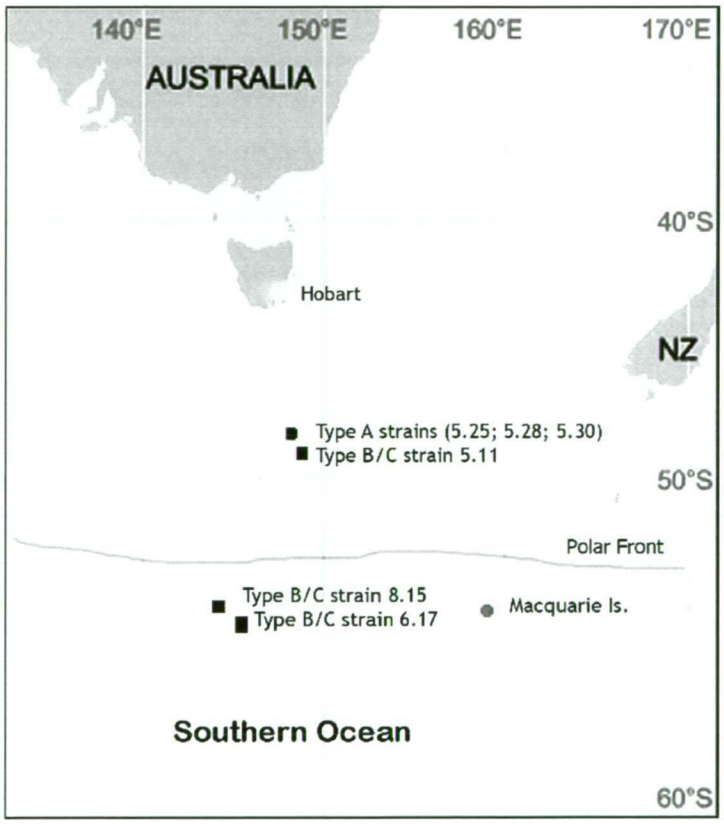

Fig. 3.1. Location map of origin of *Emiliania huxleyi* strains used in this study

Morphotypes were verified using scanning electron microscopy and published descriptions (Young *et al.* 2003). The 6 selected strains (Table 3.2) were batch cultured at 16° C in 300 mL Erhlenmeyer flasks with media using 0.2 μm - filtered natural seawater from east coast Tasmania with K medium nutrients, metals and vitamins added at recommended concentrations including a final concentration of 290 μM L^{-1} nitrate and 4 μM L^{-1} phosphate (Keller *et al.* 1987). A 12:12h L:D cycle was provided by Cool White fluorescent tubes (Sylvania 36W/w41) providing 70 μmol photons m^{-2} s^{-1}. Cultures were acclimatised for 28 d prior to the commencement of the experiments. Fresh cultures were inoculated from parental stock every 14 d. During the exponential growth phase average growth rates of 1.04 div d^{-1} for type A and 0.86 div d^{-1} for type B/C were calculated from cell counts. Prior to extraction of samples for pigment analysis semi-continuous growth conditions were initiated by removing and replacing 100 mL of homogenised media and cells on a regular basis to maintain cultures in exponential growth phase.

Table 3.2. Details of culture strains and field samples of *Emiliania huxleyi* used in this study

Culture Strain ID.	Morphotype	Location	Isolation Date	Isolator
EHSO 5.30	A	Southern Ocean		
EHSO 5.25	A	149.2500E:49.5900S	Feb 2007	S Cook
EHSO 5.28	A	(7 m depth)		
EHSO 5.11	B/C	Southern Ocean 149.2500E:49.5900S (7 m depth)	Feb 2007	S Cook
EHSO 6.17	B/C	Southern Ocean 146.1813E:54.0850S (65 m depth)	Feb 2007	S Cook
EHSO 8.15	B/C	Southern Ocean 145.5519E:53.5973S (80 m depth)	Feb 2007	S Cook
Field Samples		**Location**	**Collection Date**	
R0 05-06-8	B/C	144.1603E:55.88717E (3 m depth)	Oct 2005	
R0 05-06-4	B/C	144.6528E:53.7122S (3 m depth)	Dec 2005	

Sampling commenced within 24 h of a media replenishment event to prevent the increase of self shading. A biomass of approximately 10^6 cells mL^{-1} was reached before sampling for pigment analysis. F_v/F_m measurements showed no evidence of nutrient limitation (see Chapter 4).

3.3.2 Coccolith Morphology

Samples for among strain morphological studies were extracted from the freshly innoculated batch cultures on day 3 and day 6 of the exponential growth phase by taking 1 mL aliquot of homogenised culture and vacuum filtering onto sterile nucleopore filters, washing 3 times with 1 mL of de-ionised and filtered (0.2 μm) water before air drying, mounted on a stub, gold coated and examined with a FEI Quanta 600 MLA environmental scanning microscope

(SEM) at 20-25 kV . Prepared SEM stubs of field samples were collected from the Southern Ocean during L'Astrolabe cruise in 2005/2006 (Cubillos *et al.* 2007).

All SEM micrographs were captured at the same magnification of 30,000 times with a horizontal field width of 9.01 μm at 2048 pixels per line. In total 153 images of type A and 100 type B/C cultured coccoliths and 44 field samples were measured using ImageJ software. Morphometrics included in the statistical analysis were distal shield length and distal shield element width (Fig. 3.2).

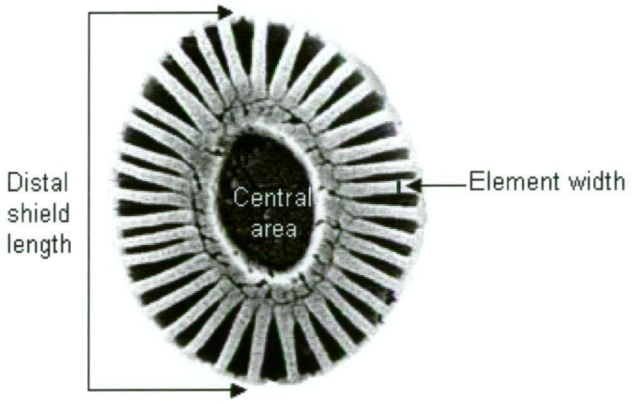

Fig. 3.2. *Emiliania huxleyi* coccolith showing distal shield and measurements taken for morphometric analysis.

3.3.3 Pigment Analysis

Pigment samples were taken by extracting a 3 mL aliquot of homogenised culture near the height of the exponential growth phase and vacuum filtered onto sterile 13 mm GF/F filters (Whatman) held in Millipore filter holders and immediately frozen in liquid nitrogen and stored at -80° C for later extraction. Filtration and freezing was conducted within 20-30 s of removal from the sample flask.

Pigments were extracted using a modification of the method of Mock and Hoch (2005). Filters were extracted in the cryotube with 300 µL dimethylformamide plus 50 µL methanol (containing 140 ng apo-8-carotenal (Fluka) internal standard) added, shaken briefly, then incubated for 1 h at -18° C. Cells were disrupted using a Mini-Bead Beater (Biospec Products) with approximately 0.6 g Zirconium beads (0.7 mm diameter, Biospec) for 20 s at 4800 rpm. The extract was cleared of particulate matter by centrifugation in a fresh tube, at 3500 rpm for 16 min at 4° C. The supernatant was transferred to an amber autosampler vial with a 300 µL micro insert. Extracts (100 µL) were automatically diluted to 80% with water immediately before injection to improve peak shape and analysed by HPLC using a Waters 626 pump, Gilson 233xL autoinjector (with the sample stage refrigerated to -10° C), Waters Symmetry C8 column (150 x 4.6 mm, 3.5 µm packing, in a water bath at 30.0 ± 0.1° C), a Waters 996 diode array detector and a Hitachi FT1000 fluorescence detector. All samples were prepared in dim light. Pigments were identified by comparison of their retention times and spectra with a sample of mixed standards from known cultures injected at the head of each daily sample queue. Peaks were integrated using Waters Empower software. Peaks were checked manually and corrected where necessary, and quantified using the internal standard method (Mantoura and Repeta 1997).

3.3.4 Statistical analysis

Descriptive statistics and ANOVAs were performed in Microsoft Excel (2003) and data checked for normality and variance. Manual Bonferroni corrections were applied where appropriate. Multi-dimensional scaling was conducted using a Euclidean distance model in SPSS v 9.1.

3.4 Results

3.4.1 Coccolith Morphology

The mean length of the distal shield of type A coccoliths was 3.68 μm (range 2.89 to 4.39 μm) and type B/C mean distal shield length was 3.65 μm (range 2.65 - 4.80 μm) (Table 1). The width of distal shield elements in type A ranged between 0.11 – 0.24 μm with a mean of 0.17 μm. In contrast, the distal shield element width of type B/C coccoliths was half that range (0.06 – 0.12 μm, mean 0.09 μm). A plot of distal shield length and distal shield element width revealed that type B/C coccolith element widths of both cultured and field samples were statistically, significantly narrower than the elements in type A. ($P < 0.001$) (Fig. 3.3).

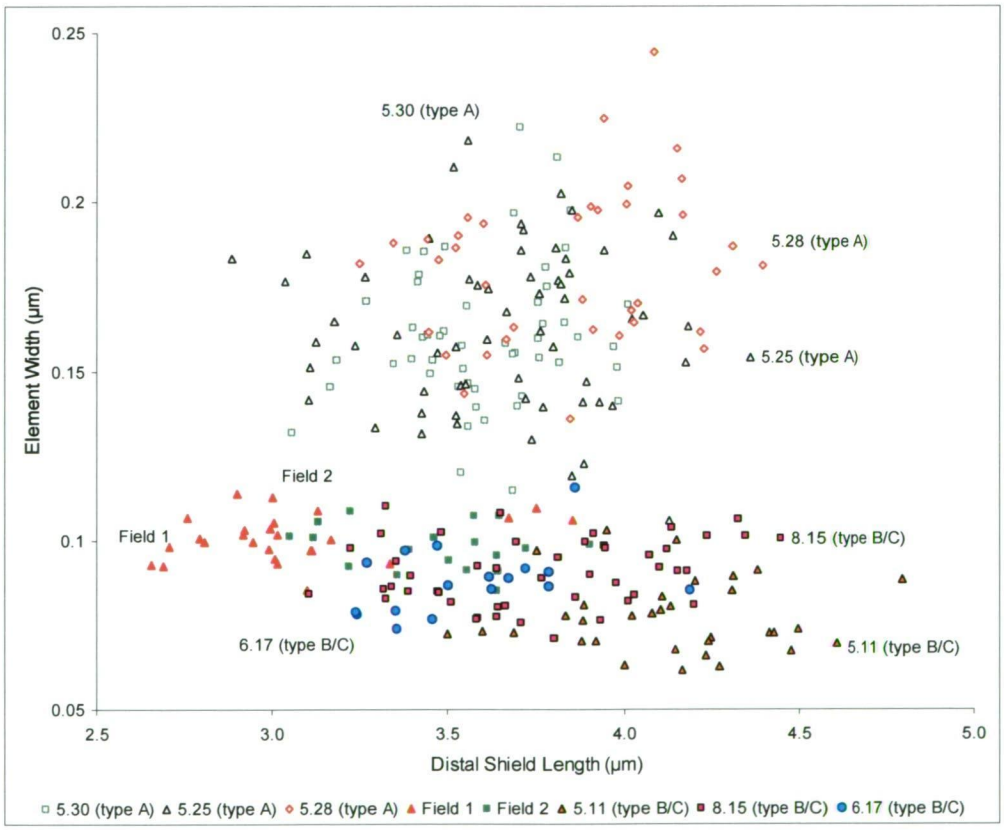

Fig. 3.3. Bivariate plot of coccolith distal shield length and distal shield element width measured from culture samples of morphotype A (open symbols) and cultured and field samples of morphotype B/C (closed symbols).

The central area of the type B/C distal shield consistently comprised a thin plate in contrast to the calcified lath elements observed in type A (Plate 3.1).

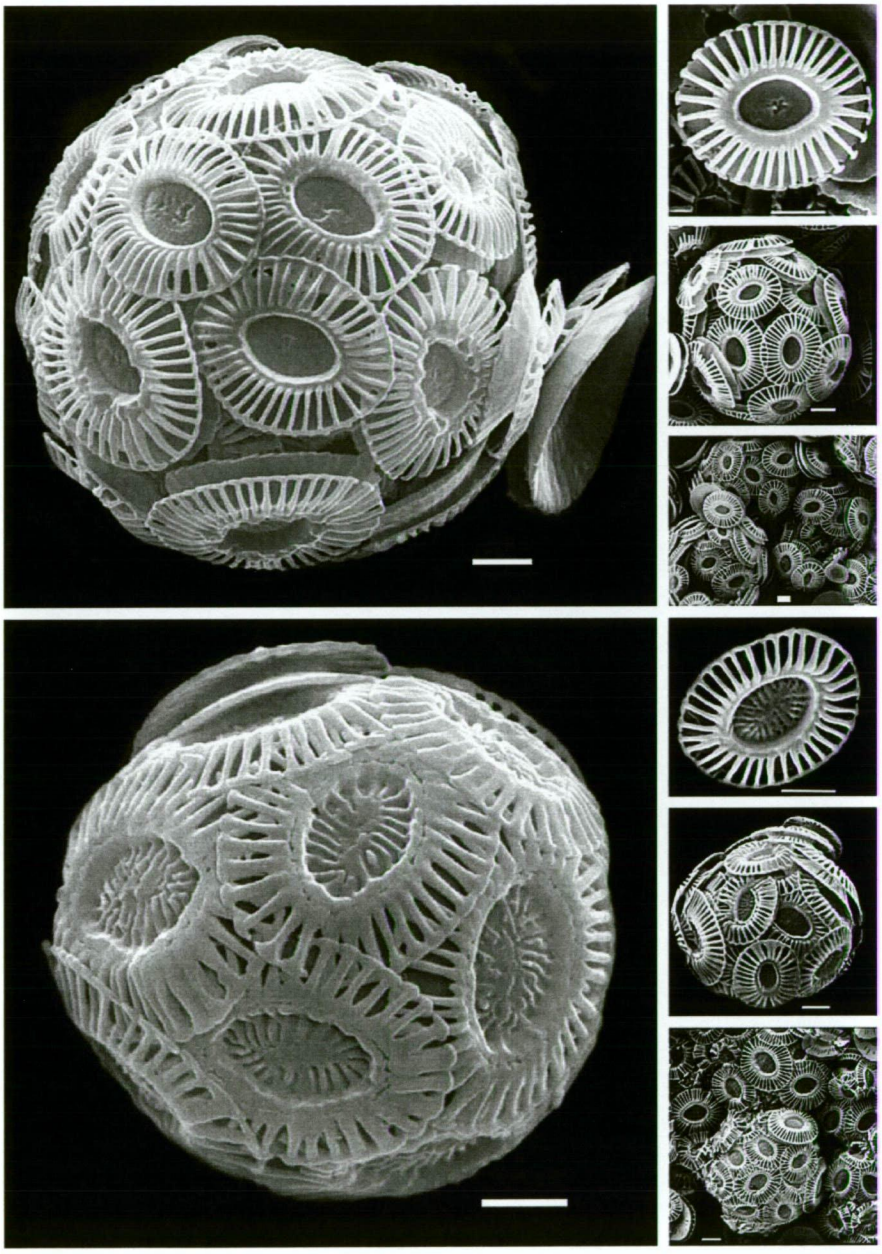

Plate 3.1. Top: Holotype *Emiliania huxleyi* var. *aurorae*. Culture strain EHSO 8.15, isolated in Feb 2007 from the Southern Ocean 145.519E;53.5973S. Bottom: *Emiliania huxleyi* type A var. *huxleyi*, culture strain EHSO 5.25 from the Southern Ocean. Small images from top to bottom: single coccolith, complete cell and group of cells of *Emiliania huxleyi* var. *aurorae*, single coccolith of type A, single cell and group image of Type A. Scale bars = 1μm .

3.4.2 Photosynthetic Pigments

Pigment content per cell was not calculated due to the problems associated with variation in cell size both within and between cultures and the large error rate experienced when conducting manual cell counts (Stolte *et al.* 2000). The two morphotypes of *E. huxleyi* exhibited considerable variation in carotenoid pigment proportions, but no significant differences were found in the percentage contribution of chlorophyll *a* or the ratios of carotenoids to total chlorophylls (Table 3.3).

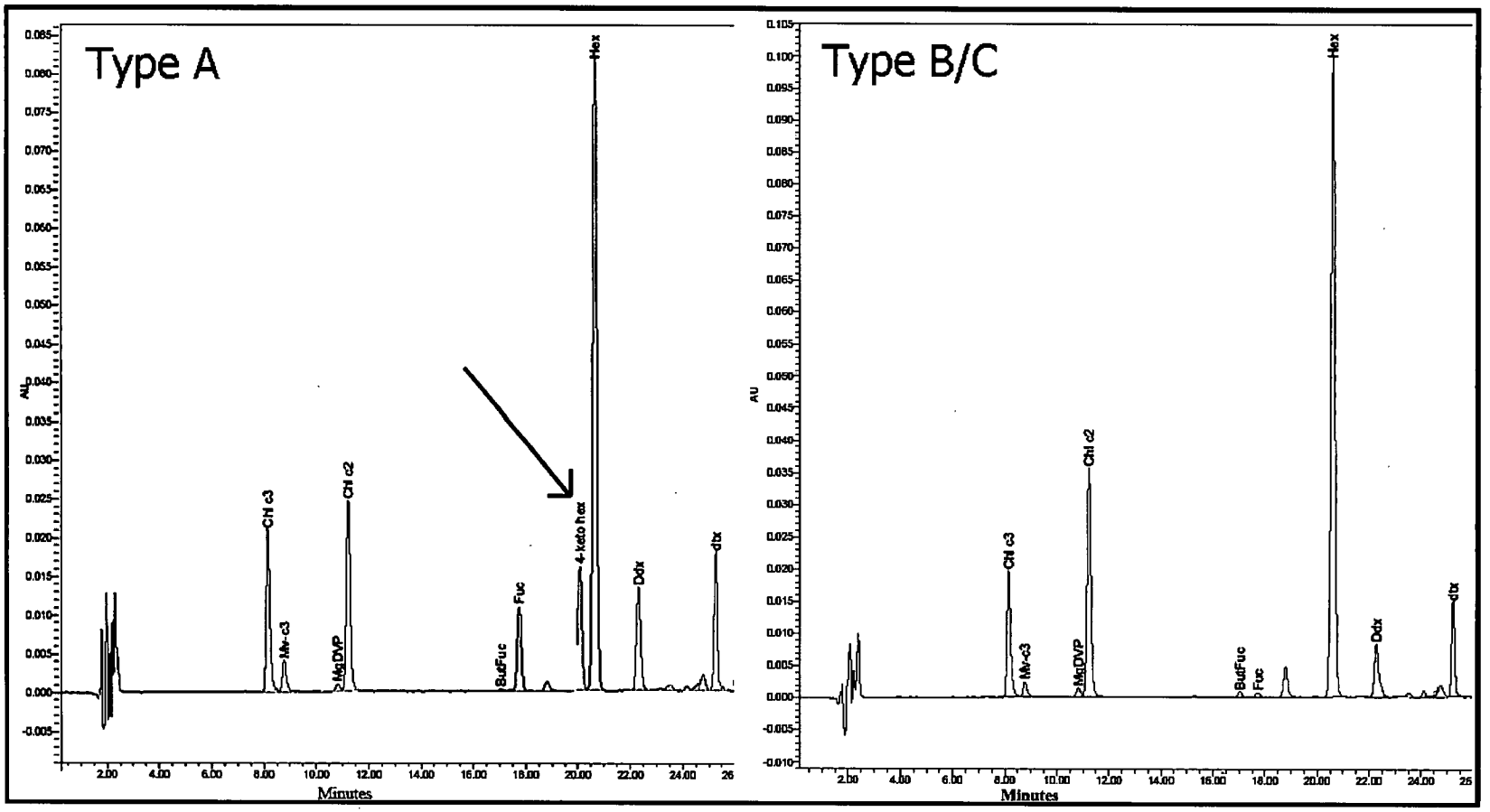

Fig. 3.4. Representative HPLC pigment chromatographs of morphotype A (left) and B/C (right) showing the presence/absence of 4-keto-19′-hexanoyloxyfucoxanthin (4-keto-hex). Other abbreviations: CH c3 = Chlorophyll c_3 ; Mv c3 = Monovinyl chlorophyll c_3 ; $_{MgDVP}$= Mg-2,4-divinyl phaeoporphyin a_5 monomethyl ester; Ch c2 = Chlorophyll c_2; But-Fuc = 19'-butanoyloxyfucoxanthin; Fuc = Fucoxanthin; Hex = 19'-hexanoyloxyfucoxanthin; Ddx = Diadinoxanthin; Dtx = Diatoxanthin

Table 3.3. Comparative pigment composition of *Emiliania huxleyi* morphotypes A and B/C. (n = 3 for each morphotype). Significance levels were obtained from ANOVAs: where * = $P < 0.05$; ** = $P < 0.01$; *** = $P < 0.001$; ns = not significant

Pigment content per unit Chlorophyll *a* (ng pigment/ng Chl *a*) *100						Proportions of total Carotenoids					
	Type A	± se	Type B/C	± se	Signif. level		Type A	± se	Type B/C	± se	Signif. level
Chlorophyll c_2 (Chl c_2)	12.37	1.29	18.86	2.97	ns	Fucoxanthin%	5.18	0.97	0.64	0.21	*
Chlorophyll c_3 (Chl c_3)	12.17	1.40	14.48	2.53	ns	Hex %	63.06	2.85	82.67	0.73	**
Non-polar-chlorophyll c_2	2.57	1.18	1.22	1.18	ns	Hex/Fuc	13.4	3.33	155.27	40.35	*
Mg-2,4-divinyl phaeoporphyin a_5 monomethyl ester (MgDVP)	0.34	0.04	0.59	0.16	ns	Tot Fuc%	78.41	1.63	83.52	0.58	*
Monovinyl chlorophyll c_3 (Mv Chl c_3)	2.38	0.32	1.95	0.25	ns	% PP pool	19.78	1.42	15.16	0.22	*
α- carotene	0.78	0.04	0.63	0.10	ns	Proportions of total Fucoxanthins					
β-carotene	1.64	0.18	1.45	0.25	ns	Fucoxanthin	6.65	1.55	0.77	0.26	*
19'-butanoyloxyfucoxanthin (But-Fuc)	0.28	0.05	0.51	0.40	ns	Hex	80.38	2.47	98.97	0.21	**
Fucoxanthin (Fuc)	7.30	0.99	1.14	0.16	**	But-Fuc	0.24	0.02	0.26	0.19	ns
Diadinoxanthin (Ddx)	25.91	1.79	27.51	4.52	ns	4-keto-Hex	12.73	1.55	0	0	**
Diatoxanthin (Dtx)	2.56	0.24	2.34	0.55	ns	Proportions of total pigments					
4-keto-19'-hexanoyloxyfucoxanthin (4-keto-Hex)	14.22	1.09	0.00	0.00	***	% Chl a	38.56	1.61	30.7	3.71	ns
violaxanthin	0.08	0.04	0.01	0.01	ns	%Chlorophylls	50.07	2.32	41.78	3.67	ns
Zeaxanthin	0.08	0.03	0.29	0.12	ns	% Hex	35.04	2.7	48.17	3.35	*
19'-hexanoyloxyfucoxanthin (Hex)	91.81	11.29	163.62	27.69	*	carot/chls	1.12	0.09	1.43	0.20	ns
						Carotenoids : Photoprotective pigments (PP)					
						carot: tot pig	0.44	0.02	0.49	0.03	ns
						PP : carots	0.25	0.02	0.18	0.00	*
						Dtx:Ddx	0.098	0.00	0.089	0.02	ns

Mean Hex:Chl *a* ratio in type B/C was greater than one, whereas in type A the ratio was less than one. All 12 type A strains analysed for pigment content by Stolte *et al.* (2000) also show a mean Hex:Chl *a* ratio of 0.8 (SD = 0.1), and lower still in type B and C of 0.5 (SD = 0.2). The pigment 19′-hexanoyloxyfucoxanthin was the most abundant carotenoid in both type A and B/C (63-83% of total carotenoids respectively), followed by the photoprotective pigments diadinoxanthin and diatoxanthin.

The proportion of total carotenoids that comprised fucoxanthin and its derivatives differed significantly between the two morphotypes, as did the relative proportions of the different components of the fucoxanthin derivative pool (Table 3.3). While 19′-hexanoyloxyfucoxanthin was the dominant fucoxanthin pigment in both morphotypes, it dominated the fucoxanthin pool in type B/C strains (99%), which possessed only trace amounts of the other fucoxanthins. In type A strains almost 20% of the fucoxanthin pool was partitioned amongst the other three components, and most importantly to 4-keto-19′-hexanoyloxyfucoxanthin (Table 3.3). The latter pigment was not detected in type B/C. As a proportion of total carotenoids the photoprotective carotenoid pool was significantly lower in type B/C cells than in type A.

To objectively classify the strains of *E. huxleyi,* a multivariate analysis was performed on the ratio of 10 carotenoids to the total carotenoid content. The two morphotypes separated clearly in the multidimensional scaling plot (Fig. 3.5).

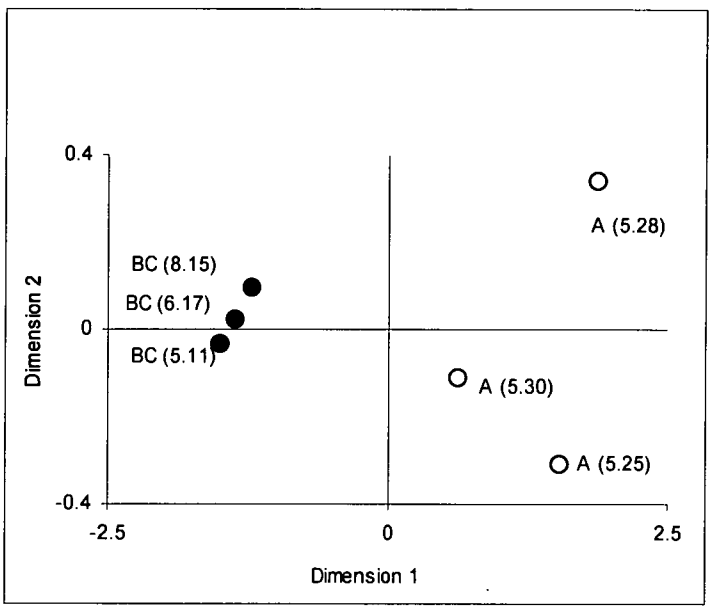

Fig. 3.5. MDS plot between *Emiliania huxleyi* strains based on the relative contribution of the carotenoids normalised to chlorophyll *a*. Euclidean distance model (SPSS)

Most of the variation between the two morphotypes related to the detection of 4-keto-19′-hexanoyloxyfucoxanthin in type A only and the relative contributions made by fucoxanthin and 19′-hexanoyloxyfucoxanthin.

3.5 Discussion

The classical criterion for distinguishing morphotypes of *E. huxleyi* relates to the biometrics of coccolith morphology (Young *et al.* 2003). However problems can arise due to the occurrence of naked cells in cultures, and the presence of overcalcified, malformed or partially dissolved coccoliths. Considerable genetic variability has been previously documented in this species (Iglesias-Rodriguez *et al.* 2006b) including a moderate to high degree (F_{ST} range 11% - 16%) of genetic differentiation between Southern Hemisphere morphotype A and the Southern Ocean type B/C (Chapter 2). This study is the first to examine ecophysiological differences between the two principal Southern Ocean morphotypes of *E. huxleyi,* type A and type B/C, based on photosynthetic pigment composition and the quantitative proportions of light harvesting carotenoids. We describe significant differences in the pigment profile and morphology of the two morphotypes examined.

There exist a number of morphometric descriptions of *E. huxleyi* type A in the literature as outlined in Table 3.1. The results from the present study fit within previously published size ranges (van Bleijswijk *et al.* 1991; Young and Westbroek 1991; Medlin *et al.* 1996). Similarly the type B/C described in the present study conforms to previously published micrographs of type B/C in Young *et al* (2003). These findings suggest that although similar in element width to *var. kleijniae* (type C), the Southern Ocean type B/C has a much larger distal shield and commonly lacks the lath-like structure of the central area. Similarly the distal shield size of the type B from the North Sea fits within the size range of the type B/C as does the element width. However, type B displays lath elements in the central area that are commonly missing in the type B/C. The morphological characterization and pigment complement differences suggests a clear difference between this and other recognized morphotypes of *E. huxleyi* .

While previous studies have characterized the pigment profile of *E. huxleyi* (Jeffrey and Wright 1994; Zapata *et al.* 2004), including pigment responses to light (Stolte *et al.* 2000; Harris *et al.* 2005; Leonardos and Harris 2006), none have compared different morphotypes.

Stolte *et al* (2000) listed three different morphotypes (A, B and C) in their strain list, but did not report differences in pigment profiles between morphotypes.

The fucoxanthin derivative carotenoid, 4-keto-19′-hexanoyloxyfucoxanthin was found only in type A strains, and was not detected in the 3 type B/C strains studied. The absence of this key fucoxanthin derivative was subsequently confirmed by the screening of a further 30 type B/C strains isolated from the Southern Ocean (unpublished data). This pigment is not unique to *E. huxleyi* and is also found in other haptophytes such as *Phaeocystis antarctica* and the dinoflagellates *Karenia brevis* and *Karlodinium veneficum* which contain haptophyte symbionts (Zapata *et al.* 2004). Its function is unknown. This carotenoid was first isolated and partly characterized by Garrido and Zapata (1998) with further structural elucidation provided by Egeland *et al* (2000) who reported that this pigment represented approximately 19% of the total carotenoids in the Norwegian strain of *E. huxleyi* from which it was isolated. In the present study the contribution of 4-keto-19′-hexanoyloxyfucoxanthin to total carotenoids was slightly less, 8-12% (averaging 12% of total fucoxanthins) but similar to the values of 7.5 – 11% of total fucoxanthins reported by Zapata *et al* (2004). These authors however did not report variability of pigments between identified *E. huxleyi* morphotypes.

Previous studies of pigment composition in *E. huxleyi* type A, have described considerably higher contributions of fucoxanthin (20.3% – 27.7%) to the carotenoid complement than we did (Stolte *et al.* 2000; Zapata *et al.* 2004; Harris *et al.* 2005). Van Leeuwe and Stefels (1998) suggested that in the haptophyte *Phaeocystis* iron limitation induced the synthesis of 19′-hexanoyloxyfucoxanthin and 19′-butanoyloxyfucoxanthin at the expense of fucoxanthin. Similarly, DiTullio *et a.l* (2007)) suggest that iron limitation increases the ratio of Hex:fuc in field populations of *P. antarctica* . Ambient iron concentrations in the Southern Ocean are routinely low (<0.2 nmol kg^{-1}), compared with values >5 nmol kg^{-1} in shallow coastal areas (Martin *et al.* 1990). In the present study type B/C strains, which exhibited an increased proportion of 19′-hexanoyloxyfucoxanthin and a significantly lower proportion of fucoxanthin than the type A, were collected from latitudes likely to be iron limited (Sedwick *et al.* 2008). By contrast, the type A cells originated from more northern waters where dissolved iron concentrations would be less likely to have been limiting.

Antarctic strains of *Phaeocystis* also contain relatively high concentrations of 19'-hexanoyloxyfucoxanthin compared to temperate strains (Vaulot *et al.* 1994). Van Leeuwe and Stefels (1998) noted that concentrations of the total fucoxanthin pigments were elevated in iron-deplete cells. In the present work type B/C showed a higher proportion of total fucoxanthins than type A. The type B/C strains used here had been maintained in culture, in identical iron-replete media, temperature and light regimes compared to the type A strains for almost 2 years. Future investigations of the expression of iron regulated proteins could determine if the type B/C fucoxanthin component proportions reflect a response to the iron-limited conditions from which they originated.

3.6 Conclusions

The differences in pigment complements and carotenoid concentrations reported here for the two morphotypes A and B/C, show that adaptation to differing environmental regimes may be occurring in the type B/C. The two morphotypes are physiologically different, with 4-keto-19′-hexanoyloxyfucoxanthin being present in type A and not detected in type B/C. Differences in Hex: Chl *a* ratios in the two morphotypes, with type A being less than one and type B/C greater than one combined with seven times the proportion of fucoxanthin in type A, suggest a difference in light harvesting capacity.

The results presented here have major ramifications for field monitoring using pigment analysis to construct phytoplankton community composition data. No longer can it be assumed that the type A pigment signature that includes 4-keto-19′-hexanoyloxyfucoxanthin as identified by Zapata *et al* (2004) will suffice to identify *E. huxleyi*, when collected from the Southern Ocean near or below the Polar Front. The role and function of 4-keto-19′-hexanoyloxyfucoxanthin is not known, nor if this pigment provides type A cells a competitive advantage or conversely why type B/C cells do not need it. The clear differences in pigment complement reported here between the two morphotypes add further evidence that *E. huxleyi* represents a species complex in the process of morphological and physiological differentiation through environmental adaptation.

In conclusion, building on Medlin *et al.*'s (1996) proposal to formally elevate three *Emiliania huxleyi* morphotypes to variety status, namely var. *huxleyi* (type A), var. *pujosae* (type B) and var. *kleijniae* (type C) (Table 1), we hereby add our description of the morphologically and ecophysiologically distinct Southern Ocean morphotype B/C (*sensu* Young *et al* . 2003) which we raise to variety status as var. *aurorae.*

Var. *aurorae* can be readily distinguished from var.*huxleyi* in the Southern Ocean in having large coccoliths, better separated narrower distal shield elements, and with the central area covered by a thin plain plate, rarely with superimposed lath elements, compared to the coarse grill of 20-23 curved rods in var. *huxleyi.* Moreover, var. *aurorae* lacks 4-keto-19′-hexanoyloxyfucoxanthin.

Emiliania huxleyi var. *aurorae* Cook et Hallegraeff var. nov.

Holotype: Plate 3.1. (Top) Culture strain EHSO 8.15, isolated Feb 2007 from the Southern Ocean 145.519E; 53.5973S.

Coccoliths large, with moderately elevated distal shield, length 2.65 - 4.80 (mean 3.65) μm (n = 144), and well separated narrow shield elements, width 0.06 - 0.12 (average 0.09) μm. Central area composed of a thin plain plate, rarely with superimposed lath elements, often completely absent in corroded specimens. The carotenoid pigment 4-keto-19'-hexanoylfucoxanthin is absent.

Coccolithi magni, scuto distale modice elevato 2.65 - 4.80 μm longo, elementis scutorum angustis valde separatis 0.06 - 0.12 μm latis; area centrali e lamina tenui inornata constanti, raro elementis tigillariis superimpositis ornata, saepe in speciminis corrosis omnino absenti; pigmento carotenoideo 4-keto-19'-hexanoylfucoxanthino nullo.

Etymology: Aurora, the Roman goddess of dawn, is the name of the Australian Antarctic research vessel *Aurora Australis*, but also refers to the low-light environment of the Southern Ocean from which this morphotype originated.

Note: type B/C *sensu* Young *et al.* 2003, figs 5,8; type B/C and type B/C-2 *sensu* Hagino *et al.* 2005, Plate 1, figs 4-6; Plate 2, figs 1-3; Plate 35-6; Cubillos *et al.*2007, figs.3 e-g, k; type C *sensu* Findlay & Giraudeau 2000, Plate 1, Figs 2,3; type K *sensu* Hiramatsu & De Deckker 1996, Fig.2.c-d.

4 Non-photochemical fluorescence quenching and xanthophyll cycle responses of *Emiliania huxleyi* morphotypes from the Southern Ocean

Submitted to Journal of Phycology as:

Ecophysiological differences between two Southern Ocean morphotypes of *Emiliania huxleyi* (Haptophyta): 2. Non-photochemical fluorescence quenching and xanthophyll cycle responses

Suellen S. Cook, Mark J. Hovenden,
School of Plant Science, University of Tasmania, Private Bag 55, Hobart, Tasmania 7001, Australia

Peter J. Ralph,
Plant Functional Biology and Climate Change Cluster (C3)
University of Technology, Sydney

Simon W Wright,
Australian Antarctic Division and Antarctic Climate and Ecosystems CRC, Kingston, Tasmania 7050, Australia

and Gustaaf M. Hallegraeff
Institute of Marine and Antarctic Studies, University of Tasmania, Private Bag 55, Hobart, Tasmania

Author for correspondence: email sscook@utas.edu.au

4.1 Abstract

The two principal Southern Ocean morphotypes of *Emiliania huxleyi* (Lohm.) Hay & Möhler contain a different photosynthetic pigment complement, suggesting physiological differentiation through adaptation to the local light environment. In this work the high light responses of the photoprotective xanthophyll cycle in triplicate strains of Southern Ocean coccolith morphotypes A and B/C are examined. By quantifying induction kinetics, non-photochemical quenching of chlorophyll fluorescence (NPQ) transformation of the xanthophyll pigments diadinoxanthin (Ddx) to diatoxanthin (Dtx) the pronounced differences in the light response of the two morphotypes are demonstrated. High light induced changes in NPQ and de-epoxidation occurred rapidly in type A (rate constants of 0.76 and 0.75 min^{-1}, respectively), while in type B/C these occurred at half those rates. The de-epoxidation state (DPS) = Dtx/(Dtx+Ddx) was highly correlated with NPQ development (r^2 = 0.98 – 0.99) and pigment conversion occurred at rates similar to NPQ development. Recovery of photosynthetic yield from high light exposure was 12.5 times faster in type A than in type B/C. Impact of the epoxidase inhibitor Dithiothreitol (DTT) and observed light induced changes on xanthophyll pigments were consistent with a dual-pool Ddx scheme, of which one pool does not undergo de-epoxidation. The speed with which de-epoxidation and NPQ development occur in type A and the subsequent rapid yield recovery are likely to confer an adaptive advantage in terms of high light handling efficiency. In contrast, the slower induction, relaxation and recovery observed in type B/C increases the trade-off between photoprotection and photochemistry but could be advantageous in the low light environment of the Southern Ocean.

Abbreviations: LL, Low light; HL, High light; DTT, Dithiothreitol; DPS, De-epoxidation state; Ddx, Diadinoxanthin; Dtx, Diatoxanthin; F_v/F_m, Maximum quantum yield; F_o, Minimum fluorescence; F_m', Maximum fluorescence; $\Delta F/F_m'$, Effective quantum yield of PSII = $(F_m' - F_t)/F_m'$; NPQ, Non-photochemical quenching of fluorescence.

4.2 Introduction

Efficient photosynthesis requires optimal utilisation of absorbed photons when light is limiting, however transport of plankton cells from depth to the surface exposes them to irradiance levels much higher than needed to drive photosynthesis at maximum capacity (Falkowski 1994; Litchman and Klausmeier 2001; Muller *et al.* 2001). To manage this variable light climate a number of highly regulated and controlled photoprotective processes have evolved to optimise light harvesting at low irradiance while at the same time minimising damage at high irradiance (Muller *et al.* 2001; Adir *et al.* 2003). Photodamage only occurs when the capacity of acclimation and protection mechanisms has been exhausted. However, photoprotective processes effectively lower the quantum yield of photosynthesis (Long *et al.* 1994). Therefore, the ability to rapidly optimise photochemistry to prevailing light is critically important for survival, growth and competitive advantage in changeable light environments (Huismann *et al.* 1999a, b, Litchman & Klausmeier, 2001, MacIntyre *et al.* 2002).

Long term photoacclimation to diurnal and seasonal changes is usually achieved by adjusting the quantity and composition of light harvesting pigments as these define the quantity and intensity of light energy transferred to the photosystems (van de Poll *et al.* 2007). This method of photosystem optimisation, however, can be a liability for aquatic microalgae exposed to rapid and large irradiance changes during vertical mixing where irradiance can regularly exceed photosynthetic requirements. This can lead to damage to the photosynthetic machinery of the cell (Falkowski and Raven 1997).

Phytoplankton possesses a number of mechanisms to manage high light intensities over short time scales (seconds to hours). These include redirecting excitation energy away from PSII (state transitions) or quenching excitation energy to heat in part by enzymatic xanthophyll pigment conversion, the xanthophyll cycle (Olaizola *et al.* 1994; Falkowski and Raven 1997; Gorbunov *et al.* 2001). This process is correlated with changes in non-photochemical quenching of chlorophyll fluorescence (NPQ) (Falkowski and Raven 1997; Gorbunov *et al.* 2001). The xanthophyll cycle is critical in preventing permanent damage during short term

exposure to high light (Falkowski and Raven 1997). In higher plants the xanthophyll cycle involves the reversible, light induced two-step conversion of the xanthophyll pigment violaxanthin via antheraxanthin to zeaxanthin by enzymatic de-epoxidation. This light stimulated conversion is also found in some algal groups notably those of the green lineage (Lohr and Wilhelm 1999; Gorbunov *et al.* 2001). However in many diatoms, dinoflagellates and haptophytes, the violaxanthin xanthophyll cycle is replaced by one that alternates diadinoxanthin (Ddx) with diatoxanthin (Dtx) through a single de-epoxidation step (Olaizola *et al.* 1994; Falkowski and Raven 1997). Xanthophyll pigments fulfill a dual function, the epoxidised forms assist in light harvesting when in low light, whereas de-epoxidised forms dissipate excessive irradiance (Olaizola *et al.* 1994; Owens 1994; Goss *et al.* 2006). The carotenoids fucoxanthin and 19'-hexanoyloxyfucoxanthin have also been implicated as precursor or derivative pigments in the biosynthesis of xanthophyll pigments in *E. huxleyi* (Stolte *et al.* 2000; Harris *et al.* 2009) and in diatoms (Lohr and Wilhelm 1999).

The ability of the coccolithophorid *E. huxleyi* to form massive blooms in ocean surface waters where incident light is high has prompted numerous investigations into the capacity of these cells to withstand photoinhibition and damage (Balch *et al.* 1992; Nanninga and Tyrrell 1996; Harris *et al.* 2005; Houdan *et al.* 2005; Trimborn *et al.* 2007). Nanninga and Tyrrell (1996) reported that this species did not show any sign of photoinhibition until light intensities exceeded 1000 - 1500 µmol photons $m^{-2} s^{-1}$. While studies have been conducted to examine xanthophyll pigment concentrations in response to variable growth irradiance in *E. huxleyi* (Harris *et al.* 2005; Leonardos and Harris 2006; van de Poll *et al.* 2007; Leonardos 2008; Ragni *et al.* 2008; Harris *et al.* 2009) the comparative photophysiology of the various coccolith morphotypes (Young and Westbroek 1991) has not previously been addressed. Chapter 3 reported significant differences in pigment complement between type A and B/C suggesting that photophysiological adaptation as a result of environmental forcing may be occurring.

Here, the similarities and differences in the photophysiological response to light between the two dominant Southern Ocean morphotypes of *E. huxleyi,* A and B/C are quantified. In a

series of laboratory experiments using pulse amplitude modulation fluorometry (PAM) and HPLC pigment analysis the kinetics of xanthophyll pigment de-epoxidation, epoxidation, the induction and relaxation of photochemical and non-photochemical quenching were examined.

4.3 Methods

4.3.1 Algal strains and culture conditions

To examine xanthophyll cycling and non-photochemical quenching, three strains of each morphotype were selected as representative, based on latitude of origin, from a collection of over 400 strains of *E. huxleyi* established from samples taken in the Southern Ocean and the south eastern Australia region (Fig. 3.1, page 50).

The six selected strains (Table 4.1) were batch cultured at 16° C in 300 mL Erhlenmeyer flasks with media using 0.2 μm - filtered natural seawater from east coast Tasmania with K medium nutrients, metals and vitamins added at recommended concentrations including a final concentration of 290 μM L^{-1} nitrate and 4 μM L^{-1} phosphate (Keller *et al.* 1987). A 12:12 h light:dark cycle was provided by Cool White fluorescent tubes (Sylvania 36W/w41) with an incident irradiance of 70 μmol photons m^{-2} s^{-1}.

Table 4.1. Details of culture strains of Emiliania huxleyi used in this study

Culture Strain ID.	Morphotype	Location	Light field (% of surface)	Isolation Date	Isolator
EHSO 5.30 EHSO 5.25 EHSO 5.28	A A A	Southern Ocean 149.2500E:49.5900S (7 m depth)	98	Feb 2007	S Cook
EHSO 5.11	B/C	Southern Ocean 149.2500E:49.5900S (7 m depth)	98	Feb 2007	S Cook
EHSO 6.17	B/C	Southern Ocean 146.1813E:54.0850S (65 m depth)	47	Feb 2007	S Cook
EHSO 8.15	B/C	Southern Ocean 145.5519E:53.5973S (80 m depth)	10	Feb 2007	S Cook

Cultures were acclimatised for 28 d prior to the commencement of the experiments. Fresh cultures were inoculated from parental stock every 14 d. Semi-continuous exponential growth conditions were maintained by regularly replacing one third (100 mL) of homogenised media and cells to maintain exponential growth and reach a biomass of approximately 10^6 cells mL^{-1}. Experimentation was commenced within 24 hours of nutrient replenishment.

High light (HL) conditions were created using two SP90 pure white E40 LED lamps (Shenzen Bang-Bell Electronics) located equidistantly on either side of the culture flask. These LED lamps, with spectral peaks at 450 nm and 570 nm, provided 1000 µmol photons m^{-2} s^{-1} at the centre of an identical flask containing 300 mL medium. Low light (LL) of 60 µmol photons m^{-2} s^{-1} was achieved by diffusing the light source. LED lights were chosen because of their low heat emission. Light intensities were measured using a Biospherical Instruments QSL 100 laboratory spherical quantum scalar irradiance meter.

4.3.2 Fluorescence measurements

Active chlorophyll *a* fluorescence was measured using a Diving-PAM (Walz, Effeltrich, Germany) under computer control. The fluorometer uses pulse modulated blue light from a light-emitting diode (LED 470 nm) as the source for the measuring light emitted at a frequency of 0.6 kHz when measuring F_o or 20 kHZ when measuring other fluorescence parameters (Heinz Walz Gmbh 1998). Actinic light and saturation pulses are provided by a miniature 8 V/20 watt halogen lamp. Fluorescence was measured using a 5.5 mm diameter fibre-optic probe held at the standard distance of 10 mm from the base of the culture flask and 10 mm below the meniscus of the culture medium..

Non-photochemical quenching was calculated as:-

$NPQ = (F_m - F_m')/F_m'$ Equation 1 (Schreiber *et al.* 1994).

Where F_m and F_m' are the maximum fluorescent measurements from a dark and light adapted sample respectively.

4.3.3 NPQ induction and relaxation

F_o and F_m were measured in homogeneous suspensions of *E. huxleyi* cells and the maximum quantum yield, F_v/F_m determined by applying saturating pulses every 2 min during the final 10 min of the 12 h overnight dark period to ensure complete relaxation of NPQ. Cultures were then exposed to LL for 1 h before HL treatment. HL was maintained for at least 45 min before returning to LL for a further 45 min. The relatively short HL period of 45 min was chosen as longer exposures (> 2 - 4 hours) can lead to changes in actual chlorophyll *a* content, a mechanism for longer term photoacclimation (Lohr and Wilhelm 2001; Harris *et al.* 2009). Recovery was measured in the dark for a further 30 min following LL treatment. Effective quantum yield of PSII ($\Delta F/F_m'$) was measured every 5 min during the initial LL period and samples for pigment analysis taken at the end of the 12 h dark period, the commencement and the end of the initial LL period. Effective quantum yield was also measured 0, 0.5, 1, 1.5, 2, 3, 5, 10, 15, 25, 35 and 45 min after HL exposure. Samples for pigment analysis were taken concurrently by extracting a 3 mL aliquot of homogenised culture and vacuum filtered onto 13 mm GF/F filters (Whatman) held in Millipore filter holders and immediately frozen in liquid nitrogen and stored at -80° C for later extraction. Filtration and freezing was conducted within 20 - 30 s of removal from the sample flask and in the same light field.

After 45 min of HL treatment, incident light was reduced to the predetermined LL level, samples for pigment analysis and $\Delta F/F_m'$ measurements were taken at the same time intervals as those for HL. During the dark recovery period pigment samples and measurements were taken at time 0, 5, 15 and 30 min.

DPS is calculated as Dtx/(Ddx+Dtx) and describes the de-epoxidation state of the xanthophyll cycle pigment diadinoxanthin to diatoxanthin. NPQ and DPS increase following exposure to HL and subsequent relaxation were described by a first order kinetics model derived from the model of Olaizola and Yamamoto (1994):-

$$NPQ(t) = NPQ_m + (NPQ_0 - NPQ_m)e^{-k_{NPQ}t} \qquad \text{Equation 2}$$

$$DPS(t) = DPS_m + (DPS_0 - DPS_m)e^{-k_{DPS}t} \quad \text{Equation 3}$$

Where NPQ_0, DPS_0, and NPQ_m, DPS_m are the values measured immediately at the beginning of the high light period and at the end of the relevant period of time being measured (respectively); k_{NPQ} and k_{DPS} are the rate constants of NPQ and DPS (respectively). k_{NPQ} and k_{DPS} were estimated by fitting Equation 2 to time 0 - 15 min and 15 - 45 min of the HL time series of NPQ and equation 3 to the same time periods of DPS respectively. Rate constants for the relaxation of NPQ and DPS in LL were similarly calculated.

4.3.4 Inhibitor Treatment

The disulfide-reducing agent, Dithiothreitol (DTT) (Aldrich Chemistry, USA) is known to prevent the de-epoxidation of xanthophylls by inactivating the de-epoxidase enzyme (Yamamoto and Kamite 1972). DTT was applied from a 1 M aqueous stock solution (2 mM final concentration) at the end of the LL period. Culture flasks were swirled for 30 s to homogeneously distribute the inhibitor. PAM measurements and samples for pigment analysis were taken at the end of the LL period prior to inhibitor addition and at 0, 15, 30 and 45 minutes during HL exposure.

4.3.5 HPLC extraction

Pigments were extracted using a modification of the method of Mock and Hoch (2005). Filters were extracted in the cryotube with 300 µL dimethylformamide plus 50 µL methanol (containing 140 ng apo-8-carotenal (Fluka) internal standard) added, shaken briefly, then incubated for 1 h at -18° C. Cells were disrupted using a Mini-Bead Beater (Biospec Products) with approximately 0.6 g Zirconium beads (0.7 mm diameter, Biospec) for 20 s at 4800 rpm. The extract was cleared of particulate matter by centrifugation in a fresh tube, at 3500 rpm for 16 min at 4° C. The supernatant was transferred to an amber autosampler vial with a 300 µL micro insert. Extracts (100 µL) were automatically diluted to 80% with water immediately before injection to improve peak shape and analyzed by HPLC using a Waters 626 pump, Gilson 233xL autoinjector (with the sample stage refrigerated to -10° C), Waters Symmetry C8 column (150 x 4.6 mm, 3.5 µm packing, in a water bath at 30.0 ± 0.1° C), a

Waters 996 diode array detector and a Hitachi FT1000 fluorescence detector. All samples were prepared in dim light. Pigments were identified by comparison of their retention times and spectra with a sample of mixed standards from known cultures injected at the head of each daily sample queue. Peaks were integrated using Waters Empower software. Peaks were checked manually and corrected where necessary, and quantified using the internal standard method (Mantoura and Repeta 1997).

4.3.6 Statistical analysis

ANOVAs and regressions were performed using SPSS software. Bonferroni corrections were applied where appropriate. Equations 2 and 3 were fitted to data using non-linear curve fitting procedures (PROC NLIN) in the statistical software package SAS® v.9.1.(SAS Institute Inc. USA).

Results

Responses to changes in irradiance of yield and non-photochemical quenching parameters as assessed by PAM fluorometry showed significant differences between the two morphotypes, A and B/C. Type A exhibited an overall greater efficiency in responding to and optimizing for HL exposure.

4.3.7 Photosynthetic Yield

Maximum quantum yield of PSII (F_v/F_m) measured just before the end of the overnight dark period was similar for both morphotypes (A = 0.59 ± 0.08; B/C = 0.60 ± 0.03). During the subsequent LL period $\Delta F/F_m'$ (effective quantum yield) initially decreased by 25% (type A) and 40% (type B/C) but after 60 min of LL recovered to reach 95 - 100 % of F_v/F_m (A = 0.59 ± 0.07; type B/C = 0.57 ± 0.03) (Fig. 4.1). At the onset of HL the $\Delta F/F_m'$ of both cell types declined dramatically by 92% (type A) and 95% (type B/C). Within 10 min of HL exposure $\Delta F/F_m'$ in both morphotypes increased, to reach 23% (type A) and 15% (type B/C) of the pre-exposure values (type A = 0.14 ± 0.01; type B/C = 0.08 ± 0.02), while recovery was rapid in both morphotypes once under LL. After 45 min of LL, $\Delta F/F_m'$ of type A had recovered to 96% of the pre-exposure values and type B/C to 82%. However the rate of recovery was significantly different between the two morphotypes, with the $\Delta F/F_m'$ of type B/C morphotypes recovering to 80% of the pre-exposure values after 25 min, compared to type A which recovered to a similar level in only 2 min ($P < 0.05$; Fig. 4.1). Both morphotypes exceeded the pre-HL values after a further 30 min of darkness but only type A reached its maximum quantum yield within that time.

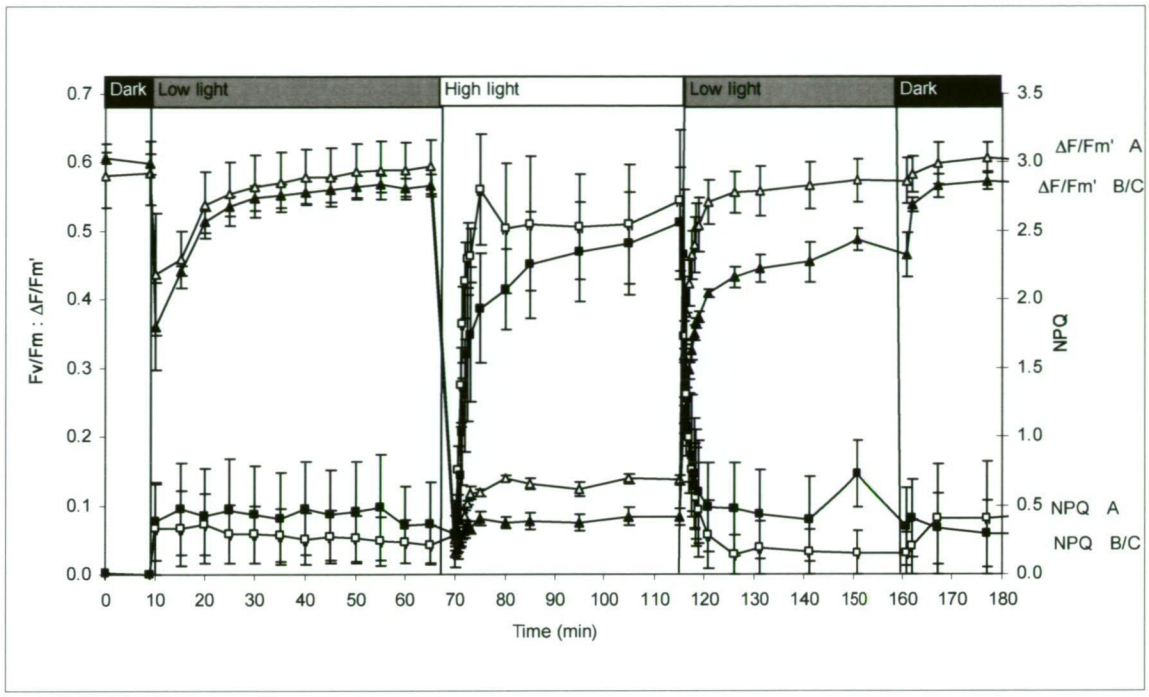

Fig. 4.1. Changes in F_v/F_m, $\Delta F/F_m'$ (triangles) and NPQ induction kinetics (squares) in dark-adapted cultures of 3 type A strains (empty symbols) and 3 type B/C strains (filled symbols) *Emiliania huxleyi* strains exposed to low (60 µmol photons m^{-2} s^{-1}) and high (1000 µmol photons m^{-2} s^{-1}) irradiance and subsequent recovery and relaxation in low light followed by darkness (means ± se, n = 3).

4.3.8 Non-Photochemical Quenching

Non-photochemical quenching (NPQ) was not present in the initial (overnight) dark period in either morphotype and only rose slightly during the initial LL period (Fig. 4.1). During exposure to HL, NPQ developed rapidly in both morphotypes, reaching a plateau after 5 min in type A but continuing to rise in type B/C. The NPQ induction rate over the first 15 min of HL exposure (k_{NPQ}) was significantly higher in type A, at 0.76 ± 0.10 min^{-1}, than in type B/C at 0.38 ± 0.03 min^{-1} ($P < 0.05$) (Table 4.2).

Table 4.2. Rate constants (k) and adjusted r^2 values of NPQ and DPS in HL and LL for morphotypes A and B/C of *Emiliania huxleyi*. ANOVAs compare means of type A and type B/C k values and empirical data with the model predictions, n=3.

HL (1000 µmol photons $m^{-2} s^{-1}$)	Time series (min)	Type A (min^{-1})	r^2/model	Type B/C (min^{-1})	r^2/model
k_{NPQ} (min^{-1})	0-15	0.76 ± 0.10 *	0.97 ***	0.38 ± 0.03	0.95 ***
	15-45	0.01 ± 0.01 ns	0.23 ns	0.03 ± 0.00	0.94 *
k_{DPS} (min^{-1})	0-15	0.75 ± 0.07 **	0.97 ***	0.32 ± 0.02	0.99***
	15-45	0.02 ± 0.00 ns	0.96 *	0.03 ± 0.01	0.99 **
LL (60 µmol photons $m^{-2} s^{-1}$)					
k_{NPQ} (min^{-1})	0-10[a]	-0.67 ± 0.24 ns	0.99 ***	-1.12 ± 0.22	0.99 ***
k_{DPS} (min^{-1})	0-45	-0.43 ± 0.02 ns	0.99 ***	-0.38 ± 0.12	0.99 ***

ANOVA of differences between type A and type B/C :* = * (P<0.05); ** (P<0.01); *** (P<0.001); ns = not significant

[a] NPQ reached stable relaxation level after 10 min

The fit of equation 2 to NPQ during the first 15 min of HL exposure was highly significant ($P < 0.001$) with the model explaining 97% of variability in type A and 95% in type B/C (Fig. 4.2, Table 2.1). A different rate constant was calculated after 15 min of HL exposure due to significant slowing of NPQ development (Table 4.2).

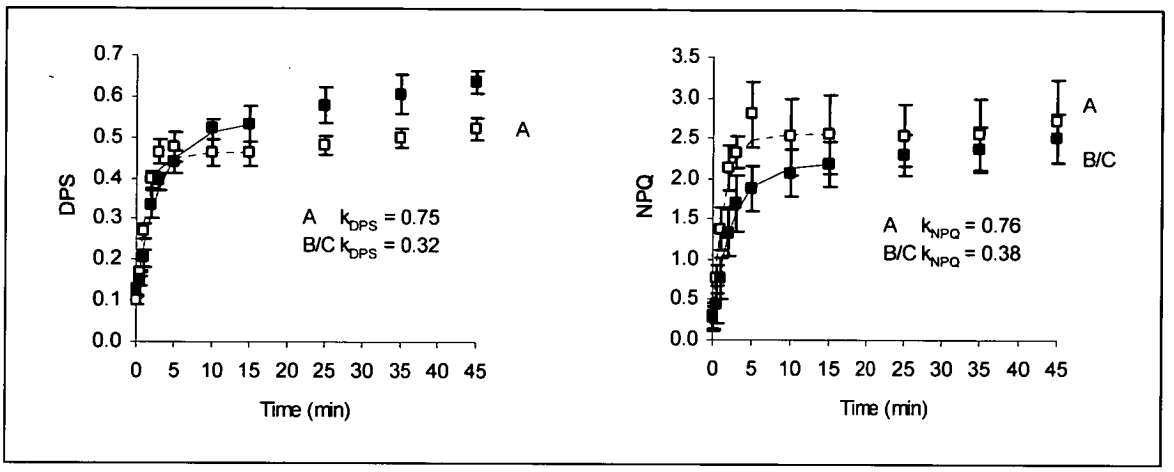

Fig. 4.2. Fit of mono-exponential function for the estimation of the rate constant over the first 15 min of exposure to 1000 µmol photons m^{-2} s^{-1}. (Left) de-epoxidation state (DPS) and (right) NPQ in morphotype A and B/C of *Emiliania huxleyi* (means ± se, n = 3).

Relaxation of NPQ following reduction of light at the end of the 45 min HL exposure was similar between the morphotypes (Fig. 4.1). NPQ reached a minimum level in type A in less than 10 min, as did type B/C, although not to the same final level (Fig. 4.1). After the dark period both morphotypes relaxed NPQ to the same level.

4.3.9 De-epoxidation/Epoxidation kinetics

At the end of the overnight dark period the Ddx proportion in both morphotypes was 90%. The proportion of the xanthophyll pool (Ddx + Dtx) that is Dtx, the de-epoxidation product represents the de-epoxidation state (DPS) of the xanthophyll pigments. Initially de-epoxidation in both morphotypes was rapid, but more so in type A (Fig. 4.2, Table 4.2).

After 5 min of HL exposure the rapid de-epoxidation of Ddx to Dtx in type A reached a plateau only to increase again after approximately 15 min (Fig. 4.2). In contrast type B/C did not reach a plateau but rather continued to increase. However in this latter period the rate of de-epoxidation was more rapid in type B/C than in type A, but rates were only 10% of the initial rate. After 10 min of HL exposure, type B/C had a significantly higher DPS than type A. The rate of de-epoxidation (k_{DPS}) over the initial 15 min of exposure was 0.75 ± 0.07

min^{-1} for type A, more than double the rate of type B/C at 0.32 ± 0.02 min^{-1} ($P < 0.01$) (Table 4.2). Overall type B/C reached a 20% higher level of de-epoxidation in HL than type A. Changes in Ddx and Dtx proportions cannot be ascribed to bleaching of chlorophyll by the irradiance treatments as regressions of chlorophyll *a* against time were not significantly different from zero ($P > 0.05$). Once in LL, DPS declined exponentially at similar rates in the two morphotypes (Table 4.2). In both HL and LL exposure there was a very strong linear relationship between NPQ and DPS induction (A: r^2 0.98; B/C: r^2 0.99) and relaxation (A: r^2 0.97; B/C: r^2 0.80) in both morphotypes (Fig 4.3).

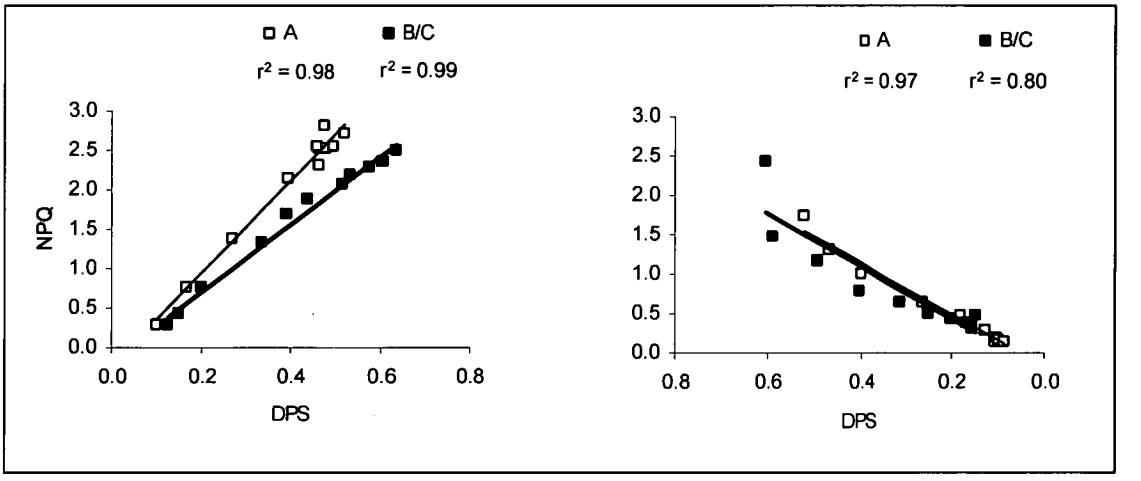

Fig. 4.3. Linear relationship between NPQ and DPS during 45 min of exposure to (left) HL (1000 µmol photons m^{-2} s^{-1}) and (right) 45 minutes exposure LL (60 µmol photons m^{-2} s^{-1}) for type A (open squares) and type B/C (closed squares) of *Emiliania huxleyi*.

The components of DPS, Ddx and its de-epoxidation product Dtx per unit chl *a*, behaved differently in the two morphotypes (Fig. 4.4).

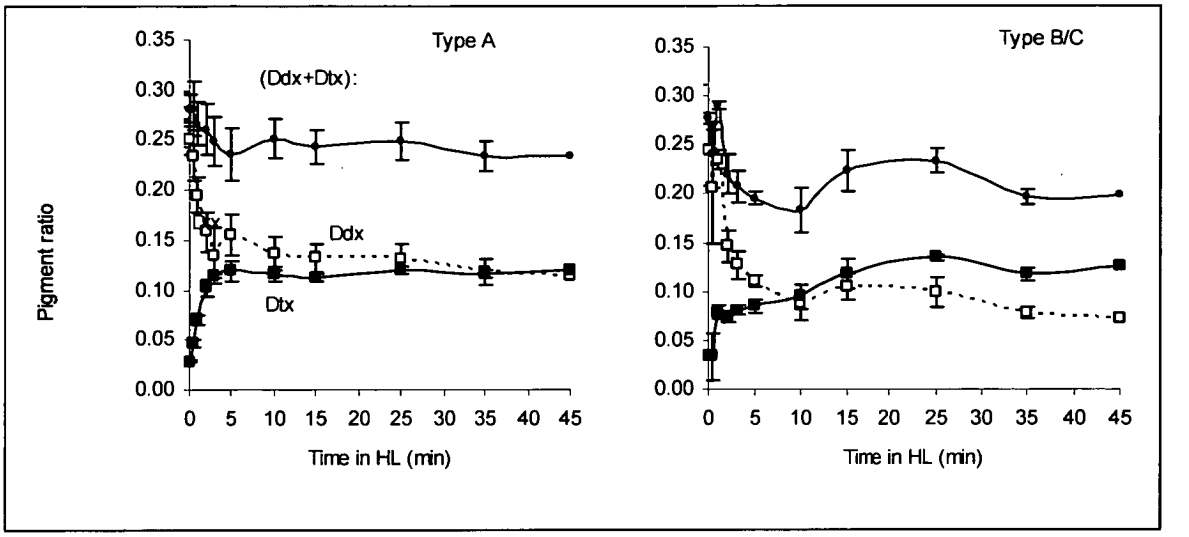

Fig. 4.4. Conversion of Ddx:Chl *a* (open squares) and Dtx:Chl *a* (closed squares) and (Ddx+Dtx):Chl *a* in (left) type A morphotype and (right) type B/C morphotype of *Emiliania huxleyi* during high light exposure. Pigment:chlorophyll *a* (ng/ng*100) values are means ± se, n=3.

In type A, Ddx did not decline to the same extent as in type B/C despite identical starting points. Furthermore, after the initial fall in Ddx, this pigment increased after 5 min of exposure to HL, without a concurrent increase in Dtx. At this point, 5 min into the HL exposure, Dtx reached its maximum level in type A and did not significantly change for the remainder of exposure time. In contrast, Ddx in type B/C declined considerably further than type A when initially exposed to HL and did not show a similar increase to type A until after 15 min of exposure to HL. Dtx in type B/C did not reach its maximum level until after 25 min of HL exposure.

4.3.10 Effect of light on Fucoxanthin and 19'-hexanoyloxyfucoxanthin

Fucoxanthin and the fucoxanthin derivative 19'-hexanoyloxyfucoxanthin (Hex) decreased during HL exposure and increased again under subsequent LL. Fucoxanthin:chl *a* fell 13% in type A cells and 46% in type B/C cells between 0 and 45 min of exposure to HL and subsequently rose in LL, 26% and 46% respectively (Fig. 4.5, upper). Hex decreased 7% in type A cells and 32% in type B/C cells during HL and increased 10% and 52% during LL and dark period (Fig. 4.5 lower).

During HL, peaks in fucoxanthin coincided with those of Ddx observed at 5 min of HL exposure in type A and at 15 min in type B/C. The correlation between fucoxanthin:chl *a* and Ddx:chl *a* from 5 to 45 min of HL exposure was 0.96 and 0.79 for type A and B/C respectively. Hex:chl *a* and fucoxanthin:chl *a*. were highly correlated ($r^2 = 0.98$) in type A during 5- 45 min of HL, but not in type B/C.

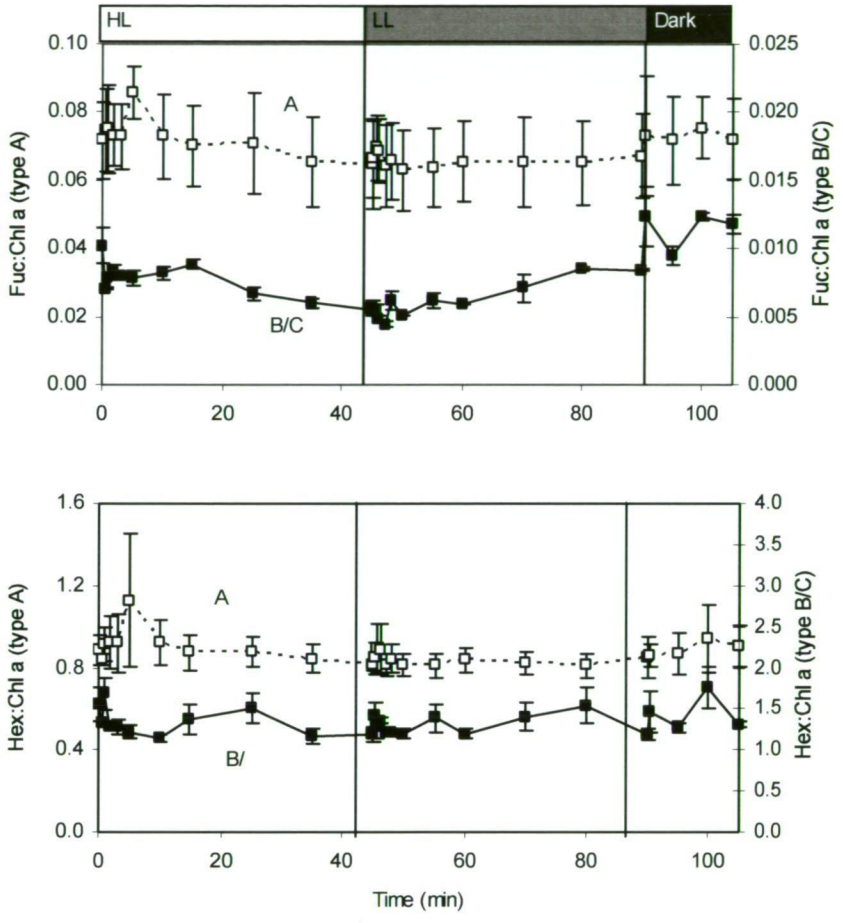

Fig. 4.5. Response of fucoxanthin:chl *a* (Fuc) (top) and 19′-hexanoyloxyfucoxanthin:chl *a* (Hex) (bottom) to high and low light exposure in *Emiliania huxleyi* type A (open squares) and type B/C (closed squares). Pigment:chlorophyll *a* (ng:ng*100) values are means ± se, n = 3.

4.3.11 Inhibitor Treatment

To examine the relationship between NPQ development and Ddx/Dtx de-epoxidation, the inhibitor DTT was used to block epoxidase activity (Lohr & Wilhelm, 1999, Olaizola *et al.*, 1994, Yamamoto & Kamite, 1972). The xanthophyll cycle pigments, Ddx and Dtx showed major changes with inhibitor treatment and/or light exposure (Fig. 4.6).

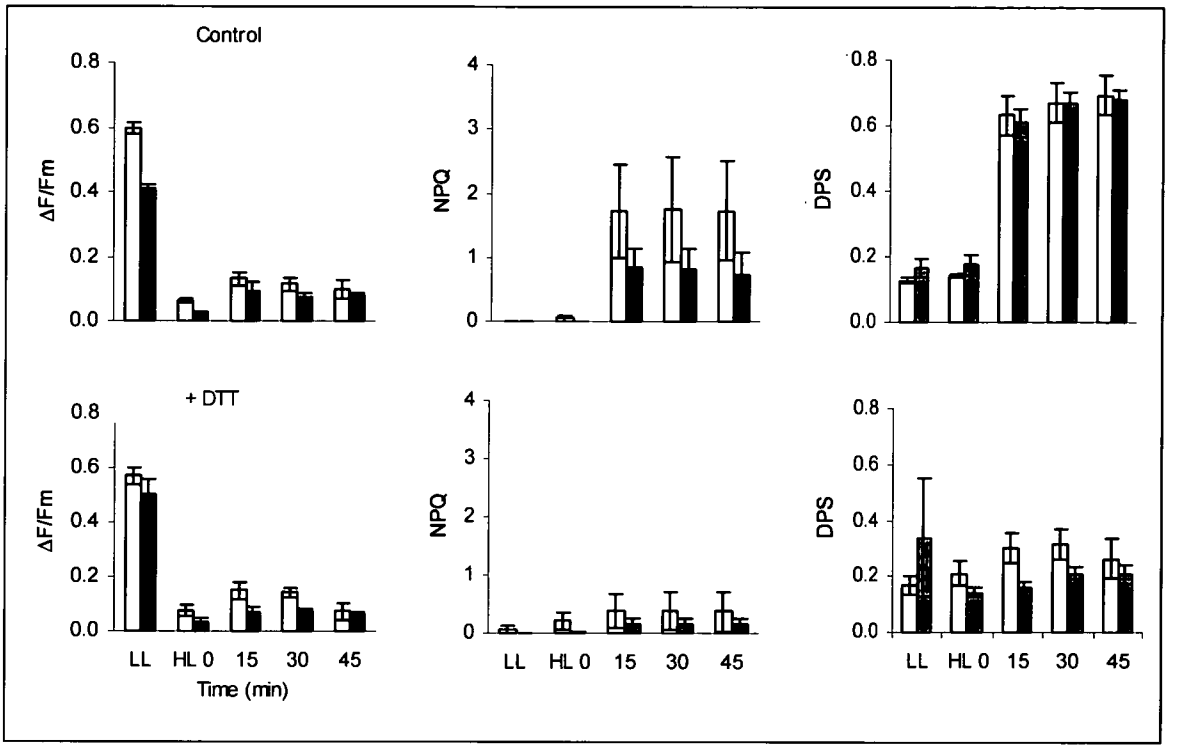

Fig. 4.6. Changes in $\Delta F/F_m'$ (left), NPQ (centre) and de-epoxidation state (DPS) (right) in morphotype A (white bars) and B/C (grey bars) strains of *Emiliania huxleyi* moving from LL into 45 min incubation in HL (1000 μmol photons m^{-2} s^{-1}). (Above) control. (Below) with the addition of the inhibitor DTT (final concentration 2 mM) at time zero (means ± se, n = 3).

DTT suppressed 56% of DPS in type A and 78% of the NPQ (average over the last 30 min of HL). In contrast, 70% of DPS in type B/C was suppressed by the inhibitor and 81% of NPQ. The degree of inhibition of de-epoxidation was significantly different between morphotypes ($P = 0.01$) despite some evidence of incomplete binding of the inhibitor. The DPS in DTT-inhibited type A was significantly higher than type B/C, 15 and 30 min after HL exposure but reached similar levels after 45 min ($P < 0.05$). Neither fucoxanthin, Hex nor $\Delta F/F_m'$ were affected by the addition of the inhibitor.

4.4 Discussion

In high light, the down regulation of photochemistry by xanthophyll cycle energy dissipation provides a safety mechanism by reducing the efficiency with which absorbed light is transferred to PSII reaction centres. In the xanthophyll cycle Ddx is rapidly and reversibly converted to the energy dissipating form Dtx (Olaizola and Yamamoto 1994) thereby reducing the energy delivered to PSII reaction centres and minimising the potential for oxidative damage to the photosynthetic apparatus (Lavaud *et al.* 2004). However at the same time photosynthetic yield is reduced. The results demonstrate that the two dominant Southern Ocean morphotypes of *E. huxleyi* differ substantially in the rate of their photochemical response to sudden shifts in light intensity imposed under the experimental conditions. Furthermore, despite the strong linear relationship between NPQ induction and DPS during de-epoxidation, the rate of photoprotective activity altered before and after 15 min of HL exposure. The difference in rate constants over the time course for both NPQ and DPS suggest the presence of slow non-variable quenching and NPQ associated with the xanthophyll cycle (Goss *et al.* 2006).

The rate of de-epoxidation when exposed to high light and epoxidation of xanthophyll pigments in low light have not previously been reported for *E. huxleyi*. Most photophysiology research with *E. huxleyi* has focused on longer term (hours - days) acclimation responses to irradiance levels (Houdan *et al.* 2005; Leonardos and Harris 2006; Trimborn *et al.* 2007; van de Poll *et al.* 2007; Leonardos 2008; Ragni *et al.* 2008; Harris *et al.* 2009). The present study is the first to examine the kinetics of de-epoxidation and relaxation of xanthophyll activity in the first seconds and minutes of exposure to high light and subsequent return to low light and darkness in the two principal Southern Ocean morphotypes of *E. huxleyi*.

4.4.1 De-epoxidation kinetics and NPQ

The results obtained on the kinetics of NPQ induction and de-epoxidation by *E. huxleyi* show that type A is faster to react initially to high light than type B/C. No previously published rates are available for *E. huxleyi*. The rate of NPQ (k_{NPQ}) induction in type A (0.76 ± 0.10)

was higher than rates published for diatoms exposed to 1700 µmol photons $m^{-2} s^{-1}$ (0.52-0.74 min^{-1}) (Serôdio *et al.* 2005) suggesting a more efficient photoprotective xanthophyll cycle in type A than in diatoms. Type B/C, however, had a k_{NPQ} rate (0.38 ± 0.03) which fell below those for diatoms and less than half that of the type A. The differences in responses to high light intensity between the two morphotypes of *E. huxleyi* have implications for the ability of the type B/C to withstand high light intensities with the same efficiency as type A. Results presented here suggest that the efficiency of xanthophyll activity in type B/C is diminished in comparison to type A at high light intensity or alternatively the type B/C could be utilising different mechanisms to gain protection from high light.

The continuous increase of NPQ and DPS during the 45 min of light stress resulted from the partial de-epoxidation of Ddx to Dtx as indicated by the decrease of the fit of the first-order kinetics model (Eq 2 and 3) for NPQ and DPS after the first 15 min of HL exposure. The slowing of NPQ after the rapid initial rise could be due to *de-novo* xanthophyll pigment synthesis or to damage caused to the photosynthetic apparatus (Arsalane *et al.* 1994). However, photodamage would have led to a larger increase in NPQ than in DPS (Arsalane *et al.* 1994; Cruz and Serodio 2008) which was not the case in the present study. The biphasic rate of NPQ and DPS development from before and after 15 minutes of HL exposure is more likely the result of PSII down regulation, the decline in $\Delta F/F_m'$ by xanthophyll activity and the presence of non-variable quenching rather than permanent photodamage (Ralph *et al.* 2002; Harris *et al.* 2005; Ralph and Gademann 2005; Goss *et al.* 2006; Kropuenske *et al.* 2009) a conclusion supported by the rapid recovery of $\Delta F/F_m'$ in LL and F_v/F_m in darkness. In addition, during HL exposure the $\Delta F/F_m'$ of type A remained at almost double the value ot type B/C indicating that more of the excitation energy is being transferred to type A PSII reaction centres than in type B/C (Ralph & Gademann 2005).

4.4.2 Diadinoxanthin pool

There is evidence that Ddx in diatoms is present in two pools with only one of these pools participating in the xanthophyll cycle, the other is suggested to serve as a precursor for fucoxanthin synthesis (Goericke and Welschmeyer 1992; Arsalane *et al.* 1994; Olaizola and Yamamoto 1994; Harris *et al.* 2009). Harris *et al.* (2009) described that initially within

minutes of being exposed to HL a rapid conversion of Ddx to Dtx occurs and subsequently, with continued exposure for 20 - 30 min the pool of Ddx returns to its original concentration. Finally, with exposures greater than 30 min a further increase in Dtx occurred without appreciable decreases in Ddx (Olaizola *et al.* 1994; Olaizola and Yamamoto 1994). Although the pattern of DPS was not exactly as described by Harris *et al.* (2009) in that Ddx did not return to original concentrations in the present study, there is some evidence for two diadinoxanthin pools. Not all Ddx was converted to Dtx. Olaizola and Yamamoto (1994) consider that the incomplete conversion of Ddx to Dtx suggests the presence of two functionally distinct pools of Ddx in the diatom *Chaetoceros muelleri*. In the present study, one Ddx pool was rapidly converted to Dtx within 0-5 min whereas the second pool (with a different rate constant) was not de-epoxidised. The second pool behaved differently in type B/C than anticipated by the dual pool scenario. In type A, Dtx did not increase along with the observed increase in Ddx at 5 min, suggesting that further de-epoxidation was halted. In type B/C, Dtx increased concomitantly with Ddx between 10 and 15 min, suggesting that Ddx was synthesised and de-epoxidation to Dtx continued. After this time, both Ddx and Dtx decreased. Olaizola and Yamamoto (1994) suggest that the second pool has a different function or there is a differential availability of the de-epoxidase. The pathway of xanthophyll biosynthesis suggested by Stolte (2000), Harris *et al.* (2009) and Lohr & Wilhelm (1999) provides a potential function for the second pool of Ddx.

4.4.3 Xanthophyll synthesis pathway

Goericke & Welschmeyer (1992) describe 3 possible biosynthetic pathways between fucoxanthin, Ddx and Dtx and propose that Ddx is not only the epoxidation product of Dtx but also a precursor for fucoxanthin leading to the suggestion of a dual Ddx pool. In *E. huxleyi* , Leonardos & Harris (2006) suggest that Hex is synthesised from fucoxanthin with light as the modulating factor with strong correlations between Hex and fucoxanthin reported by Stolte *et al.* (2000). Lohr & Wilhelm (1999) showed that violaxanthin, a xanthophyll pigment in other algae and higher plants, is the putative precursor of both Ddx and fucoxanthin in the diatom *Phaeodactylum tricornatum* all synthesised from β-carotene. Together the suggested biosynthesis pathway is summarised in Harris (2009).

Results presented in this study support the hypothesised biosynthesis pathway and links between carotenoids noting changes in fucoxanthin and 19'-hexanoyloxyfucoxanthin associated with the de-epoxidation/epoxidation of Ddx in both high and low light exposure supporting a relationship between fucoxanthin, Hex and Ddx in *E. huxleyi*. The magnitude of change in both fucoxanthin and Hex was 3 - 4 times greater in type B/C strains than in type A in both high and low light.

Harris *et al.* (2009) encountered a decrease in fucoxanthin:chl *a* in *E. huxleyi* following a shift from LL to HL and subsequent increase during a shift from HL to LL which they claim represents a dual role for fucoxanthin i.e. 1) stoichiometric conversion of fucoxanthin to the xanthophyll cycle pigments; as well as 2) acting as a light harvesting pigment under low light. The results of the current study support this view although it is pertinent that the proportion of fucoxanthin in type B/C strains was 8 - 10 times lower than type A. Furthermore, recovery of $\Delta F/F_m'$ in type B/C cells was considerably slower than in type A and could be due to the lower concentration of fucoxanthin and therefore a decreased ability to harvest sufficient light to maximise photosynthesis in light limiting conditions (Siefermann-Harms 1987).

If as suggested, the dual pool Ddx performs both functions of fucoxanthin synthesis and de-epoxidation in the xanthophyll cycle then each pool will have the opposite effect on light harvesting. Fucoxanthin, highly efficient at transferring excitation energy to the PS II reaction centres (Siefermann-Harms 1987) could be being regulated by the light energy dissipation activity of de-epoxidation (Harris *et al.* 2009). The rapidity with which type A recovered from high light exposure suggests that both Ddx pools whether present as xanthophyll pigments or as light harvesters operate in some form of stoichiometric balance. In contrast, type B/C has a predominance of Hex, a poor light harvester and very low proportions of fucoxanthin. The magnitude of change of these two pigments during irradiance change suggests that a more dynamic response controls the proportions of these carotenoids in type B/C. Speculatively, it is possible that the lower light harvesting efficiency of Hex protects type B/C cells from high light exposure to compensate for the slower de-epoxidation kinetics of the xanthophyll cycle.

In light of previous hypotheses that suggest that Ddx and Hex are synthesized from fucoxanthin (Stolte *et al.* 2000; Harris *et al.* 2009), Fig. 7 presents a schematic summary showing the principal photophysiological differences between the two morphotypes. The scheme is consistent with the dual pool of Ddx, where one pool takes part in the de-epoxidation process of the xanthophyll cycle and the other is associated with fucoxanthin and Hex biosynthesis.

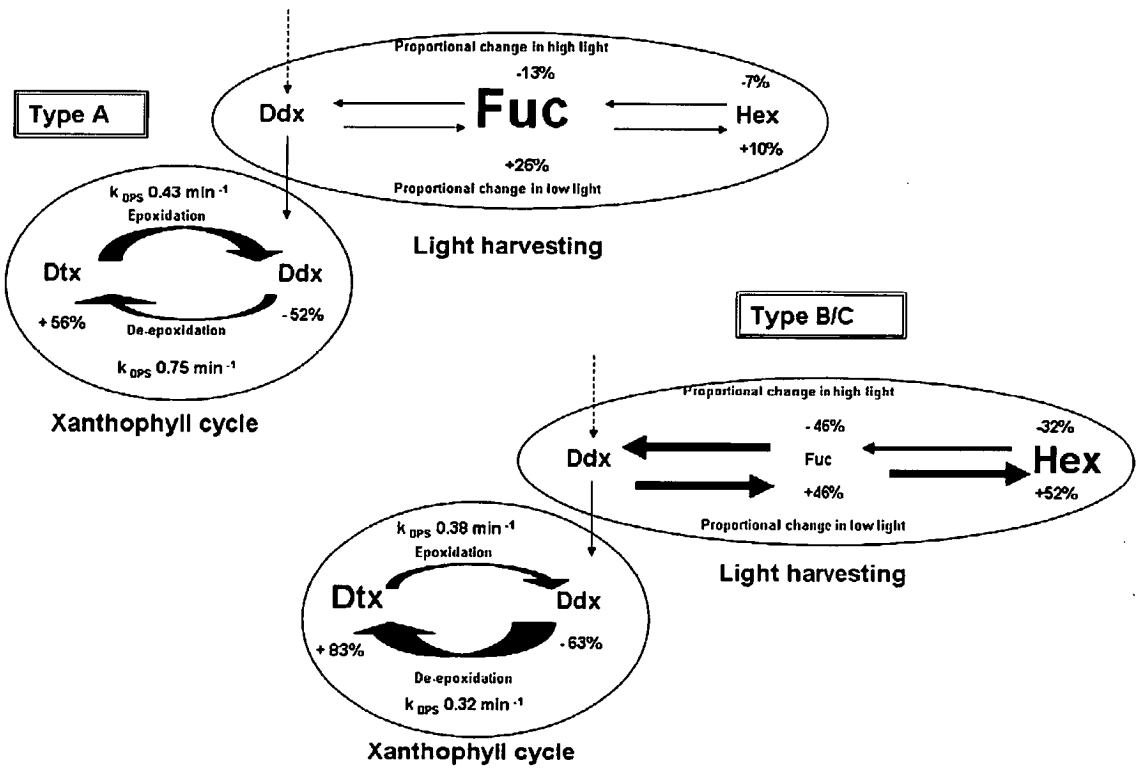

Fig. 4.7. Schematic representation of proportional changes in 19'-hexanoyloxyfucoxanthin, fucoxanthin, diadinoxanthin and diatoxanthin during exposure to high light and subsequent low light. This representation assumes the hypotheses of schemes suggested by Goerick & Welschmeyer (1992), Stolte *et al.* (2000), Lohr & Wilhelm (2001) and Harris (2009). The weight of the arrows and text represent comparison between the two morphotypes in terms of proportional quantities.

4.4.4 Inhibitor treatment

The concentration of inhibitor was determined from previous work where Olaizola *et al.* (1994) used a final concentration of 100 μM DTT which resulted in the complete blocking of de-epoxidation in the diatom *Phaeodactylum tricornutum*. Lohr & Wilhelm (1999) successfully blocked 80% of the de-epoxidation in the same diatom with 500 μM and 100% with 5 mM final concentrations of DTT. Goss *et al.* (2006) showed that 2mM DTT was able to completely inhibit de-epoxidation in 3 diatom species and based on this 2mM was used in the present study. However some incomplete binding of the inhibitor occurred, but did not affect the results.

The DTT inhibitor treatment supports the view of a two-pool scheme for diadinoxanthin concentration, one of which does not undergo de-epoxidation but is the precursor to fucoxanthin. NPQ was significantly reduced by the addition of DTT (78% and 81% in type A and B/C respectively, the remainder most likely incomplete binding of the inhibitor), however only slightly more than half the de-epoxidation was inhibited in type A. The effect of the inhibitor on de-epoxidation suppression was 14% greater in type B/C strains. This suggests that Dtx formation is linked to NPQ but that not all Ddx is linked to xanthophyll activity and NPQ development, supporting the dual pool Ddx hypothesis.

4.5 Conclusions

Differences in photoprotective mechanisms under identical growth conditions should reflect evolutionary adaptations to different oceanic environments. The differential proportions of fucoxanthin and Hex in the two morphotypes of *E. huxleyi* reflect differences in light handling capabilities between the two morphotypes under the imposed growth and experimental conditions. Differences in the time scales and responses to energy dissipation have implications for the competitive advantages of both morphotypes of *E. huxleyi* in their natural light environment. The speed with which de-epoxidation and NPQ development occur in type A and the subsequent rapid $\Delta F/F_m'$ recovery are likely to confer an adaptive advantage in terms high light handling efficiency. Type A is more efficient at minimising the potential for damage to the photosynthetic apparatus by reducing the energy delivered to PSII reaction centres whilst importantly still maintaining photochemistry. Type A cells are typically found in surface waters of temperate oceans typifying the high light environment to which it is well adapted. Accelerated xanthophyll cycling that increases the short-term photoprotective capacity of cells may be an important factor contributing to ecological success of *E. huxleyi* type A during a surface bloom where sustained high light intensities are common.

The balance between photoprotection and photochemistry is less efficient for type B/C, when in high light environments, particularly over the short-term. Type B/C is the dominant morphotype of typically low light, sub-Antarctic waters and found at considerable depth where light is often limiting to photosynthesis and growth, placing less demand on photoprotective mechanisms unless deep mixing should bring cells rapidly to the sea surface (Ross *et al.* 2008). Nevertheless, type B/C still appears capable of initiating a level of photoprotection when exposed to high light over the short term. Type B/C, with its slower response rates and longer timescales to reach its maximum de-epoxidation state and yield recovery may be compromised in its ability to adapt and optimise photosynthesis in typical bloom conditions of high irradiance therefore unlikely to reach the rapid growth rates required to form bloom proportions.

These results suggest that different selective pressures imposed on the type B/C through entrainment within the Antarctic Circumpolar Current have modified physiological characteristics to optimize adaptation to the low light environment of the Southern Ocean (Lavaud *et al.* 2007). The present evidence of differences in photophysiology together with previous evidence of differences in photosynthetic pigments and coccolith morphology strongly argue that type A (var. *huxleyi*) and type B/C (var. *aurorae*) require rigorous discrimination when conducting ecophysiological surveys in the Southern Ocean. Furthermore, if as predicted under climate change models, ocean stratification and shallow mixing increase, Southern Ocean conditions will have serious implications for the survival of the type B/C as it is likely to be exposed to longer term high light conditions and may possibly lack the capacity to adequately and rapidly adapt. In depth investigation into the intracellular processes of photoprotection for type B/C would be desirable in order to determine if the slower de-epoxidation kinetics identified here are in fact detrimental during HL exposure. The capacity of the two morphotypes to manage high light exposure over extended periods of time is explored further in Chapter 5.

5 Photoacclimation and photoinhibition in *Emiliania huxleyi* morphotypes from the Southern Ocean

Submitted to Marine Ecology Progress Series as:

Ecophysiological differences between two Southern Ocean morphotypes of *Emiliania huxleyi* (Haptophyta): Photoacclimation and Photoinhibition

Suellen S. Cook,
School of Plant Science, University of Tasmania, Private Bag 55, Hobart, Tasmania 7001, Australia

Andrew McMinn,
Institute of Marine and Antarctic Studies, Tasmania 7050, Australia

Peter J. Ralph,
Plant Functional Biology and Climate Change Cluster (C3)
University of Technology, Sydney

and Gustaaf M. Hallegraeff
Institute of Marine and Antarctic Studies, University of Tasmania, Private Bag 55, Hobart, Tasmania

Author for correspondence: email sscook@utas.edu.au

5.1 Abstract

Acclimation to high (HL = 600 µmol photons $m^{-2} s^{-1}$) and low (LL = 30 µmol photons $m^{-2} s^{-1}$) growth irradiance on triplicate strains of *Emiliania huxleyi* morphotypes A and B/C from the Southern Ocean were investigated. Short-term stress effects and recovery from 90 min exposure to simulated midday level irradiance (SMI) of 1500 µmol photons $m^{-2} s^{-1}$ using PAM fluorometry and rapid light curves (RLC) were also examined.

Under high growth irradiance and following SMI exposure, substantial photoinhibitory stress responses in both morphotypes were evident. However the effects were found not to be permanent in either morphotype when acclimated to HL. When acclimated to LL both morphotypes experienced slowly reversible or permanent photodamage when exposed to SMI. Light saturation following long-term acclimation to both light regimes was 30% - 35% higher in type A than in type B/C. During SMI exposure, the E_k values of type B/C HL grown cells more than doubled, whereas in type A E_k increased by 26% to reach similar levels to type B/C. Under LL conditions E_k of type B/C cells increased by 55% and type A by 40%.

Type A cells exhibited 30 - 40% higher $rETR_{max}$ than type B/C, indicating a greater energy sink capacity at higher light intensities. The negative impact of high growth irradiance on PSII reaction centre closure in type B/C strains was 2 fold greater than for type A. Type B/C showed a marginally greater capacity to optimise photosynthesis in low light (higher α) reaching maximum photosynthetic capacity at lower irradiance levels. Although type B/C acclimated to HL, a greater amount of damage to PSII reaction centres was incurred in comparison to type A. As a consequence it is considered that type B/C would be unlikely to form surface blooms as the priority for photoprotection may compromise growth at high irradiance levels.

Abbreviations: RLC, Rapid light curve; F_o, Minimum fluorescence of a dark adapted sample; F_v/F_m, F_v'/F_m', Maximum quantum yield of PSII in a dark-adapted state and under actinic light; F_m', Maximum fluorescence under actinic light; $\Delta F/F_m'$,Effective quantum yield of PSII; NPQ, Non-photochemical quenching of fluorescence; LL, Low light ; HL, High light;

SMI, Simulated midday irradiance; rETR, relative electron transport rate; E_k , the irradiance at which light saturation commences; α, photosynthetic efficiency in the light limited region of the RLC.

5.2 Introduction

Only two of the approximately 200 extant species of coccolithophorids (Jordan and Green 1994; Young *et al.* 2003) are known to form seasonal blooms and these can cover as much as 100,000 km^2, *Gephyrocapsa oceanica* (temperate and tropical waters) and *Emiliania huxleyi* (temperate and high latitude oceans). Such blooms are climatically of global significance through the production of dimethylsulphide, large fluxes of calcium carbonate from surface waters to the sediments and impacts on CO_2 air-sea exchange (Westbroek *et al.* 1994).

Most of the recorded blooms have occurred in northern hemisphere waters (Zondervan 2007). *Emiliania huxleyi* blooms in the Southern Ocean have been poorly documented, most likely due to poor coverage of the Southern Hemisphere oceans by CZCS imagery (Iglesias-Rodríguez *et al.* 2002). *Emiliania huxleyi* was first reported in Antarctic waters by Hentschel (1932) and subsequently by McIntyre and Bé (1967) who described *E. huxleyi* populations south of the Antarctic Polar Front. More recently, Findlay and Giraudeau (2000), Cubillos *et al.* (2007) and Mohan *et al.* (2008) described the distribution of coccolithophorids in Antarctic waters, some as far south as 64°S.

In 2002, Iglesias-Rodriguez used SeaWiFS imagery to suggest that during summer in the Southern Ocean large coccolithophorid blooms formed a belt north of the Antarctic Polar Front in the Pacific and Atlantic sectors following the Antarctic Circumpolar Current. Southern Hemisphere blooms have also been described by Siegel *et al.* (2007) off the coast of Namibia in the Atlantic Ocean. It has been found from satellite and experimental data that coccolithophorid blooms coincide with areas of low turbulence, decreasing nitrate concentrations and a stable water column with shallow mixed layers (10 - 20 m). Irradiance, however, appears to be the pivotal factor determining the occurrence of *E. huxleyi* blooms (Nanninga and Tyrrell 1996; Iglesias-Rodríguez *et al.* 2002; Siegel *et al.* 2007; Zondervan 2007).

Maximum down-welling irradiance at the sea surface can reach up to 2000 µmol photons m^{-2} s^{-1} (PAR) at midday under clear skies, although in reality values greater than 1500 µmol photons m^{-2} s^{-1} are rarely encountered as significant attenuation occurs through the mixed

layer (Kirk 1994). Ross *et al.* (2008) demonstrated that cells in turbulent environments can experience rapid and extreme shifts in irradiance from < 250 to > 1500 µmol photons m^{-2} s^{-1}. Nanninga and Tyrrell (1996) calculated that the average light intensity in a mixed layer of 15 m depth in the Southern Ocean is 780 µmol photons m^{-2} s^{-1} ($K_d \sim 0.1$ m^{-1}). Irradiances greater than 500 µmol photons m^{-2} s^{-1} have been reported (Nanninga and Tyrrell 1996) during blooms of *E. huxleyi* in shallow mixed layers (< 20 m).

Emiliania huxleyi appears to be tolerant of the effects of extreme irradiance levels, particularly in bloom conditions (Tyrrell and Taylor 1996; Nielsen 1997; Iglesias-Rodríguez *et al.* 2002; Merico *et al.* 2004; Harris *et al.* 2005; Harris *et al.* 2009). Laboratory studies show minimal photoinhibitory effects in *E. huxleyi* at high light intensities (a reduction in maximum photosynthetic rate of 5 - 20%) when light levels exceed 1000 µmol photons m^{-2} s^{-1} (Nanninga and Tyrrell 1996). Nielsen (1995) found no evidence of photoinhibition of the photosynthetic rate at irradiances up to and including 1700 µmol photons m^{-2} s^{-1}. Whereas in diatom assemblages at the same light levels, a reduction of 40-80% is likely (Kirk 1994; Lavaud *et al.* 2007).

It has been suggested that the coccoliths act as protective screens to excessive light (Nanninga and Tyrrell 1996; Harris *et al.* 2005) or that the calcification process serves as an energy sink to divert energy in excess of photosynthetic needs (Paasche 2001), although neither suggestion has been rigorously confirmed (Nanninga and Tyrrell 1996; Harris *et al.* 2005; Trimborn *et al.* 2007). Recently Leonardos *et al.* (2009) showed, that there is no mechanistic dependence of photosynthesis on calcification in *E. huxleyi*. Despite limited research, the mechanisms by which *E. huxleyi* manages the damaging impact of excessive light energy, still requires further investigation (Leonardos and Harris 2006; Ragni *et al.* 2008; Harris *et al.* 2009).

Previous work has shown that type A and type B/C morphotypes have a different pigment complement (Chapter 3). Furthermore, photophysiological differences in their responses to short term irradiance changes are evident (Chapter 4). The objective of the present study was to characterise the response of laboratory cultured Southern Ocean morphotypes A and

B/C of *E. huxleyi* to long term low and high growth irradiance and to assess their susceptibility to irradiance based photoinhibition and recovery.

5.3 Methods

5.3.1 Algal strains and culture conditions.

Three strains of each of two morphotypes of *E. huxleyi* from the Southern Ocean (Table 5.1) were selected as replicate cultures to examine and compare photoacclimation processes and evidence of photoinhibition and damage in the two Southern Ocean morphotypes. Refer to sampling location map (Fig. 3.1 , page 50)

Table 5.1. Details of culture strains of *Emiliania huxleyi* used in this study

Culture Strain ID.	Morphotype	Location	Light field (% of surface)	Isolation Date	Isolator
EHSO 5.30	A	Southern Ocean			
EHSO 5.25	A	149.2500E:49.5900S	98	Feb 2007	S Cook
EHSO 5.28	A	(7 m depth)			
EHSO 5.11	B/C	Southern Ocean 149.2500E:49.5900S (7 m depth)	98	Feb 2007	S Cook
EHSO 6.17	B/C	Southern Ocean 146.1813E:54.0850S (65 m depth)	47	Feb 2007	S Cook
EHSO 8.15	B/C	Southern Ocean 145.5519E:53.5973S (80 m depth)	10	Feb 2007	S Cook

The six selected strains were batch cultured at 16° C in 300 mL Erhlenmeyer flasks with media using 0.2 µm - filtered natural seawater from east coast Tasmania and the addition of K medium nutrients, metals and vitamins at recommended concentrations including a final concentration of 290 µM L^{-1} nitrate and 4 µM L^{-1} phosphate (Keller *et al.* 1987). A 12:12 h light dark cycle was provided by Cool White fluorescent tubes (Sylvania 36W/w41) with an incident PFD of 30 µmol photons m^{-2} s^{-1} for low light (LL) grown cultures and 600 µmol photons m^{-2} s^{-1} for high light (HL) grown cultures. Cultures were acclimatised for 28 d prior

to the commencement of the experiments. Fresh cultures were inoculated from parental stock every 14 d. Semi-continuous growth conditions were initiated and maintained for these cultures by regularly removing and replacing one third (100 mL) of homogenised media and cells to maintain exponential growth and reach a biomass of approximately 10^6 cells mL^{-1}. Experimentation was commenced within 24 hours of nutrient replenishment.

5.3.2 Fluorescence measurements

Variable fluorescence was measured using a Pulse Amplitude Modulation (PAM) fluorometer (Schreiber *et al.* 1986), a WaterPAM (Walz, Effeltrich, Germany). The PAM method is based on the supply of weak, modulated light pulses (the measuring light) that allows chlorophyll fluorescence to be monitored without inducing photosynthesis. In the dark adapted state a minimum fluorescence (F_o) is determined when the measuring light is turned on, the fluorescence results from emissions from the antenna pigments. When the sample is exposed to actinic light, i.e. light that induces photosynthesis, a much higher fluorescence results. This fluorescence rapidly peaks and then declines until an equilibrium level (F) is attained. This characteristic behaviour is referred to as the Kautsky curve (Schreiber 1994). The maximum (i.e. potential) quantum yield of PSII is determined by exposing the dark-adapted sample to a pulse of very intense light and defined as the ratio $F_v/F_m = (F_m-F_o)/F_m$ or in the case of a light adapted sample effective quantum yield, $\Delta F/F_m'$ or Φ_{PSII}(Schreiber 2004). As actinic light is applied a similar saturating pulse will lead to a maximum (light adapted) fluorescence, F_m', the maximal fluorescence yield of an illuminated sample and referred to as the effective quantum yield of charge separation in PSII, $\Delta F/F_m'$ or Φp and is defined as:-

$$\Delta F/F_m' = (F_m' - F)/F_m'$$

The relative electron transfer rate (rETR) is calculated as:-

$rETR = \Delta F/^{F}{}_m' * E$, where E is the irradiance.

Actinic light levels for the RLCs were preset at 0, 102, 150, 229, 342, 485, 671, 1094 and 1527 µmol photons m^{-2} s^{-1}. The photosynthetic parameters, E_k, $rETR_{max}$ and alpha (α) were estimated for each RLC using a non-linear regression in SPSS with the function $P=P_{max}[1-e^{(-\alpha E/Pmax)}]$ (Webb *et al.* 1974),

where P = photosynthesis (here equivalent to rETR), P_{max} is the maximum photosynthetic rate ($rETR_{max}$), α = alpha, the photosynthetic efficiency of the light limited region of the RLC, E = irradiance (PAR). E_k is derived by dividing P_{max} by α. Non-photochemical quenching was calculated as:-

$NPQ = (F_m - F_m')/F_m'$ (Schreiber *et al.* 1994).

5.3.3 Steady state light curve vs. RLC

A preliminary study of steady state light curves (SSLC) and RLCs was conducted on 3 replicate samples from just one strain of each morphotype (5.30 and 8.15) to assess the similarity between derived parameters. A dark adaption period of 15 minutes was found to be sufficient for NPQ to be completely relaxed. For the SSLC after the 15 min dark adaptation, a single saturating pulse was applied for the assessment of the maximum quantum yield of PSII (F_v/F_m) in the dark adapted state. From previous trials the dark adaptation time of 15 minutes was found to be sufficient for NPQ to fully relax. The sample was subsequently exposed to stepwise increasing irradiance levels from 19 to 1527 µmol photons m^{-2} s^{-1}. Under each irradiance level F and F_m' were measured every 60 s until a steady state was reached (minimum of 6 min). Light curve parameters, rETRmax, α and E_k were calculated in the same manner as those for RLC's in section 5.3.2. Rapid light curves were conducted with the same strains, sampled from the same flask for comparative purposes. The data derived from the steady state light curves were not significantly different from the RLC data and therefore the steady state data of representative samples of both morphotypes is presented but not analysed further.

5.3.4 Acclimation to growth irradiance

Rapid light curves (RLC) were conducted on 3 replicate light adapted samples and 3 replicate dark adapted (15 min) samples from each of the 6 strains for the two growth irradiance levels. In all experiments the PAM manufacturer's supplied stirring device was used to prevent cells from settling and/or becoming carbon limited in the cuvette of the WaterPAM.

5.3.5 Acclimation to simulated midday irradiance

To simulate typical midday irradiance (SMI) each sample was exposed to 90 min of actinic light (1500 μmol photons m^{-2} s^{-1}). From the RLCs conducted before and after SMI the the minimum light saturation point, E_k was calculated (McMinn and Hattori 2006).

5.3.6 Recovery

Following exposure to SMI all but the measuring light was extinguished. Recovery in the dark was recorded with saturating pulses every 2 min to measure $\Delta F/F_m'$ and NPQ relaxation. The degree of recovery after 1 hour and after 24 hours (as indicated in the results section) was normalised to the initial 15 minute dark adapted maximum quantum yield (F_v/F_m) and the difference is expressed as percent recovery of F_v/F_m. Samples retained for recovery assessment after 24 h were sealed with an air permeable film to prevent carbon limitation and bacterial contamination.

5.4 Results

5.4.1 Steady State Light Curves and Rapid Light Curves

Results of the preliminary comparison between steady state light curves and rapid light curves showed no significant differences between the majority of critical parameters (Table 5.2).

Table 5.2. Comparison of steady state light curve and rapid light curve parameters in 3 replicate samples of strain 5.30 (type A) and 8.15 (Type B/C) of *Emiliania huxleyi.*

Morph	Growth Irradiance	SSLC/RLC	$rETR_{max}$	A	E_k
A	HL	SS	95.9 ± 8.2 ns	0.43± 0.03 ***	227± 30 ns
		RLC	81.2± 8.5	0.29± 0.01	276± 22
	LL	SS	91.5± 9.1 ns	0.46± 0.01 ns	201± 21 ns
		RLC	84.4± 0.9	0.46± 0.01	185± 4
B/C	HL	SS	76.1± 12.6 ns	0. 44± 0.01 ***	175± 28 ns
		RLC	57.0± 4.4	0.28± 0.01	206± 16
	LL	SS	83.2± 5.1 **	0.48± 0.01 ns	173± 8 **
		RLC	63.6± 2.7	0.49± 0	130± 6

Significance refers to the comparison between SSLC and RLC derived parameters where * = $P < 0.05$, ** = $P < 0.01$; *** = $P < 0.001$, ns = not significant. (n=3)

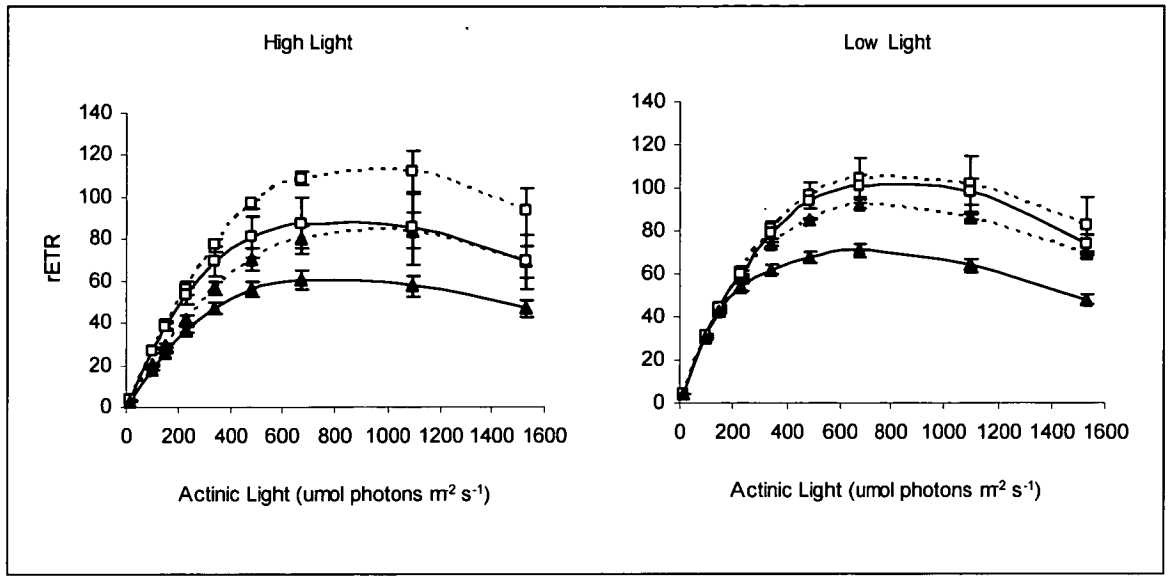

Fig. 5.1. Steady state light curves (SSLC) and rapid light curves (RLC) from 3 replicates of one type A and one type B/C strain of *Emiliania huxleyi*. Dotted lines = type A, black lines = type B/C. Open squares = SSLC and closed triangles = RLC. n = 3.

Statistically significant differences in α were observed between HL and LL growth treatments for both morphotypes. Alpha is a derived parameter is specific to the region of the curve below E_k and this study is focused on the region of the curve above E_k. Furthermore the RLCs began at a higher light level and consequently fewer measurements were performed at the lower light intensities thereby appearing to under estimate α (Ralph and Gademann 2005). The LL grown type B/C parameters, rETRmax and E_k, were statistically significantly different from the rapid light curve data but not α. For the purposes of this study considering the similarity between these two sets of results it was considered appropriate to use RLC data for further analysis of acclimation and photoinhibition.

5.4.2 Acclimation to growth irradiance

There was a significant difference in F_v/F_m ,the maximum quantum yield, between LL and HL growth treatments in both morphotypes ($P < 0.001$) (Table 5.3, "before" values).

Table 5.3. Photosynthetic parameters for morphotypes A and B/C of *Emiliania huxleyi* strains from the Southern Ocean calculated from RLCs. Before and after measures refer to values taken before exposure to 1500 µmol photons m^{-2} s^{-1} for 90 min (simulated midday irradiance, SMI) and after. All light values for growth irradiance, E_k in units of µmol photons m^{-2} s^{-1}; values marked * are the maximum quantum yield values measured after 15 min dark adaption. ΔF/Fm' measurements are those at growth irradiance. Values are means ± se; n = 9). See text for relevant statistically significant differences.

Type	Growth Irradiance	$\Delta F/F_m'$ at growth (before) or treatment (after) irradiance *F_v/F_m after 15 min dark adaption		$rETR_{max}$		α		E_k	
		Before [a]	After[b]	Before	After	Before	After	Before	After
A	HL	0.33 ±0.02 ***0.54 ± 0.01**	0.28 ±0.0	78.96 ± 9.47	73.70 ±2.15	0.21 ±0.02	0.15 ±0.02	368.98 ±36.00	496.07 ±47.30
	LL	0.65 ±0.0 ***0.65 ± 0.01**	0.44 ±0.0	92.24 ± 1.41	75.25 ±7.92	0.47 ±0.01	0.23 ±0.02	196.70 ± 5.01	327.27 ± 6.04
B/C	HL	0.32 ±0.02 ***0.53 ± 0.01**	0.30 ±0.02	49.11 ± 2.92	67.12 ±8.08	0.19 ±0.02	0.13 ±0.02	264.16 ±26.23	545.32 ±48.16
	LL	0.65 ±0.01 ***0.66 ± 0.0**	0.40 ±0.01	63.03 ± 3.02	53.56 ±3.21	0. 50 ±0.01	0.20 ±0.02	128.60 ±10.48	288.54 ±23.91

[a] Before refers to measurements taken from RLCs conducted prior to exposure to SMI

[b] After refers to measurements taken from RLCs conducted immediately after exposure to SMI

In HL grown cells the effective quantum yield ($\Delta F/F_m'$) was about 60% of the potential maximum quantum yield. In contrast, LL grown cells had an F_v/F_m and F_v'/F_m' close to the

optimal value of 0.65 (Kolber and Falkowski 1993). The two morphotypes exhibited little difference in effective quantum yield at either growth irradiance. However, there was a highly significant difference between the effective quantum yield measurements of HL and LL grown samples of the same morphotype ($P < 0.001$). LL grown $\Delta F/F_m'$ were 50% higher than $\Delta F/F_m'$ in HL.

The $rETR_{max}$ of type A was not significantly affected by the growth irradiance but type B/C $rETR_{max}$ was significantly higher in LL than in HL ($P = 0.04$) (Table 5.3). The $rETR_{max}$ of type B/C was consistently lower (32 - 38%) than for type A ($P \leq 0.05$). In low light type B/C had a significantly higher α value than type A ($P < 0.05$).

The irradiance at which photosynthesis became light saturated (E_k) was consistently higher in type A than B/C (28 - 35%). LL grown strains of both morphotype were light limited at growth irradiance of 30 μmol photons $m^{-2} s^{-1}$ (A = 6.5 times higher; B/C, 4 times higher than growth irradiance). E_k in HL grown type A reached 61% of the growth irradiance and 44% in type B/C. The E_k value differences between the morphotypes for each growth irradiance were significantly different (HL – P , 0.05; LL – $P < 0.001$).

5.4.3 Acclimation to simulated midday irradiance (SMI)

Exposure to 90 min of SMI reduced photosynthetic yield in HL grown type A by 14% and type B/C 6% (Table 5.3"after" values). In LL grown strains, type A and type B/C reduced effective quantum yield by 33% and 38% respectively. In contrast to the gradual decrease of yield before SMI exposure the "after" decrease occurred rapidly and simultaneously from the first actinic light step of the RLC (Fig. 5.2). Exposure to SMI generally had little significant effect on $rETR_{max}$ although in LL grown strains of both morphotypes a small reduction in the maximum rate was observed.

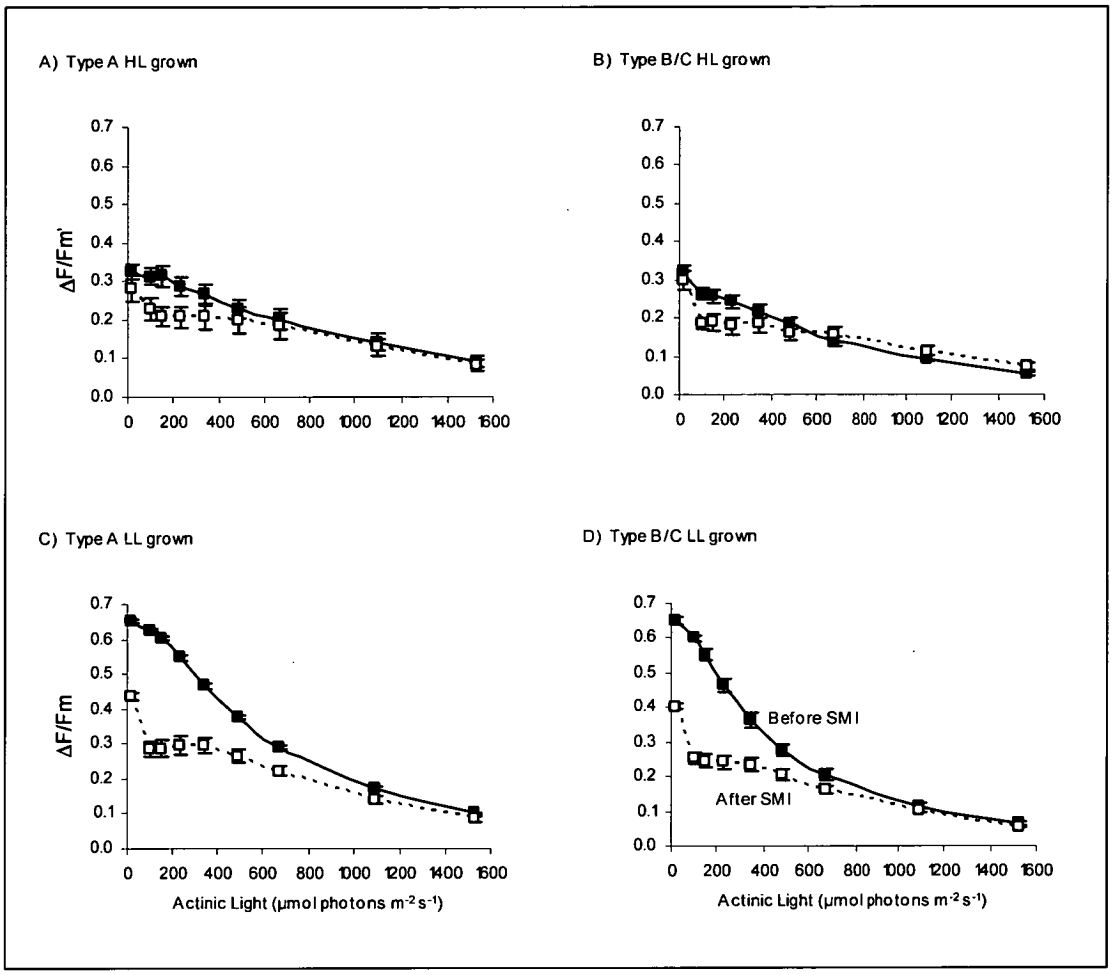

Fig. 5.2. Curves of effective quantum yield ($\Delta F/F_m'$) during RLCs from 3 replicate samples from each of the 6 HL and LL grown strains of *Emiliania huxleyi* before (closed squares) and after (open squares) exposure to SMI. (n = 9).

The major differences in response were in the level of irradiance required to saturate photosynthesis (Table 5.3). During SMI, HL grown cells were exposed to 2.5 times their growth irradiance and LL grown cells to 50 times growth irradiance. During exposure to the SMI exposure E_k of HL grown type A reached 33% of SMI (1500 µmol photons m^{-2} s^{-1}) and 22% of SMI for LL grown type A strains. Correspondingly, type B/C reached 36% and 19% of SMI respectively. Before exposure of both morphotypes to SMI, the values of E_k in both growth irradiances were significantly different ($P < 0.05$), with type A E_k 28% (HL) and 35%

(LL) higher than E_k in both HL and LL type B/C respectively. However, the increase of E_k after SMI was significantly greater in type B/C cells than in type A irrespective of growth irradiance ($P \leq 0.05$). The E_k of type B/C HL grown cells more than doubled, whereas in type A E_k increased by only 26%. In LL type B/C cells E_k increased by 55% and type A by 40% (Fig. 5.3).

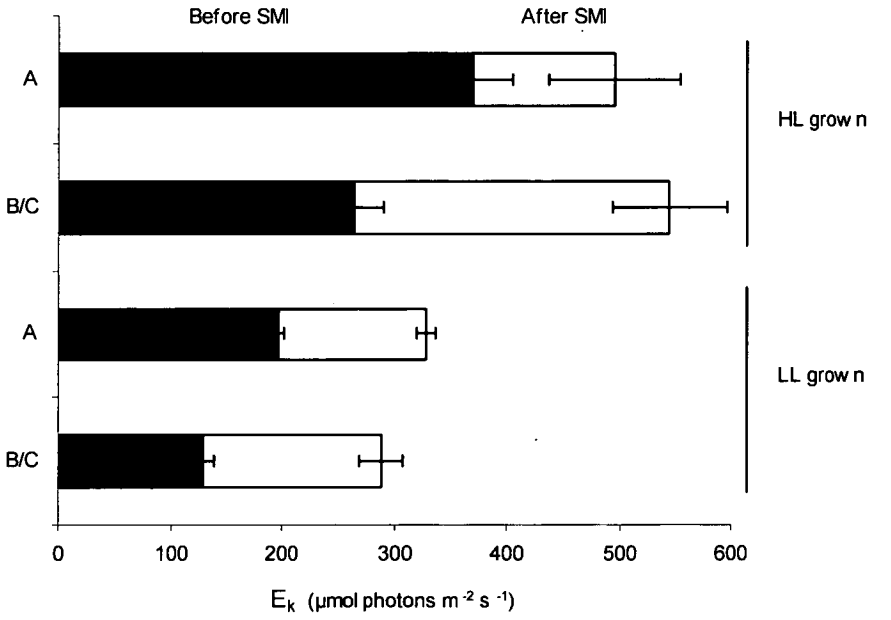

Fig. 5.3. Value of the light saturation parameter E_k before (dark bars) and after (open bars) exposure to 90 min SMI. Values are means ± se, n = 3.

Values of E_k before SMI for type A were significantly different from type B/C in both growth irradiances ($P < 0.05$). Likewise the increase in E_k after SMI was also significantly different between morphotypes grown at the same light level ($P < 0.05$).

5.4.4 *Photoprotection or photodamage*

NPQ in HL grown type A cells showed similar development patterns before and after exposure to SMI (Fig. 5.4).

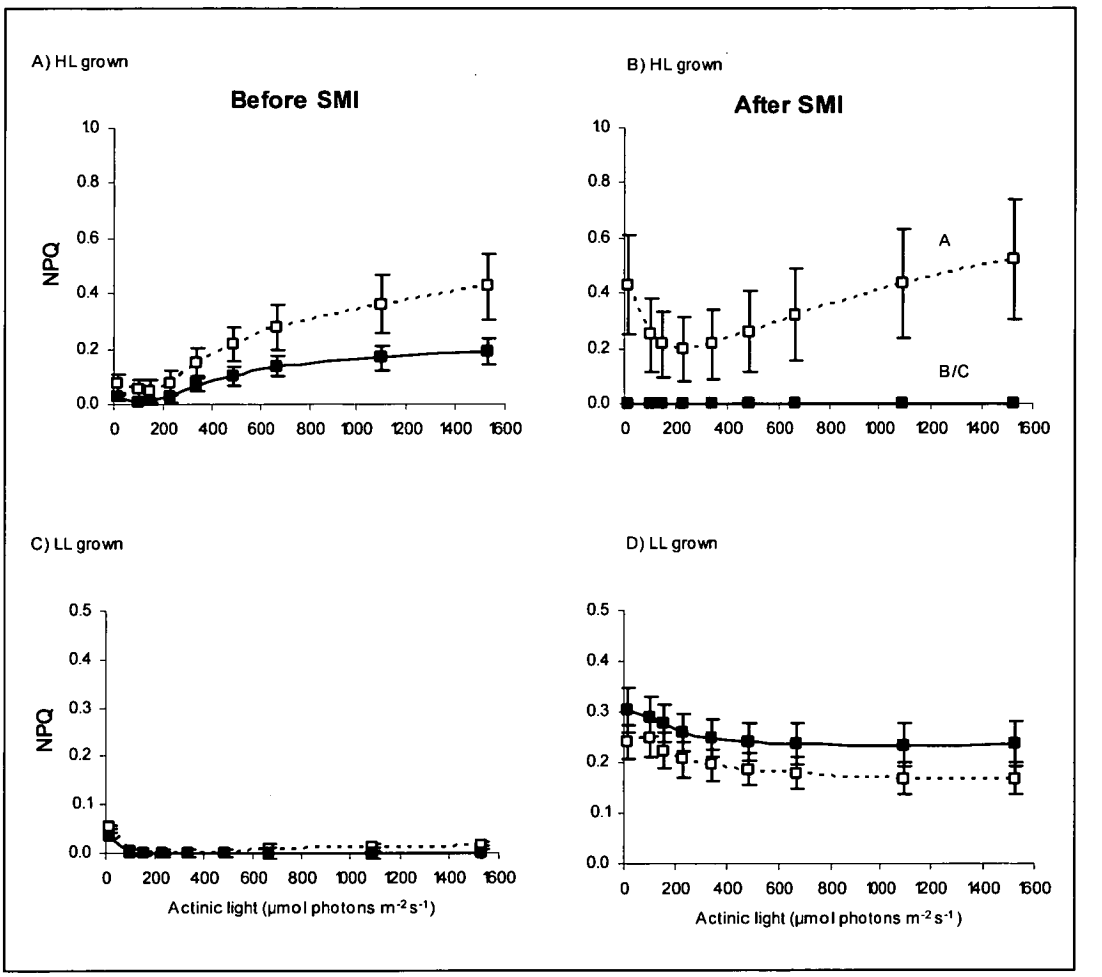

Fig. 5.4. Development of NPQ before and after exposure to SMI in HL and LL grown cells of *Emiliania huxleyi*. Type A = open squares, type B/C closed squares. Values are means ± se, n = 9.

At the low actinic light levels, NPQ relaxed, only to increase again at light levels comparable to the measured E_k values in Table 5.3. NPQ development was more rapid and reached higher levels in HL type A cells than in type B/C both before and after exposure to SMI.

NPQ development in HL cultures was more variable, particularly in type A. LL cultures did not develop NPQ in RLCs prior to SMI exposure and what had developed during SMI reduced in both LL grown A and B/C during the RLCs performed afterwards.

The nature of photoprotection can be determined by examining the development of the minimum fluorescent yield (F), maximum fluorescent yield (F_m') and 1-qP, an indicator of the proportion of reaction centres that are closed due to light saturation (Maxwell and Johnson 2000; Ralph and Gademann 2005) (Fig. 5.5). High light grown cells prior to SMI exposure showed a relatively constant F value and a sudden rise in reaction centre closure at very high light levels (Fig. 5.5). The sink capacity for the captured energy was able to deal with the full range of incoming irradiance (up to 1527 µmol photons $m^{-2} s^{-1}$). At the same time the value of F_m' decreased with increasing irradiance. After exposure to SMI HL grown cells, showed a small increase in Fat low values of actinic light (below E_k),, most likely because of insufficient pseudo dark adaptation time between SMI being extinguished and the commencement of the RLC. As the RLC progressed both F and F_m' showed a minor decline with a concurrent increase of reaction centre closure followed by re-opening as the effect of photprtoective measures increased. The pattern of change in F and F_m' was similar in both HL grown morphotypes and indicates the presence of energy dissipating NPQ from xanthophyll activity .

Prior to SMI minimum fluorescence increased rapidly in both LL grown morphotypes while F_m' remained constant. Reaction centre closure index increased rapidly after E_k (100-200 µmol photons $m^{-2} s^{-1}$) had been exceeded. After exposure to SMI the F_m' of LL grown cells remained relatively constant while F continued to rise.

Type A

Type A 5.25 HL grown before SMI

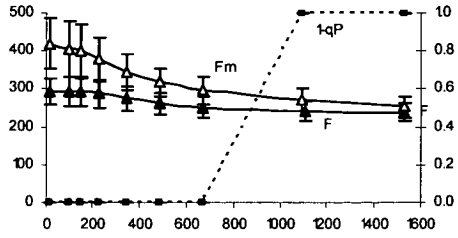

Type A 5.25 HL grown after SMI

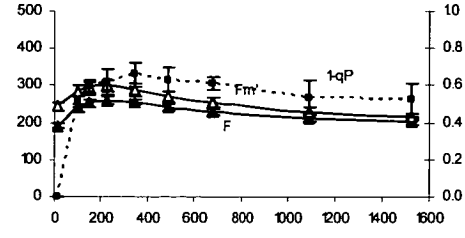

Type A 5.25 LL grown before SMI

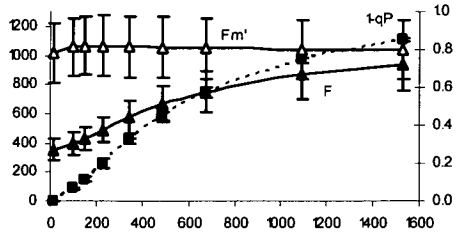

Type A 5.25 LL grown after SMI

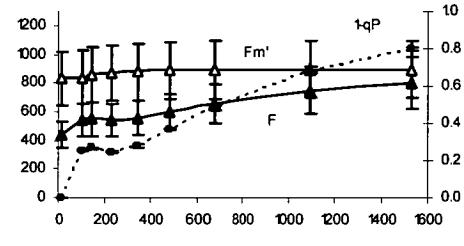

Type B/C

Type B/C 5.11 HL grown before SMI

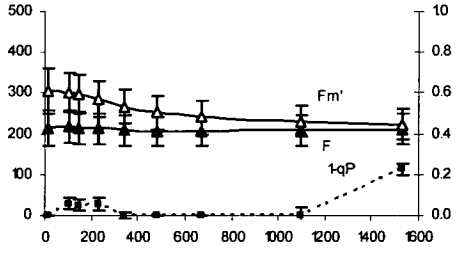

Type B/C 5.11 HL grown after SMI

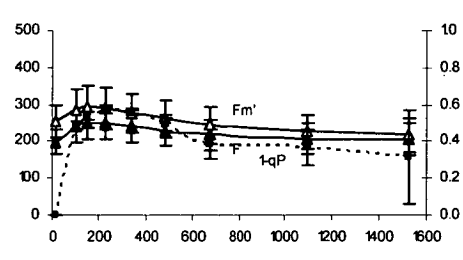

Type B/C 5.11 LL grown before SMI

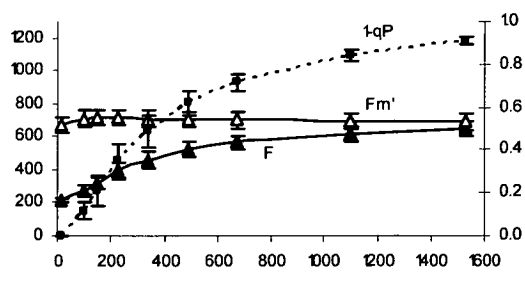

Type B/C 5.11 LL grown after SMI

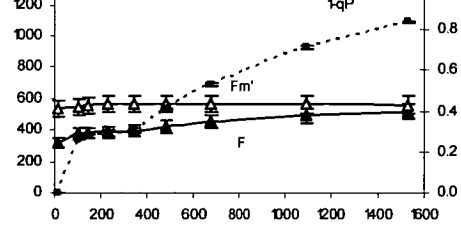

Actinic Light (µmol photons m^{-2} s^{-1})

Actinic Light (µmol photons m^{-2} s^{-1})

Fig. 5.5. Curves (1 strain of each morphotype) of F, minimum fluorescent yield (closed triangles) and F_m', maximum light-adapted fluorescence yield (open triangles;) and 1-qP, an index of reaction centre closure (closed squares) as a function of PAR from RLCs conducted before and after exposure to SMI (n=3). See Appendix 3 for remaining strains of *Emiliania huxleyi* .

After exposure to 90 min of SMI cells were held in the PAM cuvette to assess dark recovery of F_v/F_m (Fig. 5.6).

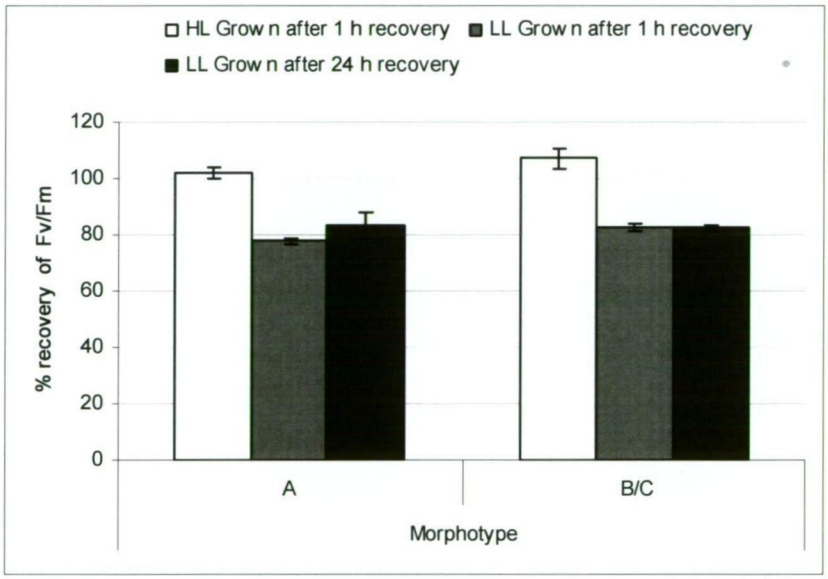

Fig. 5.6. Percentage recovery of $\Delta F/F_m'$ in type A and type B/C strains of *Emiliania huxleyi* after exposure to SMI. Values are means ± se, n = 9.

HL grown A and B/C morphotypes showed a 100% recovery within an hour of being returned to the dark, with type A samples reaching 80% of pre exposure F_v/F_m within 1 - 10 min of being placed in the dark, type B/C varied between 30 s and 20 min. However, the F_v/F_m of HL grown cultures was already 20% below the theoretical optimum 0.65 (Kolber and Falkowski 1993). Low light grown cultures of both morphotypes failed to recover to pre-SMI exposure yield levels reaching and remaining at 80% recovery after 10 min of being in the dark. After the 1 h recovery period between 20 - 72% of NPQ remained in both

morphotypes of LL cells whereas NPQ in HL acclimated cells returned to zero within the first 2 - 3 min of darkness in type A cells and between 5 and 25 min in type B/C cells.

5.5 Discussion

The ability of *E. huxleyi* to form large seasonal sea surface blooms has been attributed to its capacity to withstand high light levels (Balch *et al.* 1992; Nanninga and Tyrrell 1996; Zondervan 2007). The contribution to blooms of the various morphotypes is only rarely identified (Gayoso 1995; Iglesias-Rodríguez *et al.* 2002; Merico *et al.* 2004; Siegel *et al.* 2007; Zondervan 2007). Therefore the comparative ability of different morphotypes to manage high light conditions has not been defined. In chapter 4 the potential competitive advantage of rapid onset of xanthophyll cycling in type A and in contrast, the slower response in type B/C was reported. In those experiments both morphotypes were acclimated to the same light level of 70 μmol photons m^{-2} s^{-1}. Long-term acclimation involves adjusting the quantity and composition of the light harvesting pigment complement as these pigments define the quantity and intensity of light energy transferred to the photosystems (Leonardos and Harris 2006; van de Poll *et al.* 2007). The 28 d acclimation period prior to experimentation used here is considered sufficient for full acclimation to the two ambient light levels chosen for this study (Harris *et al.*, 2009, Leonardos, 2008, Leonardos & Harris, 2006, Ragni *et al.*, 2008).

The preliminary investigation of the comparison between steady state light curve and rapid light curve parameters showed a remarkable similarity between the two distinctly different processes. Comparisons between SSLCs and RLCs have been made on mixed benthic diatom assemblages (Serôdio *et al.* 2006; Cruz and Serodio 2008). However these studies have conducted a RLC at each steady state step on the same mixed community sample. In the present study, 2 independent samples taken from the same stock culture source were used to conduct a RLC on one and a SSLC on the other in order to prevent any additive effect from the light treatment of both methods on the same sample. Consequently derived parameters are not directly comparable. The most significant difference between the two methods found in the present study is the estimation of α, where only in HL grown cultures RLCs indicated an α half the value indicated by the SSLC. In LL grown cultures the values were identical.

Light steps of RLCs are too short to completely alter the established photoacclimation status and therefore they are a useful means of assessing photosynthetic capacity in increasing actinic light intensities given a background of an established light acclimation status (Schreiber *et al.* 1994; Falkowski and Raven 1997; Ralph 1999; White and Critchley 1999; Ralph and Gademann 2005). Further, by exposing both HL and LL grown cultures to a period of SMI, an attempt was made to simulate conditions *E. huxleyi* cells experience in the field during blooms.

5.5.1 Acclimation status of LL vs. HL grown cells

Dark-adaptation prior to a RLC allows PSII reaction centres to fully open, the electron transport chain to be oxidised and photoprotective mechanisms (xanthophyll cycle) to be relaxed allowing a measurement of maximum photochemical efficiency (F_v/F_m) of cells (Ralph 1999; Ralph and Gademann 2005). While healthy algal cells are characterised by F_v/F_m values around 0.65 (Kolber and Falkowski 1993), they may display a very different photosynthetic capacity depending on their long-term light adaptation state during growth (Schreiber 2004). For *E. huxleyi* Harris *et al* (2005) reported a relatively constant value of F_v/F_m of 0.59 and Ragni (2008) even lower values of between 0.50 and 0.55 characteristic of the single turnover FRR fluorometry used in the Ragni (2008) study. Both studies observed that irradiance did not have a significant effect on F_v/F_m. However, this was not the case here. High growth irradiance significantly lowered F_v/F_m by 18% in type A and by 20% in type B/C, from around 0.65 in LL to 0.53 in HL respectively. Given that the cells were maintained in semi continuous culture conditions replenished with nutrient replete media, lower values of F_v/F_m are an indicator of photodamage to the reaction centres rather than nutrient stress or carbon limitation (Harris *et al.* 2005).

Under high growth irradiance and SMI exposure substantial photoinhibitory stress responses in both morphotypes were evident. However, the effects were found not to be permanent in strains of either morphotype that had been previously acclimated to a high light regime. HL cells displayed rapid reversal of photoinhibitory effects and $\Delta F/F_m'$, suggesting HL acclimated cells were capable of rapid repair and were able to acclimate sufficiently to prevent long-term photodamage and were not nutrient stressed. This was not the case for LL

grown cells of either morphotype, where full recovery of $\Delta F/F_m'$ was significantly slower or non-existent. Ragni *et al.* (2008) reported similar observations of rapid recovery in HL acclimated *E. huxleyi* (type A) but significantly slower in LL acclimated cells suggesting that some PSII inactivation or damage had occurred.

Cells acclimated to HL had lower than ambient E_k values. Type A reached light saturation at 61% of growth irradiance and type B/C at 44%. Nanninga & Tyrrell (1996) reported that when *E. huxleyi* was acclimated to 200 μmol photons $m^{-2} s^{-1}$, E_k values calculated from oxygen derived P-E curves, were also well above growth irradiance (E_k = 500 μmol photons $m^{-2} s^{-1}$). Whereas Balch *et al.* (1992) acclimated cells to 1160 μmol photons $m^{-2} s^{-1}$ and calculated (carbon uptake P-I curves) E_k values of 500 μmol photons $m^{-2} s^{-1}$ that were significantly lower than growth irradiance. It appears that the optimum light intensity falls within defined lower and upper limits, in this study between 190 and 550 μmol photons $m^{-2} s^{-1}$ for type A and between 115 and 600 μmol photons $m^{-2} s^{-1}$ for type B/C depending on light acclimation status. Despite slower responses to and recovery from HL, type B/C appears to have the capacity to manage light as shown by changes in E_k and recovery of $\Delta F/Fm'$, through a wider range of intensities.

Photoprotective mechanisms appeared capable of preventing permanent photodamage or at least rapidly repairing photodamage in cells acclimated to HL both before and after SMI exposure, an observation also reported by Harris *et al* (2005). The decline in F_m' and the steady F signal of HL samples and the coincident development of NPQ indicates that growth illumination did not cause substantial permanent PSII reaction centre closure and is a pattern typical of down-regulation of photochemistry through the action of xanthophyll cycling (Ralph and Gademann 2005). The decline in $\Delta F/F_m'$ was slow and steady over the course of the RLC. After exposure to SMI and at low actinic light levels of the RLC ($< E_k$) both F and F_m' increased concurrently. A rise in F indicates PSII reaction centre inactivation however NPQ was evident indicating that some PSII reaction centres were rapidly re-opening further indicated by the drop in the reaction centre index 1-qP. Furthermore, this rise during the low light levels of the RLCs suggests that there was insufficient pseudo-dark adaption after exposure to SMI before commencing the RLC. F_m' and F are at very low levels at the end of

the period of SMI and are still recovering during the low light steps of the RLC. As irradiance increased above E_k the two values (F and F_m') decreased and converged, decreasing $\Delta F/F_m'$ due to energy loss and the down-regulation of photochemistry as PSII reaction centres temporarily cease to operate but were not actually damaged (Gorbunov *et al.* 2001; Ralph and Gademann 2005). The responses were almost identical in both morphotypes of HL grown cells. Furthermore F_v/F_m in both morphotypes recovered completely within 30 s of darkness following SMI and NPQ returned relatively rapidly to zero. The rate at which NPQ returns to zero in darkness is an indicator of tolerance to high light (Ralph and Gademann 2005). This suggests a well-developed mechanism to dissipate energy via the NPQ pathway, which was much faster in type A than it was in type B/C.

Overall, cells growing in LL were light-limited, as indicated by the higher than ambient E_k values. E_k of type A was 6.5 times greater than growth irradiance and type B/C 4.3 times. Prior to SMI exposure LL acclimated cells, showed a relatively constant F_m' corresponding with a limited capacity for non-photochemical energy dissipation. The increase in F signifies the rapid closure and inactivation of PSII reaction centres (White and Critchley 1999). E_k for both morphotypes was surpassed at step 3 of the RLC. As irradiance increased further all PSII reaction centres were effectively closed, and hence not able to transfer energy for photo-chemical usage, producing a rapid decrease in $\Delta F/F_m'$ and rapid rise in the reaction centre index, 1-qP (Maxwell and Johnson 2000; Ralph and Gademann 2005). There was a more rapid rise in F in type B/C than in A but the rate of increase slowed at about the same point in the RLC (400 - 500 μmol photons $m^{-2} s^{-1}$). With exposure to continuous high light, inhibition occurred and rETR declined (Ralph and Gademann 2005).

After SMI, the steady rate of F_m', and increase in F and rise in 1-qP confirm that photodamage had occurred in LL grown samples. NPQ decreased in both morphotypes. . The decline in NPQ, the rise in F and the sudden decrease in $\Delta F/F_m'$ (particularly in type B/C) together indicate that non-reversible damage had occurred. Furthermore, photosynthetic yield failed to recover within 24 hours of exposure to SMI in both A and B/C LL acclimated strains. The slow rate of NPQ relaxation indicated that LL acclimated cells do not tolerate sudden high light exposure and signified that damage had occurred to PSII

reaction centres that could take some time to repair (White and Critchley 1999; Ralph and Gademann 2005). Data presented by Ragni *et al.* (2008) also showed that the rate of repair is inhibited in LL adapted cells upon HL exposure.

5.5.2 Acclimation status of morphotype A vs. B/C

The two morphotypes responded slightly differently to growth irradiance levels. Type A cells had 40 % higher $rETR_{max}$ resulting in 30% higher E_k values and less down-regulation of photosynthesis indicating a greater energy sink capacity at higher light intensities (Ralph and Gademann 2005). Type B/C on the other hand showed a greater capacity to optimise photosynthesis in low light (higher α) reaching maximum photosynthetic capacity at a lower irradiance level.

Type B/C cells acclimated to HL were able to match HL type A in the degree of movement of the minimum light saturation point (E_k) during SMI, despite having a significantly lower light saturation point before exposure. However, type B/C cells acclimated to LL did not match the E_k of LL type A cells, despite doubling their light saturation point. Clearly not only was previous light history pivotal in determining SMI responses, but so was the photophysiology of each morphotype.

The proportion of PSII reaction centres that are open and available for photochemistry is directly related to $\Delta F/F_m'$ of PSII. Harris *et al.* (2005) concluded that at comparable rates of light absorption, cells acclimated to high light can maintain a greater proportion of open PSII reaction centres than cells acclimated to low light. Under the assumption of no photodamage when grown under the low growth irradiance, the fraction of chronically damaged PSII reaction centres in HL grown cells can be estimated as the difference between $(F_v/F_m)_{LLgrown}$ and $(F_v/F_m)_{HLgrown}$, normalized to $(F_v/F_m)_{LLgrown}$ (Gorbunov *et al.* 2001). Using this formula 16% of the PSII reaction centres in type A HL grown cells were chronically damaged by daily exposure to the HL growth irradiance whereas in type B/C as much as 30%. This suggests that type A has either a lower damage rate or higher repair rate of PSII reaction centres than type B/C. Thus type B/C cells growing in high light conditions are less efficient at managing that light than type A.

Both HL and LL type A cells were acclimated to an E_k value significantly higher than their respective B/C cells before exposure to SMI. E_k of B/C cells more than doubled after SMI exposure with HL B/C cells surpassing the E_k of HL type A cells indicating that the B/C morphotype is capable of withstanding short periods of high light levels regardless of its prior light history

5.6 Conclusions

Results presented here demonstrate that the two *E. huxleyi* morphotypes, A and B/C, use light and are affected by light differently according to the light level to which they have previously been acclimated. The similarity between SSLCs and RLCs may indicate an extremely rapid acclimation process within *Emiliania huxleyi*. This aspect of the study requires further investigation with a greater number of strains from each morphotype. However, the data from RLCs showed that both morphotypes, if acclimated to LL, will suffer slowly reversible or permanent photodamage if suddenly exposed to typical midday irradiance levels at the sea surface, type B/C more so than type A. The effect of SMI on minimum and maximum fluorescent yield shows that in LL grown strains of both morphotypes reaction centre closure occurs and NPQ is limited. Cells acclimated to HL maintain a greater proportion of open PSII reaction centres than cells acclimated to LL suggesting well developed D1 protein repair capacity (Long *et al.* 1994; Harris *et al.* 2005). This is an important difference between the two morphotypes when growing in HL. Type A cells experience half the reaction centre closure than type B/C and faster $\Delta F/F_m'$ recovery when in high light whereas type B/C cells have the capacity to acclimate to a wider range of irradiance levels both lower and higher than type A.

The results of this study provide important insight into the mechanisms underlying the success of *E. huxleyi* morphotypes in high light environments. Acclimation to ambient light plays a pivotal role in its success. Cells residing longer in the upper layers of the mixed layer have the acclimation capacity to endure periods of excessive irradiance as might be experienced at the sea surface. Whereas those that have been residing at greater depth or experience deep mixing and hence lower overall light availability, if brought to the sea surface experience photodamage and lengthier recovery times. This has the potential to offset photosynthetic efficiency and possibly growth. With its higher fucoxanthin content, rapid xanthophyll de-epoxidation activity and rapid recovery/repair mechanisms (chapters 3 and 4), type A has adaptations to a narrower range of light intensities but is more efficient in sustained high light conditions. In contrast, type B/C, although possessing the capacity to withstand and acclimate to high light, has adaptations to a wider range of light intensities but experiences photodamage and slow $\Delta F/F_m'$ recovery. Nevertheless, type B/C has better

adaptations for low light environments, where greater photosynthetic efficiency than type A was evident from the results presented here. Despite the apparent wider acclimation capacity to the extremes of the light environment, it is predicted that type B/C would be unlikely to form surface blooms as growth could be severely compromised by the need for photoprotection and repair.

6 Conclusions and Implications

This thesis draws together elements of coccolithophorid physiology, morphology and genetics to further our understanding of the fundamental differences between Southern Ocean *E. huxleyi* morphotypes A and B/C. This taxon has, for a long time, been considered a cosmopolitan species though examination of the literature regarding *E. huxleyi* genetics indicated significant and widespread genetic variability within type A populations, even within blooms (Brand 1982; Young and Westbroek 1991; Iglesias-Rodriguez *et al.* 2006b). The genetics study was important to determine differentiation between the two morphotypes originating from, not only the Southern Hemisphere but in particular the Southern Ocean, and to recognise the variability that exists within morphotype A. The examination of coccolith fine structure enabled the morphotaxonomy to be clarified, something that had not previously been scrutinised, particularly with respect to Southern Ocean strains. The photophysiology studies have been crucial in pinpointing major differences between the two morphotypes and identifying a novel pigment signature for the Southern Ocean type B/C. Furthermore these experiments have increased our understanding of short term and long term dynamics of light acclimation processes in both morphotypes and importantly, demonstrating a clear difference in the physiological responses to light exposure that provide insight into how type A is able to form large and sustained surface blooms whereas no such blooms of type B/C are known.

The extensive literature on *E. huxleyi* applies to a limited handful of principally Northern Hemisphere strains but little is known about Southern Hemisphere strains, including the Southern Ocean. The use of microsatellite molecular markers with 423 Southern Hemisphere strains covering both A and B/C morphotypes clearly shows the genetic differentiation between the two. In addition, despite considerable admixture, differentiation among type A populations is still clearly evident. It is suggested that ocean currents as well as environmental gradients act as potential barriers to *E. huxleyi* gene flow.

The unresolved taxonomy of the type B/C morphotype prompted a thorough assessment of the morphological differences in Southern Ocean strains held in culture and in field samples.

Measurements taken from 297 individual coccoliths showed a clear and statistically significant morphological difference in element width and fine structure of the central area of the distal shield between the type A and Southern Ocean type B/C, a conservative character that remained stable under prolonged culture conditions. Furthermore, the carotenoid pigment complement in each morphotype showed significant differences. Type A possessed the carotenoid 4-keto-19′-hexanoyloxyfucoxanthin which, despite extensive strain sampling, was undetected in some 30 type B/C strains examined. The vastly different ratios of the two major light harvesting pigments, 19′-hexanoyloxyfucoxanthin and fucoxanthin, are most likely related to differences in light handling capabilities between the two morphotypes. It was considered that these combined differences warranted the raising of the new variety of *Emiliania huxleyi* var. *aurorae* Cook et Hallegraeff for what was previously known as morphotype B/C *sensu* Young *et al.* 2003.

The laboratory experiments into the photophysiological responses to variable irradiance showed that type A and B/C use light and are affected by light differently according to the light level to which they have previously been acclimated. Differences in the time scales and responses of excess excitation energy dissipation have implications for the competitive advantages of both morphotypes of *E. huxleyi* in their natural light environment. Type A cells are commonly found in surface waters of temperate and sub-tropical oceans. The accelerated response of type A to high light whilst maintaining photochemistry and without incurring permanent or long term photodamage appears to be an adaptation to high light environments. This undoubtedly has contributed to the ecological success of this morphotype in surface blooms where sustained high light intensities are common (Nanninga and Tyrrell 1996). In contrast, type B/C, with its slower light response rates and longer recovery timescales, may be compromised in its ability to adapt and optimize photosynthesis in typical bloom conditions of high irradiance. It is unable to sustain the same degree of photochemistry in high light as does type A and hence is unlikely to attain the rapid growth rates required to form and maintain surface blooms. High irradiance would most probably prove damaging to cells over a sustained period of time.

The natural environment of type B/C is one of low-light conditions in the sub-Antarctic, where it is often found at depth where light can be limiting to photosynthesis. It is the dominant morphotype found poleward of 50° S and below the Antarctic Polar Front. The Antarctic Polar Front is characterized by a sharp change in surface water temperatures (3-4° C) which is detectable to depths > 1000 m. This Front creates an environmental gradient boundary for the distribution of species and a barrier to free north-south water exchange (Patarnello *et al.* 1996; Clarke *et al.* 2005). It is highly probably that the temperature gradient and entrainment within the Antarctic Circumpolar Current has isolated type B/C sufficiently to prevent gene flow and thus enabled physiological adaptations to the low-light environment of the Southern Ocean.

Future work should examine the role of temperature in the photophysiological responses to light and investigate in greater detail the physiological mechanisms that control the light responses of the Southern Ocean type B/C. The altered photophysiology of type B/C needs to be taken into account when considering the impact of ocean acidification and increasing CO_2 on *E. huxleyi*.

Climate change models predict that ocean stratification and shallow mixing will likely increase (Hallegraeff 2010), with the consequences of increased irradiance levels occurring for longer periods of time along with increased UV exposure (Gao *et al.* 2009). This may have serious implications for the survival of the type B/C as it may lack the capacity to adequately adapt to the changing environment. Conflicting predictions have been published as to the impact of increasing atmospheric CO_2, with some suggesting increased calcification but others are predicting a decrease (Riebesell *et al.* 2000; Iglesias-Rodriguez *et al.* 2008). Also unresolved is whether *E. huxleyi* possesses a carbon concentrating mechanism, which would impact its photosynthetic capacity in a rising CO_2 atmosphere (Raven *et al.* 2005; Beardall *et al.* 2009). Therefore increasing CO_2 may or may not increase photosynthesis but could be outweighed by the impact of ocean acidification on dissolution or malformation of coccoliths (Hallegraeff 2010),. Knowledge of the lifecycle, reproductive habits and a thorough assessment of the genetic differentiation of type B/C using targeted microsatellite molecular markers are required before definitive predictions can be made. It is imperative

that type A (var. *huxleyi*) and type B/C (var. *aurorae*) should be discriminated in future ecophysiological studies on this keystone ocean phytoplankton.

Appendix A

Allele frequencies by population and marker

Marker	Allele	Bicheno	Trumpeter Bay	EAC eddy	Cape Jaffa	Discovery Bay	Sandy Cape	Maatsuyker Is	Sthn Ocean A	Sthn Ocean B/C	Overall frequency
P02F11	N	35	27	32	26	41	44	5	12	41	
	63						0.023				0.004
	91									0.200	0.004
	93					0.016					0.002
	97		0.012	0.058							0.008
	99	0.286	0.280	0.096	0.593	0.063	0.291	0.060	0.250	0.200	0.232
	101	0.014	0.098	0.115	0.130	0.281	0.151	0.274	0.292	0.100	0.160
	103		0.012	0.115		0.078	0.093	0.107		0.200	0.059
	105						0.012				0.002
	107	0.014									0.002
	113		0.024								0.004
	115	0.014		0.077		0.031		0.036	0.042		0.021
	117					0.031			0.042		0.006
	119			0.096		0.016	0.012	0.060	0.042		0.025
	121		0.061	0.077		0.109	0.128	0.202	0.125	0.100	0.091
	123	0.114	0.183	0.058		0.031	0.058	0.071			0.074
	125	0.214	0.061		0.056	0.016	0.023	0.048	0.042		0.059
	127	0.286	0.183	0.077	0.093	0.016	0.105	0.012			0.105
	129	0.029	0.012	0.096	0.019	0.016			0.125	0.200	0.029
	131					0.031		0.012			0.006

133			0.019	0.074	0.047	0.023	0.036		0.025
135		0.012	0.038	0.019			0.012		0.010
137					0.125	0.047	0.012		0.025
139					0.078		0.036		0.015
141	0.014			0.019		0.035			0.010
143	0.014								0.002
145		0.012							0.002
147		0.024	0.019				0.024	0.042	0.011
153			0.019						0.002
155		0.012							0.002
157			0.038						0.004
161		0.012							0.002
175					0.016				0.002

Marker	Allele	Bicheno	Trumpeter Bay	EAC eddy	Cape Jaffa	Discovery Bay	Sandy Cape	Maatsuyker Is	Sthn Ocean A	Sthn Ocean B/C	Overall frequency
P02E11	N	35	39	24	22	31	35	31	10	9	
	125									0.056	0.002
	133									0.111	0.004
	179									0.056	0.002
	181									0.056	0.002
	183			0.063						0.056	0.008
	185		0.026	0.125							0.017
	187			0.021		0.032	0.016	0.043		0.056	0.017
	189					0.032	0.032	0.071	0.150		0.025
	191					0.113	0.129	0.129			0.051
	193	0.029		0.021				0.014			0.008
	195				0.591		0.129				0.072
	197			0.021	0.068						0.008
	199	0.014	0.103							0.056	0.021
	201	0.471	0.359	0.125	0.068	0.161	0.258	0.100	0.200		0.227
	203	0.143	0.103	0.021	0.045	0.016	0.016	0.057	0.050		0.059
	205		0.103	0.021	0.045		0.177	0.029			0.051
	207	0.043	0.064	0.104		0.016	0.032	0.029		0.056	0.040
	209	0.071	0.064		0.023	0.048		0.029	0.100		0.038
	211	0.114	0.026	0.104	0.023	0.016		0.029	0.050	0.167	0.049
	213				0.023		0.016	0.029		0.167	0.015
	215	0.014			0.045	0.016	0.032	0.029	0.100	0.056	0.023
	217			0.083	0.068		0.032	0.043			0.025
	219			0.021		0.161				0.056	0.025

221				0.065	0.016	0.014		0.056	0.015
223		0.077	0.083		0.048	0.029			0.032
225			0.021	0.065	0.048	0.129	0.150		0.042
227		0.013	0.104	0.081		0.086			0.036
229	0.029		0.042	0.113	0.016	0.014	0.050		0.030
231				0.016			0.050		0.004
233						0.014	0.050		0.004
235				0.032		0.043			0.011
241			0.021						0.002
245				0.016		0.029	0.050		0.008
251						0.014			0.002
255	0.043	0.026							0.011
257	0.029								0.004
265		0.026							0.004
267		0.013							0.002

Marker	Allele	Bicheno	Trumpeter Bay	EAC eddy	Cape Jaffa	Discovery Bay	Sandy Cape	Maatsuyker Is	Sthn Ocean A	Sthn Ocean B/C	Overall frequency
P01F08	N	34	38	18	17	29	44	38	11	9	
	92						0.025				0.004
	94					0.034					0.004
	102					0.017					0.002
	110				0.059			0.012			0.006
	112				0.059						0.004
	114			0.028							0.002
	116									0.056	0.002
	126					0.017					0.002
	138					0.034					0.004
	146		0.026								0.004
	150	0.029	0.013	0.056		0.241	0.050	0.250	0.273		0.105
	152	0.265	0.342	0.111	0.265	0.121	0.338	0.238			0.233
	154	0.176	0.184	0.083	0.235	0.052	0.100	0.012	0.091		0.107
	156	0.235	0.145	0.056	0.088		0.013			0.389	0.084
	158	0.029	0.105	0.194	0.147	0.103	0.163	0.190	0.318		0.134
	160	0.029	0.039				0.025		0.045		0.017
	162				0.029			0.024		0.056	0.008
	164	0.206	0.079	0.056	0.029	0.017	0.038				0.057
	166		0.026	0.056			0.038	0.024		0.056	0.021
	168	0.015		0.028				0.024			0.008
	170	0.015				0.155		0.048	0.091		0.034
	172			0.083			0.038	0.036			0.019
	174			0.028	0.029		0.025	0.012	0.091		0.015

176					0.013				0.002
178						0.024	0.091		0.008
180						0.024			0.004
188			0.059						0.004
194	0.013	0.111		0.172	0.075	0.048			0.053
196	0.026	0.111		0.017	0.038	0.012			0.023
200								0.056	0.002
208				0.017	0.025				0.006
228						0.012			0.002
230								0.111	0.004
234								0.111	0.004
236								0.111	0.004
264						0.012			0.002
298								0.056	0.002

Marker	Allele	Bicheno	Trumpeter Bay	EAC eddy	Cape Jaffa	Discovery Bay	Sandy Cape	Maatsuyker Is	Sthn Ocean A	Sthn Ocean B/C	Overall frequency
P02E09	N	34	36	26	25	27	45	42	11	9	
	73	0.029									0.004
	77	0.294	0.139			0.019	0.011	0.023			0.067
	79	0.088	0.153	0.058	0.020		0.011	0.012			0.045
	81					0.019			0.045		0.004
	83		0.014			0.019		0.023			0.008
	87						0.011				0.002
	91		0.014								0.002
	93		0.028	0.019				0.012			0.008
	95			0.058	0.040	0.019	0.045				0.020
	97	0.324	0.347	0.288	0.300	0.574	0.398	0.337	0.545	0.111	0.365
	99	0.206	0.125	0.212	0.220	0.185	0.205	0.186	0.227	0.722	0.210
	101	0.015	0.069	0.154	0.220	0.111	0.182	0.198	0.136	0.167	0.137
	103		0.069	0.096	0.060	0.019	0.080	0.081	0.045		0.057
	105			0.038	0.120		0.023	0.047			0.027
	107	0.029	0.014	0.058	0.020	0.037	0.023	0.047			0.029
	109	0.015									0.002
	113		0.028	0.019			0.011	0.012			0.010
	121							0.012			0.002
	127							0.012			0.002

Marker	Allele	Bicheno	Trumpeter Bay	EAC eddy	Cape Jaffa	Discovery Bay	Sandy Cape	Maatsuyker Is	Sthn Ocean A	Sthn Ocean B/C	Overall frequency
P02B12	N	34	34	25	25	27	44	39	11	9	
	197				0.020						0.002
	203	0.029						0.012		0.222	0.014
	205	0.265	0.221	0.080	0.220	0.111	0.146	0.060	0.045	0.333	0.157
	207	0.632	0.647	0.580	0.620	0.519	0.695	0.560	0.545	0.333	0.599
	209	0.074	0.059	0.040	0.060	0.074	0.073	0.143	0.136	0.111	0.083
	211		0.029			0.019	0.012	0.071	0.136		0.026
	213			0.060		0.074	0.024	0.107			0.036
	215			0.020		0.056	0.024	0.048	0.045		0.022
	217			0.020	0.020	0.148	0.012				0.022
	219				0.020						0.002
	221		0.044	0.040			0.012				0.012
	223			0.120	0.020						0.014
	225			0.040							0.004
	227				0.020				0.045		0.004
	229								0.045		0.002

Marker	Allele	Bicheno	Trumpeter Bay	EAC eddy	Cape Jaffa	Discovery Bay	Sandy Cape	Maatsuyker Is	Sthn Ocean A	Sthn Ocean B/C	Overall frequency
P01E05	N	35	39	25	28	32	46	42	10	1	
	102			0.020							0.002
	104	0.014							0.050		0.004
	106							0.011			0.002
	108							0.011			0.002
	114			0.020			0.023				0.006
	120		0.026								0.004
	122		0.026	0.080							0.012
	124	0.014									0.002
	126	0.171	0.064	0.100	0.036		0.023				0.050
	128	0.043			0.018						0.008
	132					0.016	0.023	0.011			0.008
	134	0.057	0.026				0.011	0.023			0.017
	136	0.043	0.090	0.040	0.018	0.109	0.068	0.091	0.150		0.072
	138	0.029	0.051		0.018		0.045	0.114			0.041
	140	0.057	0.026			0.063		0.011			0.021
	142	0.057	0.013		0.071	0.375	0.080	0.125			0.099
	144	0.014	0.090	0.200	0.018	0.156	0.182	0.114	0.150		0.112
	146	0.086	0.051	0.180	0.071	0.078	0.091	0.114	0.100	0.500	0.095
	148	0.057	0.077	0.020	0.036		0.011	0.011			0.029
	150	0.114	0.090	0.060	0.036	0.016	0.034		0.050		0.048
	152	0.029	0.038	0.020	0.232	0.031	0.057	0.057			0.060
	154		0.077	0.020	0.232		0.114	0.091	0.100		0.078

156	0.114	0.167	0.040	0.089	0.047	0.091	0.091	0.050		0.093
158	0.029	0.038	0.040		0.031	0.045	0.045	0.150		0.039
160		0.013	0.020		0.031	0.011	0.011		0.500	0.014
162		0.026	0.040			0.011				0.010
164		0.013		0.036						0.006
166				0.036		0.023	0.011			0.010
168			0.020	0.036	0.016	0.011	0.011	0.050		0.014
170						0.011	0.034	0.050		0.010
172	0.043		0.040	0.018		0.011	0.011			0.016
174			0.040			0.023				0.008
176	0.014									0.002
184					0.031					0.004
186	0.014									0.002
222								0.100		0.004

Marker	Allele	Bicheno	Trumpeter Bay	EAC eddy	Cape Jaffa	Discovery Bay	Sandy Cape	Maatsuyker Is	Sthn Ocean A	Sthn Ocean B/C	Overall frequency
P02E10	N	34	40	22	22	31	43	37	12	7	
	151				0.045						0.004
	157				0.023						0.002
	165				0.023						0.002
	167				0.068						0.006
	171	0.074	0.175	0.114	0.136	0.081	0.171	0.060	0.083	0.286	0.119
	173	0.500	0.488	0.318	0.477	0.500	0.368	0.381	0.542	0.714	0.448
	175	0.088	0.063	0.295		0.290	0.211	0.286	0.167		0.173
	177	0.324	0.200	0.136	0.227	0.113	0.211	0.238	0.167		0.204
	179	0.015		0.045		0.016	0.013	0.024	0.042		0.016
	187		0.025					0.012			0.006
	197			0.023							0.002
	199		0.013	0.023							0.004
	203		0.025	0.045							0.008
	207		0.013				0.026				0.006

Marker	Allele	Bicheno	Trumpeter Bay	EAC eddy	Cape Jaffa	Discovery Bay	Sandy Cape	Maatsuyker Is	Sthn Ocean A	Sthn Ocean B/C	Overall frequency
EHMS37	N	35	40	26	28	31	42	43	12	8	
	186									0.313	0.009
	190									0.188	0.006
	198					0.097	0.044	0.113	0.292		0.049
	200					0.032	0.022				0.008
	202			0.019			0.011	0.013			0.006
	204			0.019	0.089	0.032	0.078	0.088			0.042
	206					0.016	0.022	0.050	0.125		0.019
	212		0.013					0.025			0.006
	214			0.058					0.042		0.008
	216								0.042		0.002
	218									0.063	0.002
	220									0.063	0.002
	222		0.025	0.058						0.063	0.011
	224			0.038							0.004
	226						0.022		0.083		0.008
	228			0.038							0.004
	230								0.042		0.002
	232			0.038							0.004
	234			0.019		0.016					0.004
	238					0.032		0.013			0.006
	240			0.038		0.032	0.033	0.050			0.021
	242		0.075	0.019		0.048	0.033	0.125			0.043
	244						0.022				0.004
	246			0.019							0.002

248									0.125	0.004
254								0.042		0.002
262			0.038	0.018			0.013			0.008
264	0.029		0.038			0.011				0.009
266	0.029		0.038	0.018	0.016	0.022	0.025			0.019
268	0.057	0.025	0.038		0.016	0.033	0.038			0.028
270	0.029	0.038		0.018	0.048	0.022	0.038	0.083		0.030
272	0.057	0.125	0.077	0.018		0.067	0.050	0.042		0.057
274	0.029	0.038		0.071	0.032	0.022				0.025
276				0.036		0.011				0.006
278	0.029	0.038				0.011	0.025			0.015
280	0.071			0.036	0.016	0.044	0.038		0.063	0.030
282	0.186	0.100	0.115	0.018		0.033		0.083		0.062
284	0.186	0.238	0.038			0.011		0.042		0.068
286	0.100	0.050	0.038	0.018		0.033				0.032
288			0.038							0.004
290		0.025	0.019	0.179	0.016	0.122	0.013		0.125	0.053
292		0.025		0.054	0.048	0.011	0.025	0.083		0.025
294	0.014	0.013				0.011	0.025			0.009
296	0.029	0.050		0.018						0.013
298	0.014			0.054	0.032	0.011	0.050			0.021
300	0.014						0.025			0.006
302	0.014			0.036	0.016					0.008
304	0.057	0.025		0.018	0.242	0.022	0.038			0.051
306	0.043	0.050	0.019	0.036	0.097	0.056	0.038			0.045
308	0.014	0.050		0.179	0.097	0.111	0.050			0.066
310			0.019	0.018		0.033	0.013			0.011

312			0.016	0.013	0.004
314	0.019			0.013	0.004
316	0.019				0.002
320	0.019				0.002
322	0.019				0.002
328	0.038	0.036	0.011		0.009
332		0.018			0.002
336		0.018			0.002

Appendix B

Type A grown in HL before and after exposure to SMI. F is the minimum fluorescence, F_m' is the maximum fluorescence in the light and 1-qP (secondary Y axis) is an index of reaction centre closure.

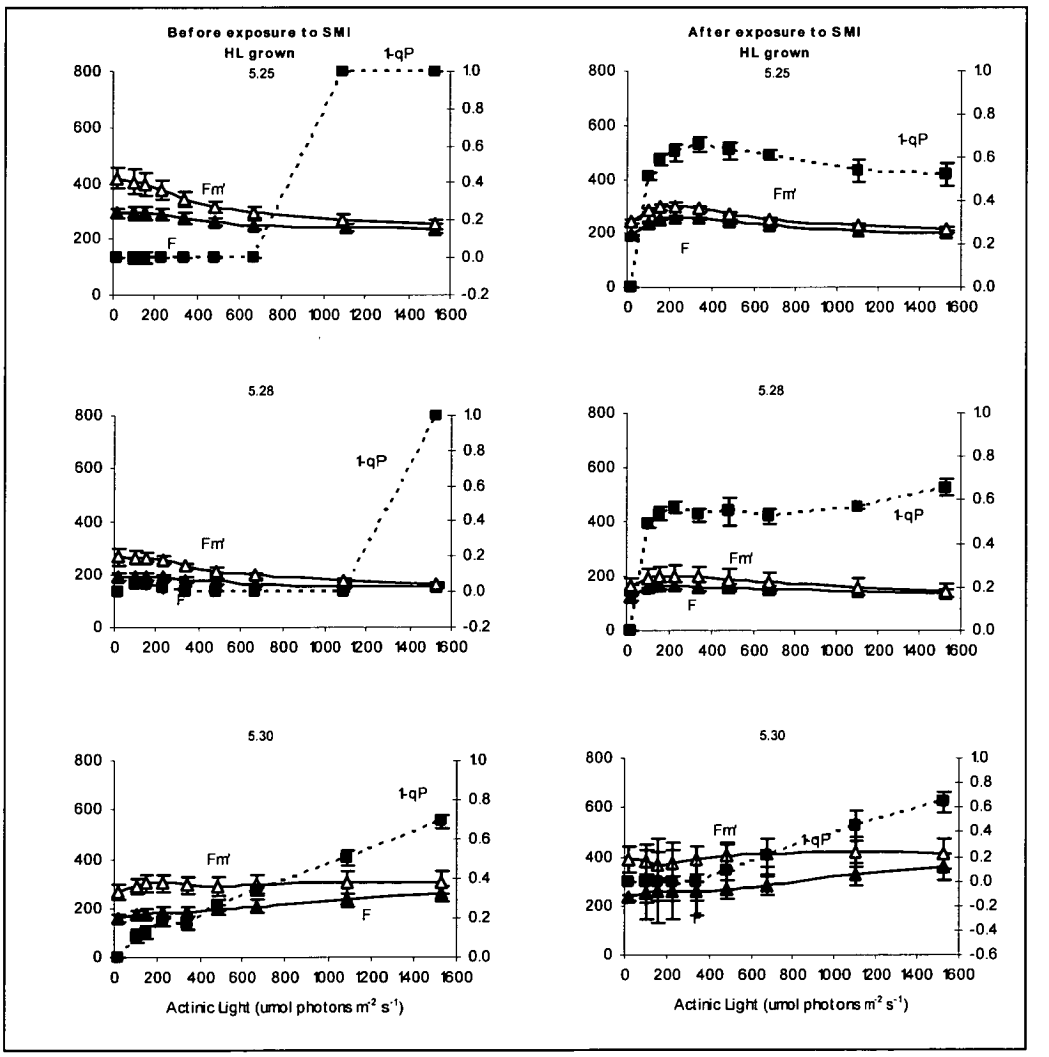

Type B/C grown in HL, before and after exposure to SMI. F is the minimum fluorescence, F_m' is the maximum fluorescence in the light and 1-qP (secondary Y axis) is an index of reaction centre closure.

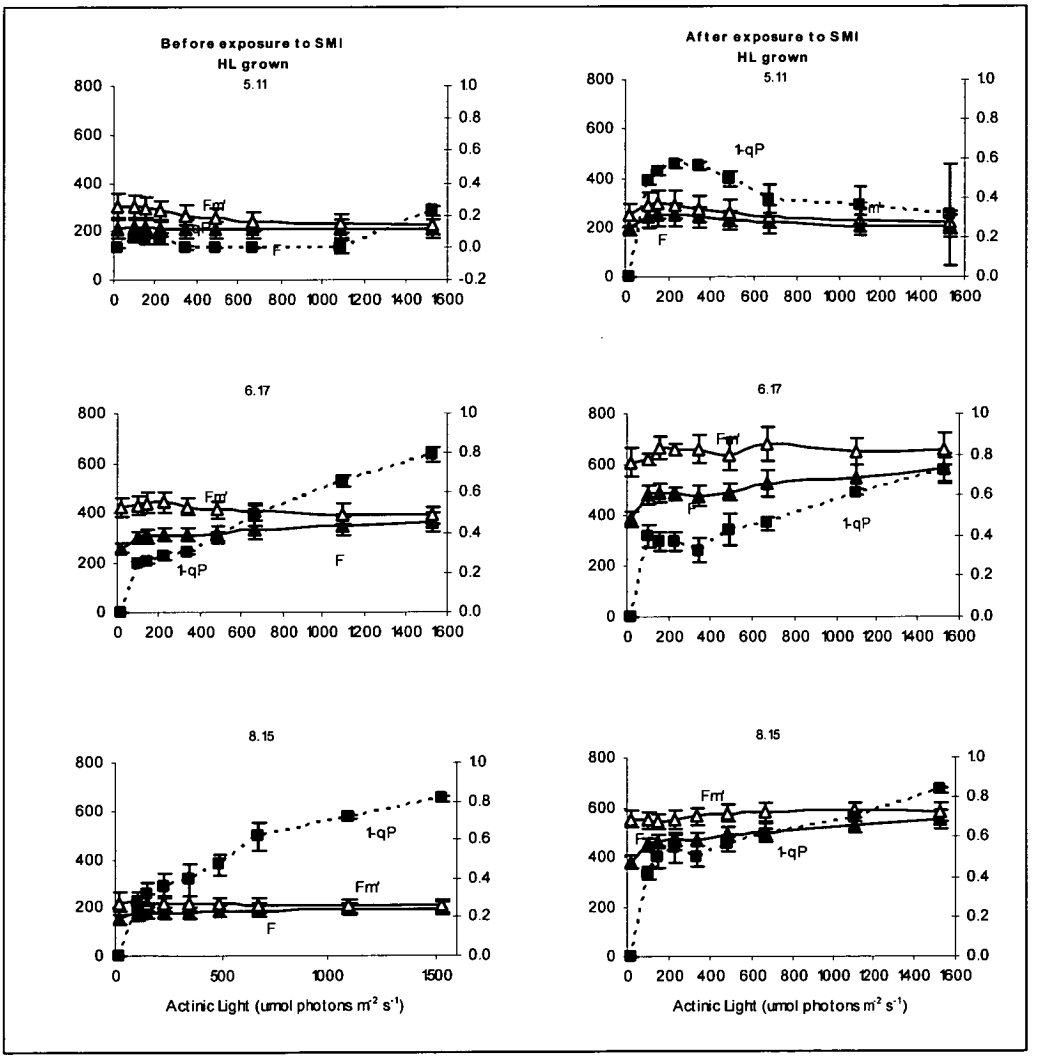

Type A grown in LL, before and after exposure to SMI. F is the minimum fluorescence, F_m' is the maximum fluorescence in the light and 1-qP (secondary Y axis) is an index of reaction centre closure.

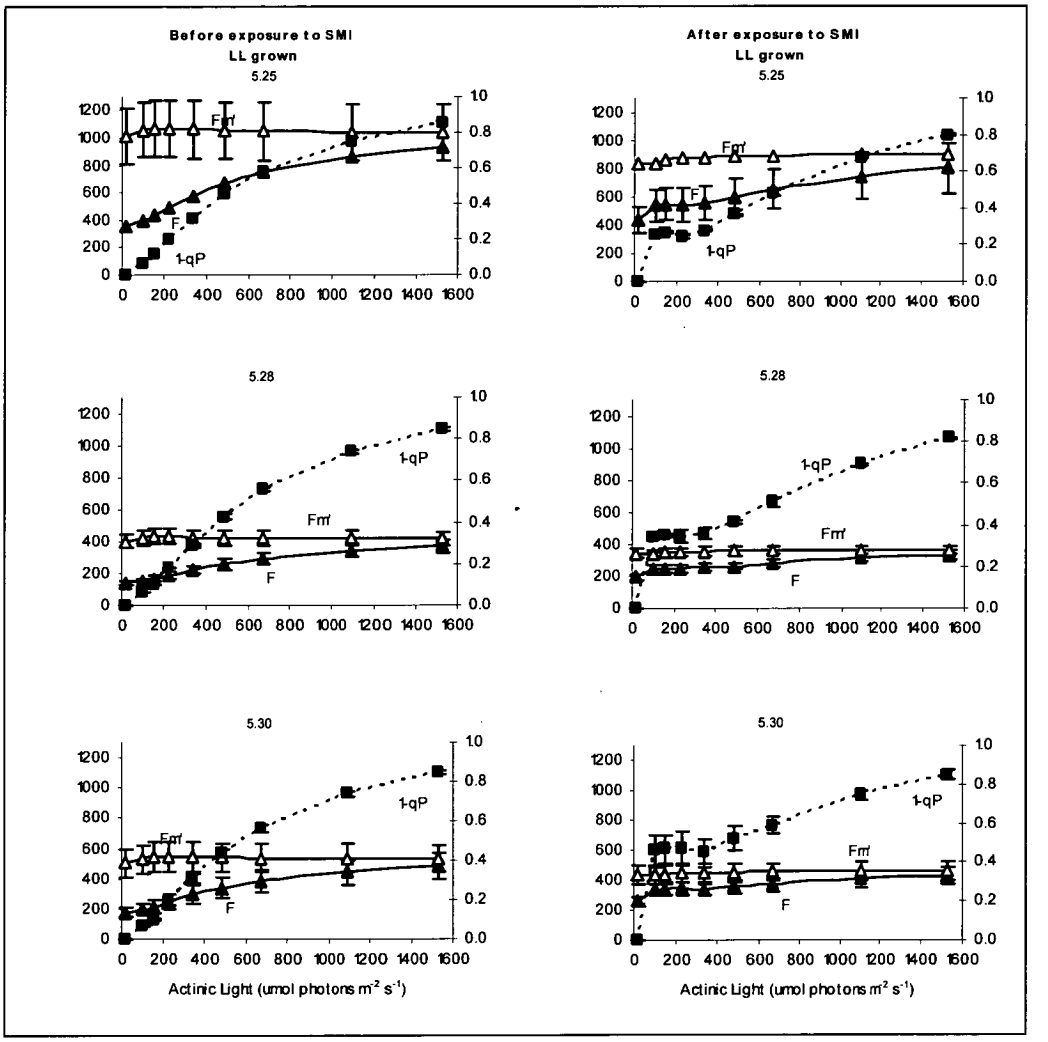

Type B/C grown in LL, before and after exposure to SMI. F is the minimum fluorescence, F_m' is the maximum fluorescence in the light and 1-qP (secondary Y axis) is an index of reaction centre closure.

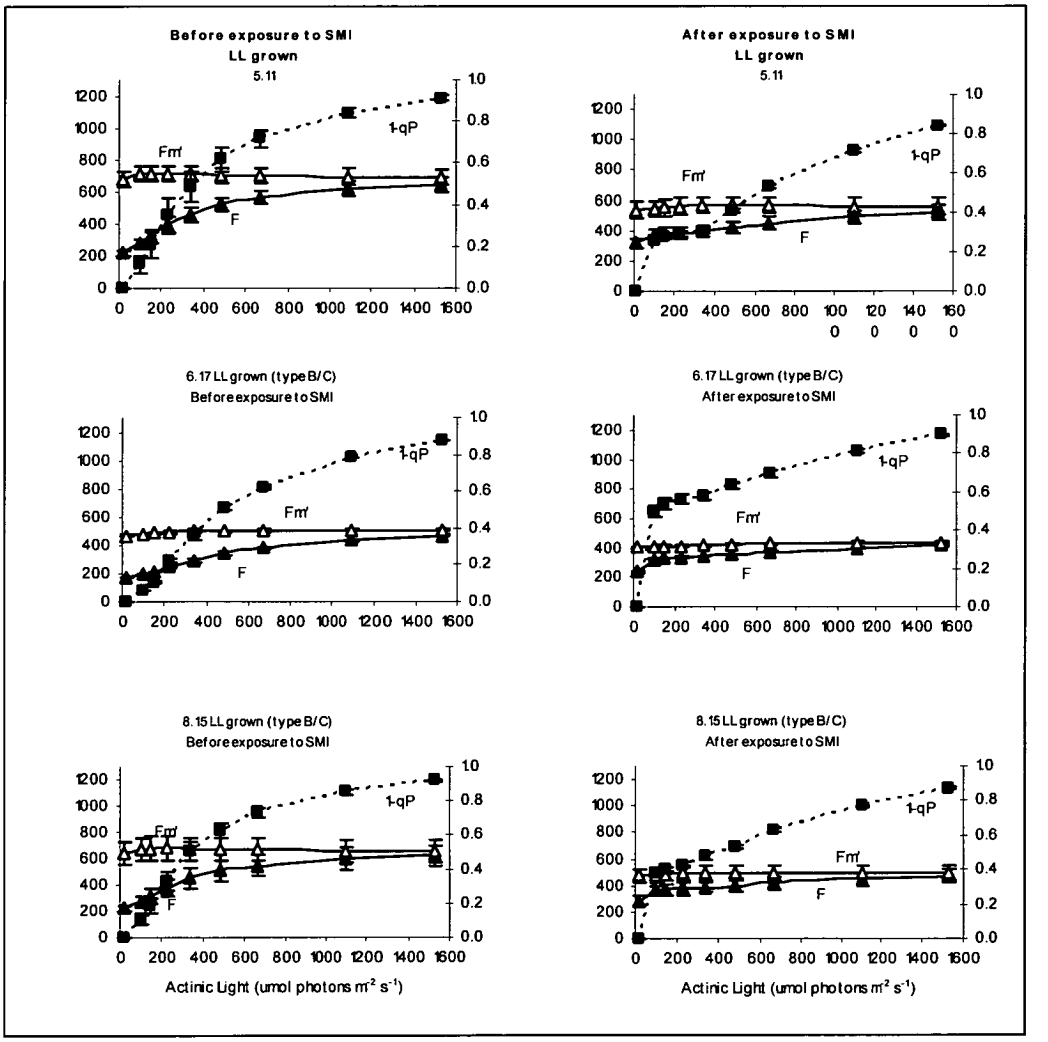

References

Adir N, Zer H, Shochat S, Ohad I (2003). Photoinhibition - a historical perspective. *Photosynthesis Research* 76, 343-370.

Arpin N, Svec WA, Liaaenjensen S (1976). New Fucoxanthin-related carotenoids from *Coccolithus huxleyi*. *Phytochemistry* 15, 529-532.

Arsalane W, Rousseau B, Duval JC (1994). Influence of the pool size of the xanthophyll cycle on the effects of light stress in a diatom - competition between photoprotection and photoinhibition. *Photochemistry and Photobiology* 60, 237-243.

Avise JC (1994). *Molecular markers, natural history and evolution*.pp. Chapman & Hall, Inc, NY.

Balch WM, Holligan PM, Kilpatrick KA (1992). Calcification, photosynthesis and growth of the bloom forming Coccolithophore *Emiliania huxleyi*. *Continental Shelf Research* 12, 1353-1374.

Banks SC, Piggott MP, Williamson JE, Bove U, Holbrook NJ, Beheregaray LB (2007). Oceanic variability and coastal topography shape genetic structure in a long-dispersing sea urchin. *Ecology* 88, 3055-3064.

Beardall J, Stojkovic S, Larsen S (2009). Living in a high CO_2 world: Impacts of global change on marine phytoplankton. *Plant Ecology and Diversity* (in press).

Beaufort L, Probert I, Buchet N (2007). Effects of acidification and primary production on coccolith weight: Implications for carbonate transfer from the surface to the deep ocean. *Geochemistry Geophysics Geosystems* 8, Article No. Q08011.

Brand LE (1982). Genetic variability and spatial patterns of genetic differentiation in the reproductive rates of the marine coccolithophores *Emiliania huxleyi* and *Gephyrocapsa oceanica. Limnology and Oceanography* 27, 236-245.

Brand LE (1994) Physiological ecology of marine coccolithophores. In 'Coccolithophores'. (Eds A Winter and WG Siesser) pp. 39-49. (Cambridge University Press: Cambridge).

Callen DF, Thompson AD, Shen Y, Phillips HA, Richards RI, Mulley JC, Sutherland GR (1993). Incidence and origin of null alleles in the (Ac)N microsatellite markers. *American Journal of Human Genetics* 52, 922-927.

Carlsson J (2008). Effects of Microsatellite Null Alleles on Assignment Testing. *Journal of Heredity* 99, 616-623.

Casteleyn G, Evans KM, Backeljau T, D'Hondt S, Chepurnov V, Sabbe K, Vyverman W (2009). Lack of population genetic structuring in the marine planktonic diatom Pseudo-nitzschia pungens (Bacillariophyceae) in a heterogeneous area in the Southern Bight of the North Sea. *Marine Biology* 156, 1149-1158.

Chapuis MP, Estoup A (2007). Microsatellite null alleles and estimation of population differentiation. *Molecular Biology and Evolution* 24, 621-631.

Chybicki IJ, Burczyk J (2009). Simultaneous Estimation of Null Alleles and Inbreeding Coefficients. *Journal of Heredity* 100, 106-113.

Clarke A, Barnes DKA, Hodgson DA (2005). How isolated is Antarctica? *Trends in Ecology & Evolution* 20, 1-3.

Crawford NG (2009). SMOGD: Software for the Measurement of Genetic Diversity. *Molecular Ecology Resources* (in press).

Cruz S, Serodio J (2008). Relationship of rapid light curves of variable fluorescence to photoacclimation and non-photochemical quenching in a benthic diatom. *Aquatic Botany* 88, 256-264.

Cubillos JC, Wright SW, Nash G, de Salas MF, Griffiths B, Tilbrook B, Poisson A, Hallegraeff GM (2007). Calcification morphotypes of the coccolithophorid *Emiliania huxleyi* in the Southern Ocean: changes in 2001 to 2006 compared to historical data. *Marine Ecology Progress Series* 348, 47-54.

Demura M, Kawachi M, Kunugi M, Nishizawa T, Kasai F, Watanabe MM (2007). Development of microsatellite markers for the red tide-forming harmful species Chattonella antiqua, C-marina, and C-ovata (Raphidophyceae). *Molecular Ecology Notes* 7, 315-317.

DiTullio GR, Garcia N, Riseman SF, Sedwick PN (2007). Effects of iron concentration on pigment composition in *Phaeocystis* antarctica grown at low irradiance. *Biogeochemistry* 83, 71-81.

Doney SC, Abbott MR, Cullen JJ, Karl DM, Rothstein L (2004). From genes to ecosystems: the ocean's new frontier. *Frontiers in Ecology and the Environment* 2, 457-466.

Doubleday ZA, Semmens JM, Smolenski AJ, Shaw PW (2009). Microsatellite DNA markers and morphometrics reveal a complex population structure in a merobenthic octopus species (Octopus maorum) in south-east Australia and New Zealand. *Marine Biology* 156, 1183-1192.

Egeland ES, Garrido JL, Zapata M, Maestro MA, Liaaen-Jensen S (2000). Algal carotenoids. Part 64. Structure and chemistry of 4-keto-19 '-hexanoyloxyfucoxanthin with a novel carotenoid end group. *Journal of the Chemical Society-Perkin Transactions 1* 8, 1223-1230.

Evanno G, Regnaut S, Goudet J (2005). Detecting the number of clusters of individuals using the software STRUCTURE: a simulation study. *Molecular Ecology* 14, 2611-2620.

Evans KM, Bates SS, Medlin LK, Hayes PK (2004). Microsatellite marker development and genetic variation in the toxic marine diatom Pseudo-nitzschia multiseries (Bacillariophyceae). *Journal of Phycology* 40, 911-920.

Evans KM, Kuhn SF, Hayes PK (2005). High levels of genetic diversity and low levels of genetic differentiation in North Sea *Pseudo-nitzschia pungens* (Bacillariophyceae) populations. *Journal of Phycology* 41, 506-514.

Falkowski P, Greene, R., Kolber, Z. (1994) Light utilization and photoinhibition of photosynthesis in marine phytoplankton. In 'Photoinhibition of photosynthesis'. (Ed. NR Baker, Bowyer, J.R.) pp. 407-432. (BIOS Scientific Publishers Ltd: Oxford).

Falkowski PG, Raven JA (1997). *Aquatic Photosynthesis*.375 pp. Blackwell Science, Oxford, UK.

Findlay CS, Giraudeau J (2000). Extant calcareous nannoplankton in the Australian sector of the Southern Ocean (austral summers 1994 and 1995). *Marine Micropaleontology* 40, 417-439.

Findlay CS, Young JR, Scott FJ (2005) Haptophytes: Order Coccolithophorales. In 'Antarctic marine protists'. (Eds FJ Scott and HJ Marchant) pp. 276-294. (Australian Biological Resources Study, Australian Antarctic Division: Canberra/Hobart).

Gaebler S, Hayes PK, Medlin LK (2007) Methods used to reveal genetic diversity in the colony-forming prymnesiophytes Phaeocystis antarctica, P-globosa and P-pouchetii - preliminary results. pp. 19-27

Gao K, Ruan Z, Villafane VE, Gattuso JP, Helbling EW (2009). Ocean acidification exacerbates the effect of UV radiation on the calcifying phytoplankter *Emiliania huxleyi*. *Limnology and Oceanography* 54, 1855-1862.

Garrido JL, Zapata M (1998). Detection of new pigments from *Emiliania huxleyi* (Prymnesiophyceae) by high-performance liquid chromatography, liquid chromatography-mass spectrometry, visible spectroscopy, and fast atom bombardment mass spectrometry. *Journal of Phycology* 34, 70-78.

Gayoso AM (1995). Bloom of *Emiliania huxleyi* (Prymnesiophyceae) in the western South Atlantic Ocean. *J. Plankton Res.* 17, 1717-1722.

Goericke R, Welschmeyer NA (1992). Pigment turnover in the marine diatom *Thalassiosira weissflogii.* 1. The $^{14}CO_2$ labeling kinetics of chlorophyll *a*. *Journal of Phycology* 28, 498-507.

Gorbunov MY, Kolber ZS, Lesser MP, Falkowski PG (2001). Photosynthesis and Photoprotection in Symbiotic Corals. *Limnology and Oceanography* 46, 75-85.

Goss R, Pinto EA, Wilhelm C, Richter M (2006). The importance of a highly active and Delta pH-regulated diatoxanthin epoxidase for the regulation of the PSII antenna function in diadinoxanthin cycle containing algae. *Journal of Plant Physiology* 163, 1008-1021.

Goudet J (2002) 'FSTAT, a programme to estimate and test gene diversities and fixation indices (available online at http://www2.unil.ch/popgen/softwares/fstat.htm)

Hagino K, Okada H, Matsuoka H (2005). Coccolithophore assemblages and morphotypes of *Emiliania huxley*i in the boundary zone between the cold Oyashio and warm Kuroshio currents off the coast of Japan. *Marine Micropaleontology* 55, 19-47.

Hallegraeff GM (2010). Ocean climate change, phytoplankton community responses, and harmful algal blooms: a formidable predictive challenge. *Journal of Phycology* 46, 220-235.

Halliburton R (2004). *Introduction to population genetics*.pp. Pearson Prentice Hall, USA.

Harris GN, Scanlan DJ, Geider RJ (2005). Acclimation of *Emiliania huxleyi* (Prymnesiophyceae) to photon flux density. *Journal of Phycology* 41, 851-862.

Harris GN, Scanlan DJ, Geider RJ (2009). Responses of *Emiliania huxleyi* (Prymnesiophyceae) to step changes in photon flux density. *European Journal of Phycology* 44, 31 - 48.

Heinz Walz Gmbh (1998). *Handbook of operation, Underwater Fluorometer Diving PAM*.pp. Heinz Walz GmbH, Germany.

Heller R, Siegismund HR (2009). Relationship between three measures of genetic differentiation G(ST), D-EST and G'(ST): how wrong have we been? *Molecular Ecology* 18, 2080-2083.

Hentschel E (1932). Die Biologischen Methoden und das Biologische Beobachtungsmaterial der Meteor Expedition. *Wiss. Ergebn. Dtsch. All Exped. 'Meteor'* 10, 1-275.

Hiramatsu C, DeDeckker P (1996). Distribution of calcareous nannoplankton near the Subtropical Convergence, south of Tasmania, Australia. *Marine and Freshwater Research* 47, 707-713.

Holligan PM (1992) Do marine phytoplankton influence global climate? In 'Primary productivity and biogeochemical cycles in the sea'. (Eds PG Falkowski and AD Woodhead) pp. 487-501. (Plenum Press: New York).

Houdan A, Probert I, Van Lenning K, Lefebvre S (2005). Comparison of photosynthetic responses in diploid and haploid life-cycle phases of *Emiliania huxleyi* (Prymnesiophyceae). *Marine Ecology-Progress Series* 292, 139-146.

Huisman J, Oostveen Pv, Weissing FJ (1999a). Critical depth and critical turbulence: Two different mechanisms for the development of phytoplankton blooms. *Limnology and Oceanography* 44, 1781-1787.

Huisman J, van Oostveen P, Weissing FJ (1999b). Species dynamics in phytoplankton blooms: Incomplete mixing and competition for light. *The American Naturalist* 154, 46-68.

Iglesias-Rodríguez MD, Brown CW, Doney SC, Kleypas J, Kolber D, Kolber Z, Hayes PK, Falkowski PG (2002). Representing key phytoplankton functional groups in ocean carbon cycle models: Coccolithophorids. *Global Biogeochemical Cycles* 16, 1-20.

Iglesias-Rodriguez MD, Halloran PR, Rickaby REM, Hall IR, Colmenero-Hidalgo E, Gittins JR, Green DRH, Tyrrell T, Gibbs SJ, von Dassow P, Rehm E, Armbrust EV, Boessenkool KP (2008). Phytoplankton calcification in a high-CO2 world. *Science* 320, 336-340.

Iglesias-Rodriguez MD, Probert I, Batley J (2006a). Microsatellite cross-amplification in coccolithophores: application in population diversity studies. *Hereditas* 143, 99-102.

Iglesias-Rodriguez MD, Saez AG, Groben R, Edwards KJ, Batley J, Medlin LK, Hayes PK (2002). Polymorphic microsatellite loci in global populations of the marine coccolithophorid Emiliania huxleyi. *Molecular Ecology Notes* 2, 495-497.

Iglesias-Rodriguez MD, Schofield OM, Batley J, Medlin LK, Hayes PK (2006b). Intraspecific genetic diversity in the marine coccolithophore *Emiliania huxleyi* (Prymnesiophyceae): The use of microsatellite analysis in marine phytoplankton population studies. *Journal of Phycology* 42, 526-536.

Jakobsson M, Rosenberg NA (2007). CLUMPP: a cluster matching and permutation program for dealing with label switching and multimodality in analysis of population structure. *Bioinformatics* 23, 1801-1806.

Jeffrey SW, Allen MB (1964). Pigments, growth and photosynthesis in cultures of two Chrysomonads, *Coccolithus huxleyi* and a *Hymenomonas* sp. *Journal of General Microbiology* 36, 277-&.

Jeffrey SW, Vesk M (2005) Introduction to marine phytoplankton and their pigment signatures. In 'Phytoplankton pigments in oceanography. Guidelines to modern methods'. (Eds SW Jeffrey, RFC Mantoura and SW Wright) pp. 37-84. (UNESCO Publishing: Paris).

Jeffrey SW, Wright SW (1994) Photosynthetic pigments in the Haptophyta. In 'The Haptophyte Algae'. (Eds JC Green and BSC Leadbeater) pp. 111-132. (Clarendon Press: Oxford).

Jordan RW, Green JC (1994). A checklist of the extant Haptophyta of the world. *Journal of the Marine Biological Association of the United Kingdom* 74, 149-174.

Jost L (2008). G(ST) and its relatives do not measure differentiation. *Molecular Ecology* 17, 4015-4026.

Keller MD, Selvin RC, Claus W, Guillard RRL (1987). Media for the culture of oceanic ultraphytoplankton. *Journal of Phycology* 23, 633-638.

Kirk JTO (1994). *Light and Photosynthesis in Aquatic Ecosystems*.509 pp. Cambridge University Press, Cambridge.

Knowlton N (2000). Molecular genetic analyses of species boundaries in the sea. *Hydrobiologia* 420, 73-90.

Kolber Z, Falkowski P (1993). Use of active fluorescence to estimate phytoplankton photosynthesis in situ. *Limnology and Oceanography* 38, 1646-1665.

Kropuenske LR, Mills MM, van Dijken GL, Bailey S, Robinson DH, Welschmeyer NA, Arrigo KR (2009). Photophysiology in two major Southern Ocean phytoplankton taxa: Photoprotection in Phaeocystis antarctica and Fragilariopsis cylindrus. *Limnology and Oceanography* 54, 1176-1196.

Langer G, Nehrke G, Probert I, Ly J, Ziveri P (2009). Strain-specific responses of *Emiliania huxleyi* to changing seawater carbonate chemistry. *Biogeosciences Discuss.* 6, 4361-4383.

Lavaud J, Rousseau B, Etienne AL (2004). General features of photoprotection by energy dissipation in planktonic diatoms (Bacillariophyceae). *Journal of Phycology* 40, 130-137.

Lavaud J, Strzepek RF, Kroth PG (2007). Photoprotection capacity differs among diatoms: Possible consequences on the spatial distribution of diatoms related to fluctuations in the underwater light climate. *Limnology and Oceanography* 52, 1188-1194.

Leonardos N (2008). Physiological steady state of phytoplankton in the field? An example based on pigment profile of *Emiliania huxleyi* (Haptophyta) during a light shift. *Limnology and Oceanography* 53, 306-311.

Leonardos N, Harris GN (2006). Comparative effects of light on pigments of two strains of *Emiliania huxleyi* (Haptophyta). *Journal of Phycology* 42, 1217-1224.

Leonardos N, Read B, Thake B, Young JR (2009). No mechanistic dependence of photosynthesis on calcification in the coccolithophorid *Emiliania huxleyi* (Haptophyta). *Journal of Phycology* 45, 1046-1051.

Lind CE, Evans BS, Taylor JJU, Jerry DR (2007). Population genetics of a marine bivalve, Pinctada maxima, throughout the Indo-Australian Archipelago shows differentiation and decreased diversity at range limits. *Molecular Ecology* 16, 5193-5203.

Litchman E, Klausmeier CA (2001). Competition of phytoplankton under fluctuating light. *American Naturalist* 157, 170-187.

Lohr M, Wilhelm C (1999). Algae displaying the diadinoxanthin cycle also possess the violaxanthin cycle. *Proceedings of the National Academy of Sciences* 96, 8784-8789.

Lohr M, Wilhelm C (2001). Xanthophyll synthesis in diatoms: quantification of putative intermediates and comparison of pigment conversion kinetics with rate constants derived from a model. *Planta* 212, 382-391.

Long SP, Humphries S, Falkowski PG (1994). Photoinhibition of Photosynthesis in Nature. *Annual Review of Plant Physiology and Plant Molecular Biology* 45, 633-662.

Lowe A, Harris S, Ashton P (2004). *Ecological genetics: Design, analysis and application*.pp. Blackwell Publishing, Oxford.

MacIntyre HL, Kana TM, Anning T, Geider RJ (2002). Photoacclimation of photosynthesis irradiance response curves and photosynthetic pigments in microalgae and cyanobacteria. *Journal of Phycology* 38, 17-38.

Mantoura RFC, Repeta DJ (1997) Calibration methods for HPLC. In 'Phytoplankton pigments in oceanography, guidelines for modern methods'. (Eds SW Jeffrey, RFC Mantoura and SW Wright) pp. 407-428. (Unesco Publishing: Paris).

Martin JH, Gordon RM, Fitzwater SE (1990). Iron in Antarctic waters. *Nature* 345, 156-158.

Masseret E, Grzebyk D, Nagai S, Genovesi B, Lasserre B, Laabir M, Collos Y, Vaquer A, Berrebi P (2009). Unexpected Genetic Diversity among and within Populations of the Toxic Dinoflagellate Alexandrium catenella as Revealed by Nuclear Microsatellite Markers. *Applied and Environmental Microbiology* 75, 2037-2045.

Maxwell K, Johnson GN (2000). Chlorophyll fluorescence - a practical guide. *Journal of Experimental Botany* 51, 659-668.

McIntyre A, Be AWH (1967). *Coccolithus neohelis* sp. n., a coccolith fossil type in contemporary seas. *Deep-Sea Research* 14, 369-&.

McMinn A, Hattori H (2006). Effect of time of day on the recovery from light exposure in ice algae from Saroma Ko lagoon, Hokkaido. *Polar Bioscience* 20, 30-36.

Medlin L, Barker GL, Baumann N, Hayes PK, Lange M (1994a) Molecular biology and systematics. In 'The Haptophyte Algae'. (Eds JC Green and BSC Leadbeater) pp. 394-411. (Clarendon Press: Oxford).

Medlin LK (2007). If everything is everywhere, do they share a common gene pool? *Gene* 406, 180-183.

Medlin LK, Barker GL, Campbell L, Green JC, Hayes PK, Marie D, Wrieden S (1996). Genetic characterisation of *Emiliania huxleyi* (Haptophyta). *Journal of Marine Systems* 9, 13-31.

Medlin LK, Lange M, Baumann MEM (1994b). Genetic differentiation among 3 colony-forming species of Phaeocystis - further evidence for the phylogeny of the Prymnesiophyta. *Phycologia* 33, 199-212.

Medlin LK, Lange M, Nothig EM (2000). Genetic diversity in the marine phytoplankton: a review and a consideration of Antarctic phytoplankton. *Antarctic Science* 12, 325-333.

Merico A, Tyrrell T, Lessard EJ, Oguz T, Stabeno PJ, Zeeman SI, Whitledge TE (2004). Modelling phytoplankton succession on the Bering Sea shelf: role of climate influences and trophic interactions in generating *Emiliania huxleyi* blooms 1997-2000. *Deep-Sea Research Part I-Oceanographic Research Papers* 51, 1803-1826.

Mock T, Hoch N (2005). Long-term temperature acclimation of photosynthesis in steady-state cultures of the polar diatom *Fragilariopsis cylindrus*. *Photosynthesis Research* 85, 307-317.

Mohan R, Mergulhao LP, Guptha MVS, Rajakumar A, Thamban M, AnilKumar N, Sudhakar M, Ravindra R (2008). Ecology of coccolithophores in the Indian sector of the Southern Ocean. *Marine Micropaleontology* 67, 30-45.

Muller P, Li XP, Niyogi KK (2001). Non-photochemical quenching. A response to excess light energy. *Plant Physiology* 125, 1558-1566.

Nagai S, McCauley L, Yasuda N, Erdner DL, Kulis DM, Matsuyama Y, Itakura S, Anderson DM (2006a). Development of microsatellite markers in the toxic dinoflagellate Alexandrium minutum (Dinophyceae). *Molecular Ecology Notes* 6, 756-758.

Nagai S, Yamaguchi S, Lian CL, Matsuyama Y, Itakura S (2006b). Development of microsatellite markers in the noxious red tide-causing algae Heterosigma akashiwo (Raphidophyceae). *Molecular Ecology Notes* 6, 477-479.

Nanninga HJ, Tyrrell T (1996). Importance of light for the formation of algal blooms by *Emiliania huxleyi*. *Marine Ecology Progress Series* 136, 195-203.

Nei M (1978). Estimation of average heterozygosity and genetic distance from a small number of individuals. *Genetics* 89, 583-590.

Nielsen MV (1995). Photosynthetic characteristics of the coccolithophorid *Emiliania huxleyi* (Prymnesiophyceae) exposed to elevated concentrations of dissolved inorganic carbon. *Journal of Phycology* 31, 715-719.

Nielsen MV (1997). Growth, dark respiration and photosynthetic parameters of the coccolithophorid *Emiliania huxleyi* (Prymnesiophyceae) acclimated to different day length-irradiance combinations. *Journal of Phycology* 33, 818-822.

Norris RD (2000). Pelagic Species Diversity, Biogeography, and Evolution. *Paleobiology* 26, 236-258.

Okada H, Honjo S (1973). The distribution of oceanic coccolithophorids in the Pacific. *Deep-Sea Research* 20, 355-374.

Olaizola M, Laroche J, Kolber Z, Falkowski PG (1994). Nonphotochemical florescence quenching and the diadinoxanthin cycle in a marine diatom. *Photosynthesis Research* 41, 357-370.

Olaizola M, Yamamoto HY (1994). Short-term response of the diadinoxanthin cycle and fluorescence yield to high irradiance in *Chaetoceros muelleri* (Bacillariophyceae). *Journal of Phycology* 30, 606-612.

Owens TG (1994) Excitation energy transfer between chlorophylls and carotenoids. A proposed molecular mechanism for non-photochemical quenching. In 'Photoinhibition of photosynthesis : from molecular mechanisms to the field '. (Eds NR Baker and JR Bowyer) pp. 95-107. (BIOS Scientific: Oxford).

Paasche E (2001). A review of the coccolithophorid *Emiliania huxleyi* (Prymnesiophyceae), with particular reference to growth, coccolith formation and calcification - photosynthesis interactions. *Phycologia* 40, 503-529.

Paasche E, Brubak S, Skattebol JR, Young JR, Green JC (1996). Growth and calcification in the coccolithophorid *Emiliania huxleyi* (Haptophyceae) at low salinities. *Phycologia* 35, 394-403.

Paetkau D, Slade R, Burden M, Estoup A (2004). Genetic assignment methods for the direct, real-time estimation of migration rate: a simulation-based exploration of accuracy and power. *Molecular Ecology* 13, 55-65.

Page TJ, Linse K (2002). More evidence of speciation and dispersal across the Antarctic Polar Front through molecular systematics of Southern Ocean Limatula (Bivalvia : Limidae). *Polar Biology* 25, 818-826.

Palumbi SR (1994). Genetic divergence, reproductive isolation and marine speciation. *Annual Review of Ecology and Systematics* 25, 547-572.

Patarnello T, Bargelloni L, Varotto V, Battaglia B (1996). Krill evolution and the Antarctic ocean currents: Evidence of vicariant speciation as inferred by molecular data. *Marine Biology* 126, 603-608.

Peakall R, Smouse PE (2006). GENALEX 6: genetic analysis in Excel. Population genetic software for teaching and research. *Molecular Ecology Notes* 6, 288-295.

Pemberton JM, Slate J, Bancroft DR, Barrett JA (1995). Nonamplifying alleles at microsatellite loci - a caution for parentage and population studies. *Molecular Ecology* 4, 249-252.

Piry S, Alapetite A, Cornuet JM, Paetkau D, Baudouin L, Estoup A (2004). GENECLASS2: A Software for Genetic Assignment and First-Generation Migrant Detection. *J Hered* 95, 536-539.

Pritchard JK, Stephens M, Donnelly P (2000). Inference of population structure using multilocus genotype data. *Genetics* 155, 945-959.

Ragni M, Airs RL, Leonardos N, Geider RJ (2008). Photoinhibition of PSII in *Emiliania huxleyi* (Haptophyta) under high light stress: The roles of photoacclimation, photoprotection, and photorepair. *Journal of Phycology* 44, 670-683.

Ralph PJ (1999). Light-induced photoinhibitory stress responses of laboratory-cultured Halophila ovalis. *Botanica Marina* 42, 11-22.

Ralph PJ, Gademann R (2005). Rapid light curves: A powerful tool to assess photosynthetic activity. *Aquatic Botany* 82, 222-237.

Ralph PJ, Polk SM, Moore KA, Orth RJ, Smith WO (2002). Operation of the xanthophyll cycle in the seagrass *Zostera marina* in response to variable irradiance. *Journal of Experimental Marine Biology and Ecology* 271, 189-207.

Rannala B, Mountain JL (1997). Detecting immigration by using multilocus genotypes. *Proceedings of the National Academy of Sciences of the United States of America* 94, 9197-9201.

Raven JA, Ball LA, Beardall J, Giordano M, Maberly SC (2005). Algae lacking carbon-concentrating mechanisms. *Canadian Journal of Botany-Revue Canadienne De Botanique* 83, 879-890.

Riebesell U, Zondervan I, Rost B, Tortell PD, Zeebe RE, Morel FMM (2000). Reduced calcification of marine plankton in response to increased atmospheric CO_2. *Nature* 407, 364-367.

Rosenberg NA (2004). DISTRUCT: a program for the graphical display of population structure. *Molecular Ecology Notes* 4, 137-138.

Ross ON, Moore CM, Suggett DJ, MacIntyre HL, Geider RJ (2008). A model of photosynthesis and photo-protection based on reaction center damage and repair. *Limnology and Oceanography* 53, 1835-1852.

Ryman N, Leimar O (2009). G(ST) is still a useful measure of genetic differentiation - a comment on Jost's D. *Molecular Ecology* 18, 2084-2087.

Rynearson TA, Armbrust EV (2000). DNA fingerprinting reveals extensive genetic diversity in a field population of the centric diatom *Ditylum brightwellii*. *Limnology and Oceanography* 45, 1329-1340.

Rynearson TA, Armbrust EV (2005). Maintenance of clonal diversity during a spring bloom of the centric diatom *Ditylum brightwellii*. *Molecular Ecology* 14, 1631-1640.

Rynearson TA, Armbrust VE (2004). Genetic differentiation among populations of the planktonic marine diatom *Ditylum brightwellii* (Bacillariophyceae). *Journal of Phycology* 40, 34-43.

Scholin CA, Anderson DM (1994). Identification of group and strain-specific genetic markers for globally distributed Alexandrium (Dinophyceae). 1. RFLP amalysis of SSU rRNA genes 1. *Journal of Phycology* 30, 744-754.

Schreiber U (2004) Pulse-amplitude-modulation (PAM) fluorometry and saturation pulse method: an overview. In 'Chlorophyll fluorescence: a signature of photosynthesis'. (Eds GC Papageorgiou and Govindjee) pp. 279-319. (Kluwer Academic Publishers: Dordrecht, The Netherlands).

Schreiber U, Bilger W, Neubauer C (1994) Chlorophyll fluorescence as a nonintrusive indicator for rapid assessment of in vivo photosynthesis. In 'Ecophysiology of photosynthesis'. (Eds ED Shulze and MM Caldwell) pp. 49-70. (Springer: Berlin).

Schreiber U, Schliwa U, Bilger W (1986). Continuous recording of photochemical and nonphotochemical chlorophyll fluorescence quenching with a new type of modulation fluorometer *Photosynthesis Research* 10, 51-62.

Schroeder DC, Biggi GF, Hall M, Davy J, Martinez JM, Richardson AJ, Malin G, Wilson WH (2005). A genetic marker to separate *Emiliania huxleyi* (Prymnesiophyceae) morphotypes. *Journal of Phycology* 41, 874-879.

Sedwick PN, Bowie AR, Trull TW (2008). Dissolved iron in the Australian sector of the Southern Ocean (CLIVAR SR3 section): Meridional and seasonal trends. *Deep-Sea Research Part I-Oceanographic Research Papers* 55, 911-925.

Serôdio J, Vieira S, Cruz S, Barroso F (2005). Short-term variability in the photosynthetic activity of microphytobenthos as detected by measuring rapid light curves using variable fluorescence. *Marine Biology* 146, 903-914.

Serôdio J, Vieira S, Cruz S, Coelho H (2006). Rapid light-response curves of chlorophyll fluorescence in microalgae: relationship to steady-state light curves and non-photochemical quenching in benthic diatom-dominated assemblages. *Photosynthesis Research* 90, 29-43.

Siefermann-Harms D (1987). The light-harvesting and protective functions of carotenoids in photosynthetic membranes. *Physiologia Plantarum* 69, 561-568.

Siegel H, Ohde T, Gerth M, Lavik G, Leipe T (2007). Identification of coccolithophore blooms in the SE Atlantic Ocean off Namibia by satellites and in-situ methods. *Continental Shelf Research* 27, 258-274.

Stolte W, Kraay GW, Noordeloos AAM, Riegman R (2000). Genetic and physiological variation in pigment composition of *Emiliania huxleyi* (Prymnesiophyceae) and the potential use of its pigment ratios as a quantitative physiological marker. *Journal of Phycology* 36, 529-539.

Thierstein HR, Geitzenauer KR, Molfino B (1977). Global Synchroneity of Late Quaternary Coccolith Datum Levels - Validation by Oxygen Isotopes. *Geology* 5, 400-404.

Thornhill DJ, Mahon AR, Norenburg JL, Halanych KM (2008). Open-ocean barriers to dispersal: a test case with the Antarctic Polar Front and the ribbon worm Parborlasia corrugatus (Nemertea: Lineidae). *Molecular Ecology* 17, 5104-5117.

Trimborn S, Langer G, Rost B (2007). Effect of varying calcium concentrations and light intensities on calcification and photosynthesis in *Emiliania huxleyi*. *Limnology and Oceanography* 52, 2285-2293.

Tyrrell T, Taylor AH (1996). A modelling study of *Emiliania huxleyi* in the NE Atlantic. *Journal of Marine Systems* 9, 83-112.

van Bleijswijk J, van der Wal P, Kempers R, Veldhuis M (1991). Distribution of two types of *Emiliania huxleyi* (Prymnesiophyceae) in the Northeast Atlantic region as determined by immunofluorescence and coccolith morphology. *Journal of Phycology* 27, 566-570.

van de Poll WH, Visser RJW, Buma AGJ (2007). Acclimation to a dynamic irradiance regime changes excessive irradiance sensitivity of *Emiliania huxleyi* and *Thalassiosira weissflogii*. *Limnology and Oceanography* 52, 1430-1438.

van Leeuwe MA, Stefels J (1998). Effects of iron and light stress on the biochemical composition of Antarctic *Phaeocystis* sp. (Prymnesiophyceae). II. Pigment composition. *Journal of Phycology* 34, 496-503.

van Oosterhout C, Weetman D, Hutchinson WF (2006). Estimation and adjustment of microsatellite null alleles in nonequilibrium populations. *Molecular Ecology Notes* 6, 255-256.

Vaulot D, Birrien JL, Marie D, Casotti R, Veldhuis MJW, Kraay GW, Chretiennot-Dinet MJ (1994). Morphology, ploidy, pigment composition and genome size of cultured strains of *Phaeocystis* (Prymnesiophyceae). *Journal of Phycology* 30, 1022-1035.

Webb WL, Newton M, Starr D (1974). Carbon dioxide exchange of *Alnus rubra* - a mathematical model. *Oecologia* 17, 281-291.

Weir BS, Cockerham CC (1984). Estimating F-statistics for the analysis of population structure. *Evolution* 38, 1358-1370.

Weisse T (2008). Distribution and diversity of aquatic protists: an evolutionary and ecological perspective. *Biodiversity and Conservation* 17, 243-259.

Westbroek P, Van Hinte JE, Brummer GJ, Veldhuis M, Brownlee C, Green JC, Harris R, Heimdal BR (1994) *Emiliania huxleyi* as a key to biosphere-geosphere interactions. In 'The Haptophyte Algae'. (Eds JC Green and BSC Leadbeater) pp. 321-334. (Clarendon Press: Oxford).

White AJ, Critchley C (1999). Rapid light curves: A new fluorescence method to assess the state of the photosynthetic apparatus. *Photosynthesis Research* 59, 63-72.

Winter A, Elbrachter M, Krause G (1999). Subtropical coccolithophores in the Weddell Sea. *Deep-Sea Research Part I-Oceanographic Research Papers* 46, 439-449.

Wright S (1978). *Evolution and the genetics of populations* pp. Chicago University Press, Chicago.

Yamamoto HY, Kamite L (1972). Effects of Dithiothreitol on violaxanthin deepoxidation and absorbance changes in 500-nm region. *Biochimica et Biophysica Acta* 267, 538-&.

Young J, Geisen M, Cros L, Kleijne A, Sprengel C, Probert I, Ostergaard J (2003). A guide to extant coccolithophore taxonomy. *Journal of Nannoplankton Research* Special Issue, 8-9.

Young JR (1994) Functions of coccoliths. In 'Coccolithophores'. (Eds A Winter and WG Siesser) pp. 63-82. (Cambridge University Press: Cambridge).

Young JR, Westbroek P (1991). Genotypic variation in the coccolithophorid species *Emiliania huxleyi*. *Marine Micropaleontology* 18, 5-23.

Zapata M, Jeffrey SW, Wright SW, Rodriguez F, Garrido JL, Clementson L (2004). Photosynthetic pigments in 37 species (65 strains) of Haptophyta: implications for oceanography and chemotaxonomy. *Marine Ecology-Progress Series* 270, 83-102.

Zondervan I (2007). The effects of light, macronutrients, trace metals and CO2 on the production of calcium carbonate and organic carbon in coccolithophores - A review. *Deep-Sea Research Part 11-Topical Studies in Oceanography* 54, 521-537.